

ผลของตัวเติมต่อสมบัติทางกายภาพและการย่อยสลายทางชีวภาพของฟิล์มผสมจาก  
พอลิবিวทิลีนอะดิเพตโคเทรฟทาเลตกับพอลิแล็กติกแอซิด



นางสาว กัญญ์รวี บ่อสุวรรณ

ศูนย์วิทยทรัพยากร  
จุฬาลงกรณ์มหาวิทยาลัย  
วิทยานิพนธ์นี้เป็นส่วนหนึ่งของการศึกษาตามหลักสูตรปริญญาวิทยาศาสตรมหาบัณฑิต

สาขาวิชาปิโตรเคมีและวิทยาศาสตร์พอลิเมอร์

คณะวิทยาศาสตร์ จุฬาลงกรณ์มหาวิทยาลัย

ปีการศึกษา 2552

ลิขสิทธิ์ของจุฬาลงกรณ์มหาวิทยาลัย

EFFECTS OF FILLERS ON PHYSICAL PROPERTY AND BIODEGRADABILITY OF POLY  
(BUTYLENE ADIPATE-CO-TEREPHTHALATE)/POLYLACTIC ACID BLENDED FILM



Miss Kanrawee Bosuwan

ศูนย์วิทยทรัพยากร  
จุฬาลงกรณ์มหาวิทยาลัย

A Thesis Submitted in Partial Fulfillment of the Requirements

for the Degree of Master of Science Program in Petrochemistry and Polymer Science

Faculty of Science

Chulalongkorn University

Academic Year 2009

Copyright of Chulalongkorn University

Thesis Title EFFECTS OF FILLERS ON PHYSICAL PROPERTY AND BIODEGRADABILITY OF POLY (BUTYLENE ADIPATE-CO-TEREPHTHALATE)/POLYLACTIC ACID BLENDED FILM

By Miss Kanrawee Bosuwan

Field of Study Petrochemistry and Polymer Science

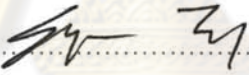
Advisor Associate Professor Dr. Amorn Petsom

---

Accepted by the Faculty of Science, Chulalongkorn University in Partial Fulfillment of the Requirements for the Master's Degree

..... Dean of the Faculty of Science  
(Professor Supot Hannongbua, Dr.rer.nat)

THESIS COMMITTEE

..... Chairman  
(Associate Professor Supawan Tantayanon, Ph.D.)

..... Thesis Advisor  
(Associate Professor Amorn Petsom, Ph.D.)

..... Examiner  
(Associate Professor Wimonrat Trakarnpruk, Ph.D.)

..... Examiner  
(Professor Sophon Roengsumran, Ph.D.)

..... External Examiner  
(Damrong Sommit, Ph.D.)

กัญญ์รวี บ่อสุวรรณ: ผลของตัวเติมต่อสมบัติทางกายภาพและการย่อยสลายทางชีวภาพของฟิล์มผสมจากพอลิบิวทิลีนอะดิเพตโคเทเรฟทาเลตกับพอลิแล็กติกแอซิด (EFFECTS OF FILLERS ON PHYSICAL PROPERTY AND BIODEGRADABILITY OF POLY (BUTYLENE ADIPATE-CO-TEREPHTHALATE)/POLYLACTIC ACID BLENDED FILM) อ.ที่ปรึกษาวิทยานิพนธ์หลัก: รศ. ดร. อมร เพชรสม, 94 หน้า.

งานวิจัยนี้ศึกษาพอลิเมอร์ผสมระหว่างพอลิบิวทิลีนอะดิเพตโคเทเรฟทาเลตกับพอลิแล็กติกแอซิดที่ถูกเสริมแรงด้วยตัวเติมอนุภาคระดับนาโนประเภทไฮโดรฟิสิกซิลิกา ไฮโดรโฟบิกซิลิกา และแคลเซียมคาร์บอเนตด้วยอัตราส่วนผสมที่ 1, 3 และ 6 ส่วนในพอลิเมอร์ 100 ส่วน โดยเตรียมพอลิเมอร์ผสม ด้วยเครื่องผสมอัดรีดแบบเกลียวหนอนคู่ จากนั้นนำไปอัดขึ้นรูปเป็นแผ่นฟิล์ม ศึกษาผลจากการเติมตัวเติมทั้ง 3 ประเภทในพอลิเมอร์ผสมด้านฐานวิทยาศาสตร์ โดยกล้องจุลทรรศน์อิเล็กตรอนแบบส่องกราดแล้วพบว่าตัวเติมทำให้การกระจายวัฏภาคของพอลิพอลิบิวทิลีนอะดิเพตโคเทเรฟทาเลตในเนื้อพื้นพอลิแล็กติกแอซิดดีขึ้น สมบัติเชิงกลด้านความทนแรงดึง มอดุลัส และความยืดเพิ่มขึ้นจากการเพิ่มการเข้ากันได้ สมบัติทางความร้อนวิเคราะห์ด้วยเครื่องวิเคราะห์การเปลี่ยนแปลงทางความร้อนชี้ให้เห็นการเพิ่มความสามารถในการเกิดผลึก วัดสมบัติเชิงกลไดนามิกด้วยเครื่องวิเคราะห์การเปลี่ยนแปลงสมบัติเชิงกลแบบไดนามิก พบการเพิ่มขึ้นของอุณหภูมิเปลี่ยนสภาพแก้ว สมบัติด้านความทนต่อโมเลกุล ของน้ำจากการวัดอัตราการซึมผ่านของไอน้ำพบว่า การซึมผ่านของไอน้ำลดลง ด้านสมบัติทางแสงตัวเติมทำให้พอลิเมอร์ผสมทึบแสงมากขึ้น การย่อยสลายทางชีวภาพด้วยเอนไซม์ Proteinase K ของพอลิเมอร์ผสมที่มีตัวเติมจะย่อยสลายได้ช้ากว่าพอลิเมอร์ผสมที่ไม่มีตัวเติม หลังจากการย่อยสลายด้วยเอนไซม์พบว่า มีช่องว่างกระจายตัวอยู่บนผิวหน้าของแผ่นฟิล์มผสมซึ่ง เกิดจากพื้นผิวพอลิเมอร์ถูกทำลาย

สาขาวิชาปิโตรเคมีและวิทยาศาสตร์พอลิเมอร์  
ปีการศึกษา: 2552

ลายมือชื่อนิสิต กัญญ์รวี บ่อสุวรรณ  
ลายมือชื่อ อ.ที่ปรึกษาวิทยานิพนธ์หลัก อมร เพชรสม



# #4973423823: MAJOR PETROCHEMISTRY AND POLYMER SCIENCE

KEYWORDS : POLY (LACTIC ACID)/ POLY (BUTYLENE ADIPATE-CO-TEREPHTHALATE)/ FILLERS/ POLYMER BLEND NANOCOMPOSITE

KANRAWEE BOSUWAN: EFFECTS OF FILLERS ON PHYSICAL PROPERTY AND BIODEGRADABILITY OF POLY (BUTYLENE ADIPATE-CO-TEREPHTHALATE)/POLYLACTIC ACID BLENDED FILM. THESIS ADVISOR: ASSOC.PROF. AMORN PETSOM, Ph.D., 94 pp.

Blends of PBAT and PLA filled with hydrophilic silica, hydrophobic silica and calcium carbonate nanoparticles were prepared by twin screw extruder and compression molding with fillers content at 1, 3 and 6 phr. Effects of fillers on morphology was investigated by SEM from which better distribution of the PBAT dispersed phase in PLA matrix was found in polymer blend nanocomposite. The incorporation of fillers increased the tensile strength, tensile modulus and elongation resulted from enhanced interfacial compatibility. DSC thermograms indicated that the crystallization rate was enhanced by fillers. DMA results revealed the storage modulus imparted by fillers. The permeability by WVTR of PBAT/PLA blends was decreased by fillers addition. The light transmittance of PBAT/PLA blends was decreased by the addition of fillers. The biodegradability test using by Proteinase K method of PBAT/PLA blends decreased by fillers addition. After the enzymatic degradation, pores were widely distributed on the surface of the films. The filler hampered enzymatic degradation.

Field of Study : Petrochemistry and Polymer Science

Academic Year : .....2009.....

Student's Signature Kanralee Bosuwan

Advisor's Signature Amorn Petsom

## ACKNOWLEDGEMENTS

The author would like to express her sincere gratitude to her advisor, Assoc. Prof. Dr. Amorn Petsom for his encouraging guidance, supervision and helpful suggestion throughout this research. The author also would like to acknowledge Assoc. Prof. Dr. Supawan Tantayanon, Assoc. Prof. Dr. Wimonrat Trakarnpruk, Prof. Dr. Sophon Roengsumran and Dr. Damrong Sommit for serving as chairman and members of the thesis committee, respectively and for their worthy comments and suggestions.

Many thanks are going to staffs of the Program of Petrochemistry and Polymer Science. The author gratefully acknowledges the funding support from Program of Petrochemistry and Polymer Science and National Center of Excellence for Petroleum, Petrochemicals, and Advanced Materials, NCE-PPAM and CU Graduate School Thesis Grant, Chulalongkorn University.

Eventually, the author would like to express her gratitude to family members for their love, understanding and great support throughout her study. Also, special thanks are extended to her friends for friendship, encouragements and cheerful moral support.



ศูนย์วิทยทรัพยากร  
จุฬาลงกรณ์มหาวิทยาลัย

## CONTENTS

	Page
ABSTRACT (Thai).....	iv
ABSTRACT (English).....	v
ACKNOWLEDGEMENTS.....	vi
CONTENTS.....	vii
LIST OF TABLES.....	x
LIST OF FIGURES.....	xi
CHAPTER I INTRODUCTION.....	1
1.1 General introduction.....	1
1.2 Objective.....	5
1.3 Scope of research.....	5
CHAPTER II THEORY AND RESEARCH BACKGROUNDS.....	6
2.1 The effect of plastic waste on the environment.....	6
2.2 Definitions of biodegradable polymers.....	6
2.3 Biodegradable polymers classification.....	8
2.4 Polymer blends.....	10
2.5 Poly (lactic acid) (PLA) properties.....	12
2.6 Poly (butylenes adipate-co-terephthalate) (PBAT) properties.....	14
2.7 Polymer composites.....	16
2.7.1 Types and components of polymer composites.....	16
2.7.2 Effects of fillers/reinforcements-functions.....	17
2.7.3 Functional fillers.....	18
2.8 Fillers and their functions.....	22
2.8.1 Silica.....	22
2.8.1.1 Fumed silica.....	22
2.8.1.2 Reactivity of silanes toward the filler.....	24
2.8.2 Calcium carbonate.....	26

2.9 Nanoparticles in material chemistry and in the natural sciences .....	27
2.9.1 Classification of nanoparticles by size.....	29
2.9.2 Nanoparticle modifying action on polymers.....	31
2.10 Determination of polymer/polymer miscibility.....	32
2.11 Polymer degradation.....	32
2.12 Literature review.....	35
CHAPTER III EXPERIMENTAL.....	38
3.1 Materials.....	38
3.1.1 Poly (lactic acid) (PLA).....	38
3.1.2 Poly (butylenes adipate-co-terephthalate) (PBAT).....	38
3.1.3 Hydrophilic Fumed silica (SiO <sub>2</sub> ) nanoparticles.....	38
3.1.4 Hydrophobic Fumed silica (mSiO <sub>2</sub> ) nanoparticles.....	38
3.1.5 Nano-sized precipitated calcium carbonate (NPCC).....	38
3.1.6 Proteinase K.....	39
3.1.7 Sodium Azide (NaN <sub>3</sub> ).....	39
3.1.8 TRIS hydrochloride buffer.....	39
3.2 Instruments and apparatus.....	39
3.3 Polymer blend nanocomposites preparation.....	40
3.4 Thermal analysis and dynamic mechanical analysis.....	42
3.4.1 DSC analysis.....	42
3.4.2 DMA analysis.....	43
3.5 Morphological observation.....	44
3.6 FT-IR analysis.....	45
3.7 Mechanical properties.....	45
3.8 Water vapor transmission rate (WVTR) and water vapor permeability (WVP).....	46
of the films.....	46
3.9 Optical transprence analysis.....	47
3.10 Enzyme degradation observation.....	47
CHAPTER IV RESULTS AND DISCUSSION .....	49
4.1 Thermal analysis of PBAT/PLA blends.....	49
4.1.1 DSC measurement of PBAT/PLA polymer blend.....	49



4.1.2 DSC measurement of PBAT/PLA polymer blend nanocomposites.....	51
4.2 Morphology of PBAT/PLA blend in the absence and presence of SiO <sub>2</sub> ,.....	58
mSiO <sub>2</sub> and NPCC by SEM.....	
4.3 Mechanical properties of PBAT/PLA blend in the absence and presence of...	61
fillers content.....	
4.3.1 Mechanical properties of PBAT/PLA blends.....	61
4.3.2 Mechanical properties of PBAT/PLA polymer blend nanocomposites.....	64
4.4 Optical transprence of the blend films.....	68
4.5 Interactions between PBAT/PLA blends in the absence and presence of.....	69
Fillers.....	
4.6 Dynamic mechanical properties.....	73
4.7 Water vapor transmission rate (WVTR) and water vapor permeability (WVP)....	77
4.8 Enzymatic degradation study of PBAT/PLA blend in the absence and.....	78
presence of SiO <sub>2</sub> at 1 phr.....	78
4.8.1 Observation by SEM.....	78
4.8.2 Weight loss investigation.....	81
4.8.3 Mechanical properties after enzymatic degradation on digestion times.	82
CHAPTER V CONCLUSION AND FUTURE DIRECTION.....	83
5.1 Conclusion.....	83
5.2 Future direction.....	84
REFERENCES.....	85
APPENDICES.....	88
BIOGRAPHY.....	94

## LIST OF TABLES

Table		Page
2.1	Commercially available aromatic copolyesters.....	15
2.2	Chemical families of fillers for plastics.....	19
2.3	Particle morphology of fillers.....	20
2.4	Fillers and their functions.....	21
2.5	Classification of nanoparticles and clusters by size.....	31
2.6	Reaction catalyzed and reactive bonds of different classes of enzyme..	34
3.1	Compositions and sample code name of PBAT/PLA/fumed silica and NPCC polymer blend nanocomposite.....	41
4.1	T <sub>m</sub> and T <sub>c</sub> of PBAT/PLA blends with various PBAT contents(1 <sup>st</sup> heating, cooling and 2 <sup>nd</sup> heating, 10 <sup>o</sup> C/min).....	49
4.2	Thermal properties of PBAT/PLA blends with various filler types and content.....	52
4.3	The optical transparence (T%) at different wavelengths for the film.....	68
4.4	The storage modulus of the PBAT/PLA blend filled with fillers nanoparticle.....	74
A-1	Mechanical properties of PBAT/PLA blend with various PBAT contents	91
A-2	Mechanical properties of PBAT/PLA blend with absence and presence of fillers content.....	92
A-3	Thermal properties (T <sub>g1</sub> and T <sub>g2</sub> ) of PBAT/PLA blends with various filler types and content (2 <sup>nd</sup> heating scan, 10 <sup>o</sup> C/min).....	93
A-4	The glass temperature (T <sub>g</sub> ) from DMA analysis of the PBAT/PLA blend filled with fillers nanoparticle.....	94

## LIST OF FIGURES

Figure		Page
2.1	Possible fate of polymer degradation.....	7
2.2	Classification of the biodegradable polymer.....	10
2.3	Chemical structure of polylactic acid (PLA).....	12
2.4	Biodegradable polyester families.....	14
2.5	Chemical structure of poly(butylenes adipate-co-terephthalate)(PBAT)	14
2.6	Surface area-to-volume ratio, $A / V$ , of a cylindrical particle plotted versus aspect ratio ( maximizing $A/ V$ and particle-matrix interaction through the interface requires $\alpha \gg 1$ for fibers and $1/\alpha \ll 1$ for platelets).....	18
2.7	Mode of reaction between a silanol and an inorganic material.....	25
2.8	Overview of a silanized surface.....	25
2.9	Size correlation between synthetic and natural structures.....	29
2.10	The main stages of the transformation metal atoms into a bulk metal.....	31
2.11	Different analytical techniques to analyze the polymer durability.....	33
2.12	Hydrolysis reaction of PLA.....	35
3.1	TRIS hydrochloride .....	39
3.2	Twin screw extruder for blending.....	42
3.3	Typical DSC: Differential Scanning Calorimeter.....	43
3.4	Typical DMA: Dynamic Mechanical Analysis cells.....	44
3.5	SEM : Scanning Electron Microscope.....	44
3.6	Fourier Transform Infrared (FT-IR) spectroscopy.....	45
3.7	Tensile testing apparatus and dumbbell test specimen.....	46
3.8	Dual-beam Spectrophotometer.....	47
4.1	DSC thermograms of PLA, PBAT and their blends: (a) neat PLA (b) neat PBAT(c) PL40PB60 (d) PL30PB70(e) PL50PB50.....	50

Figure	Page
4.2	Enthalpy of Tm and Tc of PLA, PBAT and their blends (2 <sup>nd</sup> heating&cooling) (A) Enthalpy of melting temperature (B) Enthalpy of crystallization temperature..... 53
4.3	DSC thermograms of PLA, PBAT and their blends with SiO <sub>2</sub> : ..... 54 (a) PL50PB50 (b) PL50PB50S1 (c) PL50PB50S3 (d) PL50PB50S6.....
4.4	DSC thermograms of PLA, PBAT and their blends with mSiO <sub>2</sub> : ..... 55 (a) PL50PB50 (b) PL50PB50MS (c) PL50PB50MS3 (d) PL50PB50MS6..
4.5	DSC thermograms of PLA, PBAT and their blends with NPCC: ..... 56 (a) PL50PB50 (b) PL50PB50C1 (c) PL50PB50C3 (d) PL50PB50C6....
4.6	DSC thermograms, comparison of PBAT/PLA blends filled with SiO <sub>2</sub> , mSiO <sub>2</sub> and NPCC at 1 phr : (a) PL50PB50 (b) PL50PB50S1 (c) PL50PB50MS1 (d) PL50PB50C1..... 57
4.7	SEM images of the blend: (a) PL50PB50 (b) PL50PB50S3 (c) PL50PB50MS3 (d) PL50PB50C3 (e) zoom of image b (f) zoom of image c and (e) zoom of image d..... 60
4.8	Tensile strength of neat PLA, PBAT and their blends..... 62
4.9	Tensile modulus of neat PLA, PBAT and their blends..... 63
4.10	The elongation of neat PLA, PBAT and their blends..... 63
4.11	Tensile strength of PBAT/PLA (50/50 wt %) and their composites..... 66
4.12	Tensile modulus of PBAT/PLA (50/50 wt %) and their composites..... 66
4.13	The elongation of PBAT/PLA (50/50 wt %) and their composites..... 67
4.14	IR spectra of PLA (a), PBAT (b), SiO <sub>2</sub> (c), PL50PB50 (d), and PL50PB50S6 (e)..... 70
4.15	IR spectra of PLA (a),PBAT (b),PL50PB50 (c),andPL50PB50MS6 (d).. 71
4.16	IR spectra of PLA (a),PBAT (b), PL50PB50 (c), and PL50PB50C6 (d). 72
4.17	(a) Temperature dependence of storage modulus at 60 °C..... 73 (b) Temperature dependence of tan delta (T <sub>g</sub> of PBAT)..... 74
4.18	Water vapor transmission rate (WVTR) of films..... 78

Figure		Page
4.19	Scanning electron micrographs after 8 hours of enzymatic exposure at 15 kV 1,000 x (a) PL50PB50 (control) (b) PL50PB50 (8 hrs) (c) PL50 PB50S1 (control) (d) PL50PB50S1 (8hrs).....	79
4.20	Scanning electron micrographs after 120 hours of enzymatic exposure (a) PL50PB50 (control) (b) PL50PB50 (120 hrs)(c) PL50 PB50S1 (control) (d) PL50PB50S1 (120hrs).....	80 81 82
4.21	Weight loss of the PL50PB50 and PL50PB50S1 on digestion times.....	83
4.22	Comparison of tensile modulus between PL50PB50 and PL50PB50S1..	
4.23	Comparison of yield stress between PL50PB50 and PL50PB50S1.....	90
A-1	$T_m$ and $\Delta H_m$ of PLA in neat form and blends at various PBAT contents (1 <sup>st</sup> heating scan, 10°C/min).....	



## CHAPTER I

### INTRODUCTION

#### 1.1 General Introduction

The environmental pollution problems with domestic waste from consumed conventional polymers has become increasing serious, particularly from packaging materials and one-off plastic bags and cups. Application of biodegradable polymers instead of conventional polymers plastic is one promising way to solve this problem has been developed for more than 10 years [1]. Development of consumer products from biodegradable and renewable materials is currently an area of great interest for research. However, there are some limitations to the application of biodegradable plastic due to its poor mechanical properties and high sensitivity to moisture. Many studies have concentrated on improving mechanical and water barrier properties of biodegradable plastic for wide applications by comparable to conventional plastics, while maintaining the overall biodegradability of the product.

Generally, biodegradable polymers can be classified by resources into two major groups: (1) natural resource polymers, such as starch, cellulose, polylactic acid (PLA), and polyhydroxyalkanoate (PHA); (2) petrochemical resource polymers, such as polycaprolactone (PCL), aliphatic-aromatic copolyester (AACs) and polyvinyl alcohol (PVA). Biodegradability is exclusively a function of the polymer structure and does not depend on the origin of the raw materials – whether petrochemical resource or from natural resources. At present, petrochemically based plastic provide a number of advantages compared to those made from naturally produced macromolecules. Better use properties, processability comparable to conventional plastics, constant material quality and in many cases a significantly lower price point in favour of petrochemically based materials, at least as components in biodegradable plastic compositions. In order to overcome disadvantages such as poor mechanical properties of plastic from natural resource polymers, or to offset the high prices of petrochemical resource polymers, various blends and composites have been developed over the last decade. Starch

blended with polyvinyl alcohol has been studied as a potential biodegradable polymer. The mechanical properties and biodegradability of starch/PVA blended films have been reported by several researchers. However, their wide applications are limited by the lack of water resistance and poor mechanical property of starch/PVA blended films. The starch/PVA blended films were modified by nano-SiO<sub>2</sub>. Improving results were increased both tensile strength and breaking elongation [2]. Blends can also aid in the development of low cost commercialized biodegradable plastic products with better performance. These blends and composites are extending the utilization of biodegradable plastic from biodegradable polymer into new value added commercial products.

Poly(lactic acid) (PLA) is a kind of linear aliphatic polyester derived from biomass through bioconversion and polymerization. PLA is environmentally biodegradable and can eventually be converted to be carbon dioxide, water, and humus. PLA has high strength (over 50 MPa) and modulus (over 3 GPa) comparable to that of many petroleum-based plastic, but its low toughness limit its application, so that neat PLA is hard to be designed for film extrusion. To retain the integrity of biodegradability, blending PLA with other biodegradable polymers is particularly interesting. Blending PLA with other polymers presents a practical and economic measure to obtain toughened products. PLA/poly ( $\epsilon$ -caprolactone) (PCL) blends have been extensively studied and have shown greatly improved mechanical properties compared to neat PLA. In a recent study, introduced PLA/poly (butylene adipate-co-terephthalate)(PBAT) as biodegradable aliphatic-aromatic copolyester, which is fully biodegradable and demonstrated a significant toughening effect. In view of its high toughness and biodegradability, PBAT was considered a good candidate for the toughening of PLA. It has been studied that the elongation and toughness of the blends of PLA and PBAT increased dramatically with the increase of PBAT content (5-20 wt %) but the blend showed decreased tensile strength and modulus [3]. Hence, in order to improve the mechanical properties of these polymers, some additives as reinforcement fillers are used to blend with them. It has been reported that blending polymer with inorganic materials is considered a powerfully method to produce new materials called

polymer composites or filled polymers. However, due to the significant development in nanotechnologies in recent years, nanoscale inorganic materials such as  $\text{SiO}_2$ ,  $\text{Al}_2\text{O}_3$  and  $\text{TiO}_2$  have brought much attention to this research field. Many studies indicate that nano-materials can improve the performance of polymer materials such as plastic and rubber. A new area of composites called nanocomposites, in which the reinforcing material has nanometric scale, has emerged and seems to be very promising. For instance, at low level of nanofillers incorporation (less than 5 wt %), the reinforcement efficiency of nanocomposites can match that of conventional composites with 40-50wt% of loading with classical fillers. This improvement is due to the dispersion of nanoscale fillers into the matrix, which results in a high surface area with high interaction between nanofillers and the polymer matrix. In recently study, the starch/PVA blend films were modified by nano- $\text{SiO}_2$ . The mechanical properties, transmittance, and water resistance of this blend films were all improved significantly with the addition of nano- $\text{SiO}_2$ . Silica is one of the most commonly used nanofillers. Nano- $\text{SiO}_2$  deviates from a stable silicon-oxygen structure for lack of oxygen in its surface. Because of its small size, large specific surface area, high surface energy, as well as a lot of unsaturated chemical bonds and hydroxyl groups on the surface, nano- $\text{SiO}_2$  is easy to disperse into the macromolecular chains. If dispersed to the scale of 10-50 nm, it can improve the modulus, heat distortion temperature and the barrier properties of the matrix. Many research efforts have been devoted to the surface modification of silica leading to hydrophobic silica. The aim is to reduce the high surface energy and the particle interactions. Additionally, filler treatment will lead to a better dispersion due to the more probable interactions of the polymer with the modification than with the inorganic particle surface. Fumed silica nanoparticle has been used as filler for thermoplastics as PP, LLDPE, PET, PEN, and blends of PS/PP, PC/LCP, and PP/EPDM [4]. Although, nano- $\text{SiO}_2$  with nanoscale fine structure are usually used to reinforce and improve polymer blend properties, but the price is higher than that of other fillers. As an important exception composites of biodegradable polymer with calcium carbonate have been studied extensively.

Calcium carbonate ( $\text{CaCO}_3$ ) is extensively used as an additive or modifier in plastic, paper, paints, inks, adhesives and pharmaceuticals, to mention but a few. New discoveries and refined processes in the plastic, paper and pharmaceutical industries call for high-end type of products consisting of particles, whose crystalline phase, morphology, size and distribution of sizes are strictly controlled and can be modulated according to specific requirements.  $\text{CaCO}_3$  is traditionally used in plastics as bulking and reinforcing agent to substitute the expensive polymers. All properties of the pure polymer are subject to change as a result of filling, and in fact a new material is created by blending a polymer with inorganic fillers.  $\text{CaCO}_3$  particles of an aspect ratio close to unity are expected to modify the viscosity of the polymer melt. Their good thermal conductivity contributes to the homogeneity of the melt and good dispersion in the polymer matrix. Nano-sized precipitated calcium carbonate (NPCC) is commonly synthesized by a recarbonizing process from natural calcium carbonate. The reinforcing effect of NPCC particles has been studied in polymer systems such as linear low density polyethylene (LLDPE), polypropylene (PP), high density polyethylene (HDPE), polystyrene (PS) and poly (lactic acid) (PLA). The tensile and/or impact toughness was found to be significantly improved by the addition of the fine  $\text{CaCO}_3$  particles [5].

To cope with the obvious limitations of biodegradable polymers for example, low strength, modulus and barrier, and to expand their applications in different sectors, inorganic particulate fillers, such as nano- $\text{SiO}_2$  and  $\text{CaCO}_3$  particles are often added to process biodegradable polymer blends. The particulate fillers modify the physical and mechanical properties of biodegradable polymers in many ways. It has been report that blending biodegradable polymer with inorganic nano-sized materials such as  $\text{SiO}_2$ , and  $\text{CaCO}_3$  as fillers is considered a powerful method to improved physical and mechanical properties. In relevant studies on PBAT/PLA composites filled with nano- $\text{SiO}_2$  and  $\text{CaCO}_3$  have not yet been reported. Therefore, in this study, silica nanoparticle both modified and unmodified and nano-sized precipitated calcium carbonate (NPCC) as reinforcement fillers were dispersed in biodegradable PBAT/PLA polymer blends matrix by melt extrusion method. The effects of the filler content and the filler surface chemistry

on the structure, physical properties and biodegradability of the polymer blends nanocomposites were studied.

## 1.2 Objective

This research aims to study effect of unmodified fumed silica ( $\text{SiO}_2$ ), modified fumed silica ( $\text{mSiO}_2$ ) nanoparticles and nano-sized precipitated calcium carbonate (NPCC) as reinforcement fillers on structure, morphology, mechanical, thermal, dynamic mechanical and optical properties, permeability and biodegradability of PBAT/PLA blend films.

## 1.3 Scope of research

This research will focus on fillers of PBAT/PLA blended films on the following topics.

- 1.3.1 Study of polymer blending on mechanical and thermal properties with various ratios of PBAT/PLA polymer blends by melt extrusion and compression molding process.
- 1.3.2 Comparison of filler type and filler content of unmodified fumed silica ( $\text{SiO}_2$ ), modified fumed silica ( $\text{mSiO}_2$ ) nanoparticles and nano-sized precipitated calcium carbonate (NPCC) as reinforcement fillers on structure, morphology, mechanical, thermal, dynamic mechanical and optical properties, permeability and biodegradability of PBAT/PLA blended film by melt extrusion and compression molding process.

ศูนย์วิทยทรัพยากร  
จุฬาลงกรณ์มหาวิทยาลัย



## CHAPTER II

### THEORY AND RESEARCH BACKGROUNDS

#### 2.1 The effect of plastic waste on the environment

Presently, the world economy depends almost entirely on the use of plastic. Since plastics are polymers that generally designed to combine light weight with excellent resistance to mechanical, biological, and chemical resistance. Plastic have become an important material for human in everyday life. The amount of plastic products in the world is increasing every year. The disposal of plastic wastes after used is major problem.

Many approaches have been proposed for solving the worldwide problem of plastic waste such as recycling or land filling. However, with increase in the world population and industrialization, the disposal of plastic waste is unable to solve this environmental problem. Much attention was focused on biodegradable polymer material to potentially apply new degradable products in the future.

#### 2.2 Definitions of biodegradable polymers

The field of polymer degradation has an extensive and sometimes confusing literature. Researchers from various fields use different definitions for biodegradable. It is important to recognize the need for accurate definitions and for test methods consistent with those definitions.

Environmental degradation includes biodegradation, photodegradation, oxidation, and/or hydrolysis leading to some change in polymer structure and physical properties. One of the first steps toward international consensus on terminology was taken by the American Society for Testing and Materials (ASTM)(1993), with these definitions:

- **Degradable polymer** : a polymer designed to undergo a significant change in its chemical structure under specific environment conditions, resulting in a loss of some properties that may vary as measured by standard test methods appropriates to the polymer and the application in a period of time that determines its classification.

- **Biodegradable polymer** : a degradable polymer in which the degradation results from the action of naturally occurring microorganisms such as bacteria, fungi, and algae.
- **Hydrolytically degradable polymer** : a degradable polymer in which the degradation results from hydrolysis.
- **Oxidatively degradable polymer** : a degradable polymer in which the degradation results from oxidation.
- **Photodegradable polymer** : a degradable polymer in which the degradation results from the action of natural light.

Biodegradation can play the key role in ultimately defining environmentally acceptable polymer. In Figure 2.1, all degradation pathways lead to fragmentation of the polymer backbone chain. However, the polymer fragments and residues (i.e. metabolites) may remain in the environment, or they may completely biodegrade and convert to carbon dioxide and water [6].

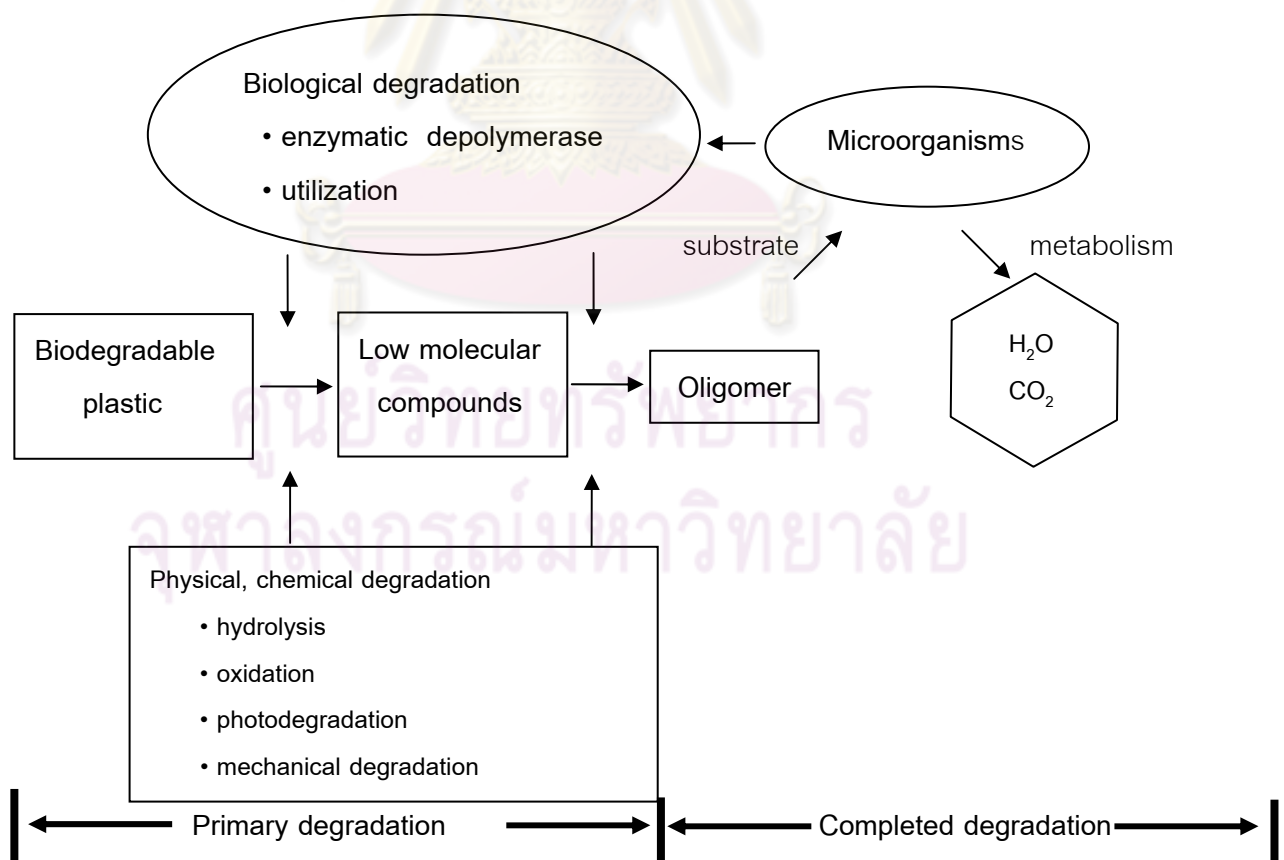


Figure 2.1 Possible fate of polymer degradation.

### 2.3 Biodegradable polymers classification

A vast number of biodegradable polymers (biopolymers) are chemically synthesized or biosynthesized during the growth cycles of all organisms. Some micro-organisms and enzymes capable of degrading them have been identified. Fig. 2.2 proposes a classification with four different categories, depending on the synthesis:

1. **Biomass products:** Polymers directly extracted or removed from biomass (i.e. polysaccharides, starch, cellulose, proteins, and polypeptides).

a. *Polysaccharides* : The most important polysaccharides of concern to material applications are cellulose and starch. Increasing attention is being given recently to more complex carbohydrate polymers produced by bacteria and fungi, such as xanthan, curdlan, pullulan, and hyaluronic acid.

- *Starch* : Starch is well-known polymer, naturally produced by plants in the form of granules (mainly from potatoes, corn, and rice). Starch granules vary from plant to plant but are in general composed of a linear polymer, amylose, and a branched polymer, amylopectin.

- *Cellulose* : Cellulose is another widely known polysaccharide produced by plants. The molecular chain of cellulose is very long, consisting of one repeating unit (cellobiose), and occurs naturally in a crystalline state.

- *Chitin and chitosan* : Chitin is a macromolecule found in the shells of crabs, lobsters, shrimp, and insects. It consists of 2-acetamido-2-deoxy- $\beta$ -D-glucose through the  $\beta$ -(1-4)-glycoside linkage.

b. *Polypeptides of natural origin* : The proteins that have found applications as materials are, for the most part, neither soluble nor fusible without degradation, so they are used in the form in which they are found in nature.

2. **From micro-organisms** : Polymers produced from microbial fermentation. This category includes natural polyesters, which are produced from renewable resources by a wide variety of bacteria as intracellular reserved materials, such as polyhydroxybutyrate (PHB).

3. **From biotechnology:** Polymers produced by classical chemical synthesis using renewable bio-based monomers, such as polylactic acid (PLA)

4. **From petrochemical products:** Polymers produced by petrochemical feedstock. Between the nonbiodegradable petrochemical polymers and the renewable/natural source biodegradable polymers, the chemical industry is also thinking in terms of aliphatic/aromatic ratio by using chemical process engineering to achieve petrochemical biodegradable polymers, such as aliphatic polyester based, blends, alloys, and graft copolymers of natural polymers and polyester. (i.e. poly(glycolic acid);PGA, poly(butylene adipate-co- terephthalate);PBAT, poly( $\epsilon$ -caprolactone); PCL, poly (vinyl alcohol); PVA, etc.)

- *Polyesters* : Polyesters derived from diacids of medium sized monomers (C6-C12) [e.g., poly(glycolic acid)] are more readily degraded by fungi, than those derived from longer or shorter monomers. The reason for that, as well as for the fact that flexible aliphatic polyesters are degradable, whereas rigid aromatic polyesters are not, is that biodegradability by enzyme catalysts requires that the synthetic polymer chain fit into the enzyme's active site. Poly(glycolic acid )(PGA) is the simplest linear, aliphatic polyester. Beside the natural polyesters (e.g.PHB), many other synthetic aliphatic polyesters are susceptible to microbial attack. It was shown that synthetic copolyesters containing aromatic constituents (i.e aliphatic-aromatic copolyester; AAC) are also degraded by microorganisms. The degradation decreases as the amount of aromatic components increases. Poly (butylene adipate-co-terephthalate); PBAT, as aliphatic-aromatic copolyester, was truly biodegradable in the composting environments without adverse ecotoxicological effect.

- *Polycaprolactone:* Poly ( $\epsilon$ -caprolactone) (PCL) is generally prepared from the ring-opening polymerization of  $\epsilon$ -caprolactone. PCL is biodegraded by fungi and can be degraded enzymatically.

- *Poly (vinyl alcohol) and poly (vinyl acetate):* Poly (vinyl alcohol) (PVA) is the most readily biodegradable of vinyl polymers (microbial degradation as well as enzymatic degradation by secondary alcohol peroxidase isolated from soil

bacteria. Most of the biodegradable vinyl polymers contain an easily oxidizable functional group and catalysts are added to promote their oxidation or photooxidation, or both [7].

Of these, only categories (1) – (3) are obtained from renewable resources. The different biodegradable polymers are sorted into main families, the agro-polymers (category 1) and the biodegradable polyesters (categories 2-4), also called biopolyesters.

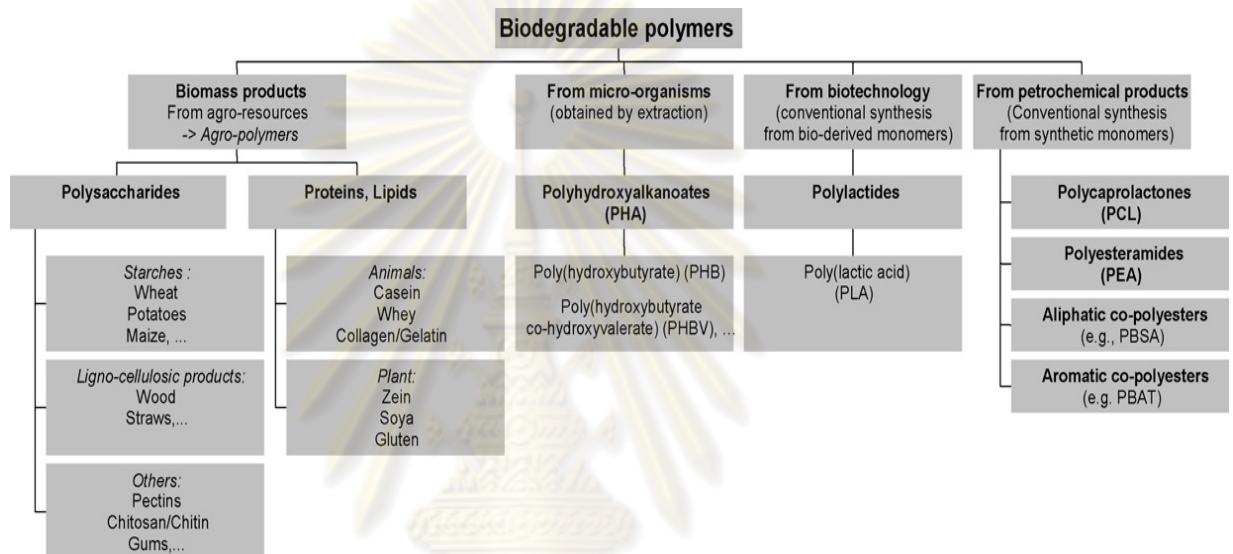


Figure 2.2 Classification of the biodegradable polymer [8]

## 2.4 Polymer blends

Biodegradable polymers have attracted an increasing amount of attention over the last two decades, predominantly due to two major reasons: firstly environmental concerns, and secondly the realization that our petrochemical polymer from petroleum resources are finite. Like numerous other petrochemical-based polymers, many



properties of biodegradable polymer can also be improved through blending and composite formation.

By definition, any physical mixture of two or more different polymer of copolymers that are not linked by covalent bonds is a polymer blend. Development of a new polymer to meet a specific need is a costly enterprise. If the desired properties can be realized simply by mixing two or more existing polymers, there is an obvious pecuniary advantage.

A number of technologies have devised to prepare polymer blend. It so happens that most polymers are not compatible. Rather, they separate into discrete phase on being mixed, although an increasing number of completely miscible blends are being developed. Differences between the two types are manifested in appearances, miscible blends are usually clear, immiscible blends are opaque and in such properties as glass transition temperature, miscible blends exhibit a single  $T_g$  intermediate between those of the individual components, whereas immiscible blend exhibit separate  $T_g$ s characteristic of each component. Miscibility is by no means prerequisite to commercial utility.

Homogeneous polymer blends are more convenient from the standpoint of being able to predict properties of processing characteristics. If additives are used, for example, there are no problems of migration from one phase to another. Physical or mechanical properties usually reflect to a degree, the weighted average of the properties of each component.

In general, the properties of blend are usually determined by miscibility of the polymeric constituents. Miscibility implies that a single phase is produced. The most polymer blend category is the partially miscible system. The most common system is one in which two completely immiscible polymer are made compatible with a third organic agent.

Miscible polymer blend is a polymer mixture which is homogeneous down to the molecular level. Thermodynamically, this is associated with the negative value of the free energy of mixing i.e  $\Delta G_m = \Delta H_m < 0$  ; where  $\Delta G_m$  is the Gibb's free energy of mixing and  $\Delta H_m$  is the enthalpy of mixing. Miscible polymer blend has a single phase,

in contrast, immiscible blend polymers is a polymer mixture in which polymer- A forms a separate phase from polymer-B. The thermodynamically immiscible blend is associated with the positive value of the Gibb's free energy of mixing i.e  $\Delta G_m = \Delta H_m > 0$

The compatibility of a polymer-polymer system determines polymer system properties. In general, compatible polymer blend is a homogeneous polymer mixture to the eye with physical and other polymer properties. Polymer blends that are heterogeneous on a macroscopic level are called incompatible polymer blends. The compatibilization can in principle interact in complex ways to influence final blend properties [9].

### 2.5 Poly (Lactic Acid) (PLA) properties

Poly (lactic acid) (PLA) is linear aliphatic polyester which has chemical structure in Figure 2.3.

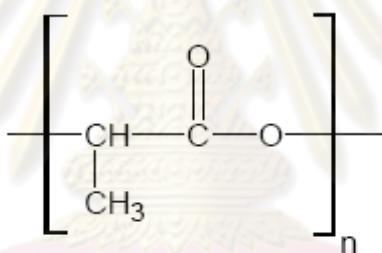
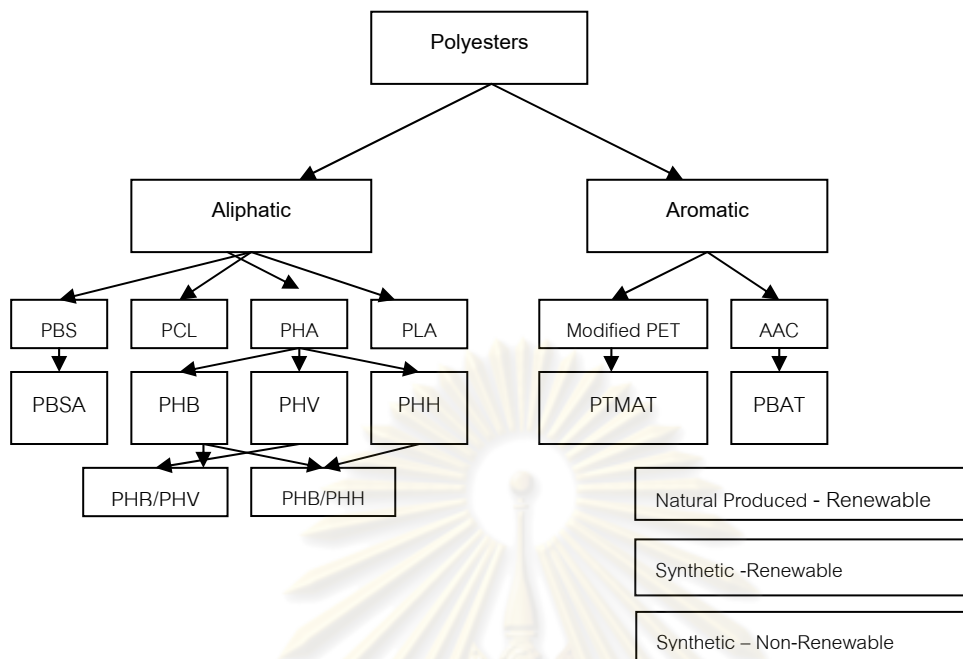


Figure 2.3 Chemical structure of polylactic acid (PLA) [10]

It produced by poly-condensation of naturally produced lactic acid or by ring opening polymerization of lactides which are the cyclic dimers of lactic acids and are typically derived from corn starch fermentation. PLA is one of biodegradable polyester family. PLA has been found to be environmentally biodegradable through a two-step process that begins with the high molecular weight polyester chains hydrolyzing to lower molecular weight oligomers under an appropriate temperature and moisture environment. In the second step, microorganisms convert these lower molecular weight components to carbon dioxide, water, and humus. Lactide is the cyclic dimer of lactic acid that exists as two optical isomers, d and l. The l-lactide is the naturally occurring isomer, and dl-lactide is the synthetic blend of d-lactide and l-lactide. The homopolymer

of L-lactide(LPLA) semicrystalline polymer. These types of materials exhibit high tensile strength, low elongation, and consequently high modulus that make them more suitable for load-bearing applications such as in orthopedic fixation and sutures. d,l-lactide (DLPLA) is amorphous polymer, exhibiting a random distribution of both isomeric forms of lactic acid, and accordingly is unable to arrange into an organized crystalline structure. This material has lower tensile strength, high elongation, and a much more rapid degradation time, making it more attractive as a drug delivery system. Standard-grade PLA has high modulus (3 GPa) and strength (50-70 MPa) comparable to that of many petrochemical-based polymers but its low toughness and physical aging present problems for its applications in medical devices and consumer products. Poly(L-lactide) about 37% crystalline, with a melting point of 175-178°C and a glass-transition temperatures of 60-65°C. The degradation time of LPLA is much slower than that of DLPLA. PLA is fully biodegradable when composted in a large-scale operation with temperatures of 60 °C and above. The first stage of degradation of PLA(two weeks) is via hydrolysis to water soluble compounds and lactic acid. Rapid metabolisation of these products into CO<sub>2</sub>, water and biomass by a variety of microorganisms occurs after hydrolysis. PLA does not biodegrade readily at temperatures less than 60 °C due to its glass transition temperature being close to 60 °C. Biodegradable polyester family is showed in Figure 2.4. Characteristic of PLA is ester linkages which are sensitive to both chemical hydrolysis and enzymatic chain cleavage. A number of companies produce PLA, such as Cargill Dow LLC. PLA produced by Cargill Dow originally sold under the name EcoPLA, but now is known as NatureWorks PLA, which is actually a family of PLA polymers that can be used alone or blended with other natural-based polymer. The applications for PLA are thermoformed products such as drink cups, take-away food trays, containers and planter boxes. The material has good rigidity characteristics, allowing it to replace polystyrene and PET in some application [10,11].



PHA - polyhydroxyalkanoates

PHB – polyhydroxybutyrate

PHH - polyhydroxyhexanoate

PHV - polyhydroxyvalerate

PLA - polylactic acid

PCL - polycaprolactone

PBS - polybutylene succinate

PBSA - polybutylene succinate adipate

AAC - Aliphatic-Aromatic copolyesters

PET - polyethylene terephthalate

PBAT - polybutylene adipate/terephthalate

PTMAT- polymethylene adipate/terephthalate

Figure 2.4 Biodegradable polyester families[11]

## 2.6 Poly (butylenes adipate-co-terephthalate) (PBAT) properties

Poly (butylenes adipate-co-terephthalate) (PBAT) is an aliphatic-aromatic copolyester (AAC) which has chemical structure in Figure 2.5.

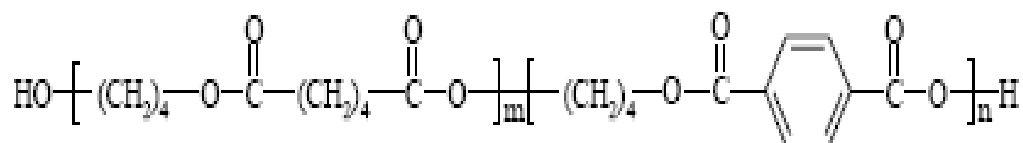


Figure 2.5 Chemical structure of poly (butylenes adipate-co-terephthalate) (PBAT)

AAC is synthetic copolyester obtained from fossil resources and known to be fully biodegradable. It is fully biodegrades to carbon dioxide, water and biomass. Typically, in an active microbial environment the polymer becomes invisible to the naked eye within 12 weeks. The extent and rate of biodegradation, apart from the inherent biodegradability of the polymer itself, depends on several environmental factors such as moisture, temperature, surface area and the manufacturing method of the finished product. To improve the use properties of aliphatic polyester, an attempt was made to combine the biodegradability of aliphatic polyesters with the good material performance of aromatic polyesters in novel aliphatic-aromatic copolyesters (AAC). AAC produced from 1,4-butanediol, terephthalic acid and adipic acid exhibit acceptable thermal and mechanical properties for the appropriate ratios of aliphatic and aromatic acids. This class of biodegradable plastics is seen by many to be the answer to making fully biodegradable plastics with property profiles similar to those of commodity polymers such as polyethylene. To reduce cost AACs are often blended with thermoplastics. Although AACs have obvious benefits, their market potential may be affected by legislation, such as that in Germany, which distinguishes between biodegradable plastics made from renewable resources and those, like AAC, which use basically the same raw materials as commodity plastics and petrochemicals. Currently in Germany, biodegradable plastics must contain greater than 50% renewable resources to be accepted. Commercially available aromatic copolyesters are given in Table 2.1 [11,12].

Table 2.1 Commercially available aromatic copolyesters

Tradename	Supplier	Origin	Website
Biomax R® Poly(butylene succinate terephthalate)PBST	DuPont	USA	www.dupont.com
Eastar Bio ® Poly (butylene adipate terephthalate) PBAT	Eastman Chemicals	Japan	www.castman.com
Ecoflex ® Poly(butylenc adipate terephthalate) PBAT	BASF	Germany	www.basf.com



## 2.7 Polymer Composites

Modification of organic polymers through the incorporation of additives yields, with few exceptions, multiphase systems containing the additive embedded in a continuous polymeric matrix. The resulting mixtures are characterized by unique microstructures or macrostructures that are responsible for their properties. The primary reasons for using additives are:

- property modification or enhancement;
- overall cost reduction;
- improving and controlling of processing characteristics.

Important types of modified polymer systems include polymer composites, polymer-polymer blends, and polymeric foams.

### 2.7.1 Types and Components of Polymer Composites

Polymer composites are mixtures of polymers with inorganic or organic additives having certain geometries (fibers, flakes, spheres, particulates). Thus, they consist of two or more components and two or more phases. The additives may be continuous, e.g. long fibers or ribbons; these are embedded in the polymer in regular geometric arrangements that extend throughout the dimensions of the product as high performance polymer composites, familiar examples are the well-known fiber-based thermoset laminates. On the other hand, the additives may be discontinuous (short), as, for example, short fibers (say <3cm in length), flakes, platelets, spheres or irregulars; these are dispersed throughout the continuous matrix. Such systems are usually based on a thermoplastic matrix as lower performance polymer composites compared to their counterparts with continuous additives.

Additives for polymer composites have been variously classified as reinforcements, fillers or reinforcing fillers. Reinforcements, being much stiffer and stronger than the polymer, usually increase its modulus and strength. Thus, mechanical property modification may be considered as their primary function, although their presence may significantly affect thermal expansion, transparency, thermal stability, etc.

The term reinforcement will be mostly used for long, continuous fibers or ribbons, whereas the terms filler, performance filler or functional filler will mostly refer to short, discontinuous fibers, flakes, platelets or particulates.

In general, parameters affecting the properties of polymer composites, whether continuous or discontinuous, include:

- the properties of the additives (inherent properties, size, shape);
- composition;
- the interaction of components at the phase boundaries, which is also associated with the existence of a thick interface, known also as the interphase; this is often considered as a separate phase, controlling adhesion between the components;
- the method of fabrication;
- the concentration and inherent properties of the additive, as well as its interaction with the matrix, are important parameters controlling the processability of the composite.

### 2.7.2 Effects of Fillers/Reinforcements-Functions

Traditionally, fillers were considered as additives, which, due to their unfavorable geometrical features, surface area or surface chemical composition, could only moderately increase the modulus of the polymer, while strength ( tensile, flexural) remained unchanged or even decreased. Their major contribution was in lowering the cost of materials by replacing the more expensive polymer; other possible economic advantages were faster molding cycles as result of increased thermal conductivity and fewer rejected parts due to warpage. Depending on the type of filler, other polymer properties could be affected; for example, melt viscosity could be significantly increased through the incorporation of fibrous materials. On the other hand, mold shrinkage and thermal expansion would be reduced, a common effect of most inorganic fillers.

The term reinforcing filler has been coined to describe discontinuous additives, the form, shape, and/or surface chemistry of which have been suitably modified with the objective of improving the mechanical properties of the polymer, particularly strength.

Inorganic reinforcing fillers are stiffer than the matrix and deform less, causing an overall reduction in the matrix strain, especially in the vicinity of the particle as a result of the particle/matrix interface. Reinforcing fillers are characterized by relatively high aspect ratio,  $\alpha$ , defined as the ratio of length to diameter for a fiber, or the ratio of diameter to thickness for platelets and flakes. For spheres, which have minimal reinforcing capacity, the aspect ratio is unity. A useful parameter for characterizing the effectiveness of a filler is the ratio of its surface area,  $A$ , to its volume,  $V$ , which needs to be as high as possible for effective reinforcement in Figure 2.6.

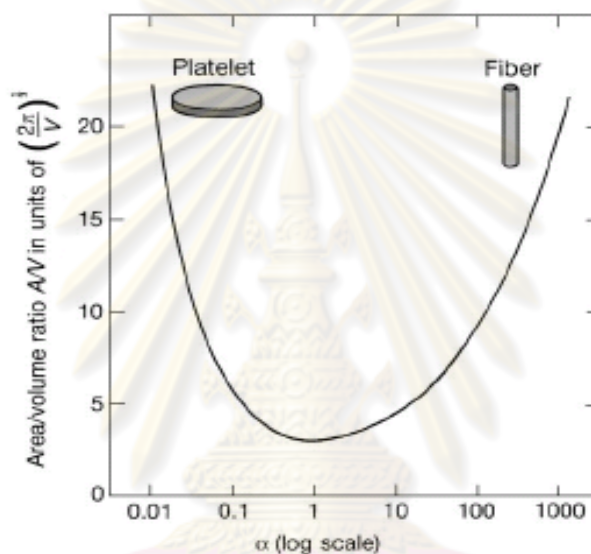


Figure 2.6 Surface area-to-volume ratio,  $A/V$ , of a cylindrical particle plotted versus aspect ratio (maximizing  $A/V$  and particle-matrix interaction through the interface requires  $\alpha \gg 1$  for fibers and  $1/\alpha \ll 1$  for platelets).

### 2.7.3 Functional Fillers

The term filler is very broad and encompasses a very wide range of materials. In this paper, fillers are defined as variety of solid particulate materials (inorganic, organic) that may be irregular, acicular, fibrous or plate-like in shape and which are used in reasonably large volume loadings in plastics. Pigments and elastomeric matrices are not normally included in this definition.

There is significant diversity in the chemical structures, forms, shapes, sizes, and inherent properties of the various inorganic and organic compounds that are used as

fillers. They are usually rigid materials, immiscible with the matrix in both the molten and solid states, and, as such, form distinct dispersed morphologies. Their common characteristic is that they are used at relatively high concentrations (>5% by volume), although some surface modifiers and processing aid are used at lower concentrations. Fillers may be classified as inorganic or organic substances, and further subdivided according to chemical family (Table 2.2) or according to their shape and size or aspect ratio (Table 2.3). More than 70 types of particulates or flakes and more than 15 types of fibers of natural or synthetic origin are reported that have been used or evaluated as fillers in thermoplastic and thermoset. The most commonly used particulate fillers are industrial minerals such as talc, calcium carbonate, mica, kaolin, wollastonite, feldspar, and barite.

Table 2.2 Chemical families of fillers for plastics

Chemical Family	Examples
<i>Inorganics</i>	
Oxides	Glass (fibers, spheres, flakes), MgO, SiO <sub>2</sub> , Sb <sub>2</sub> O <sub>3</sub> , Al <sub>2</sub> O <sub>3</sub>
Hydroxides	Al(OH) <sub>3</sub> , Mg(OH) <sub>2</sub>
Salts	CaCO <sub>3</sub> , BaSO <sub>4</sub> , CaSO <sub>4</sub> , phosphates
Silicates	Talc, mica, kaolin, wollastonite, montmorillonite, nanoclays, asbestos
Metals	Boron, steel
<i>Organics</i>	
Carbon, graphite	Carbon fibers, graphite fibers and flakes, carbon nanotubes, carbon black
Natural polymers	Cellulose fibers, wood flour and fibers, starch
Synthetic polymers	Polyamide, polyester, aramid, polyvinyl alcohol fibers

Table 2.3 Particle morphology of fillers

Shape	Aspect ratio	Examples
Cube	1	Calcite
Sphere	1	Glass spheres
Block	1-4	Quartz, calcite, silica, barite
Plate	4-30	Kaolin, talc, hydrous alumina
Flake	50-200++	Mica, graphite, montmorillonite nanoclays
Fiber	20-200++	Wollastonite, glass fibers, carbon nanotubes, wood fibers, asbestos fibers, carbon fibers

A more convenient scheme, first proposed for plastics additives, is to classify fillers according to their specific function, such as their ability to modify mechanical, electrical or thermal properties, flame retardancy, processing characteristics, solvent permeability, or simply formation costs. Fillers, however, are multifunctional and may be characterized by a primary function and a plethora of additional functions (Table 2.4). The scheme adopted involves classification of fillers according to five primary functions, as follows[13] :

- mechanical property modifiers (and further subdivision according to aspect ratio);
- fire retardants;
- electrical and magnetic property modifiers;
- surface property modifiers;
- processing aids.

Additional functions may include degradability enhancement, barrier characteristics, anti-aging characteristics, bioactivity, radiation absorption, warpage minimization, etc. Such attributes will be identified in subsequent sections of this paper.



Table 2.4 Fillers and their functions

Primary Function	Examples of Fillers	Additional Functions	Examples of Fillers
Modification of mechanical properties	High aspect ratio: Glass fibers, mica, nano-clays, carbon nanotubes, carbon / graphite fibers, aramid / synthetic / natural fibers Low aspect ratio: talc, CaCO <sub>3</sub> , kaolin, wood flour, wollastonite, glass spheres	Control of permeability	Reduced permeability : impermeable plate-like fillers: mica, talc, nanoclays, glass flakes Enhanced permeability: CaCO <sub>3</sub> dispersed polymers
Enhancement of fire retardancy	Hydrated fillers: Al(OH) <sub>3</sub> , Mg(OH) <sub>2</sub>	Bioactivity	Bone regeneration: hydroxyapatite, tricalcium phosphate, silicate glass
Modification of electrical and magnetic properties	Conductive, non-conductive, ferromagnetic metals, carbon fibers, carbon black, mica	Degradability	Organic fillers, starch, cellulose
Modification of surface properties	Antiblock, lubricating silica, CaCO <sub>3</sub> , PTFE, MoS <sub>2</sub> , graphite	Radiation absorption	Metal particles, lead oxide
Enhancement of processability	Colloidal silica, bentonite, hydrotalcite	Improved dimensional stability	Particulate fillers, mica
		Modification of optical properties	Nucleators, clarifiers, mica hybrids
		Control of damping	Flake fillers, glass, BaSO <sub>4</sub>

## 2.8 Fillers and their Functions

### 2.8.1 Silica

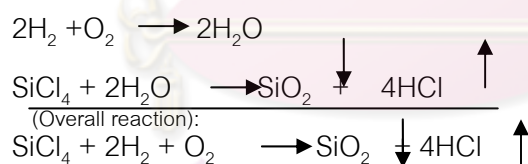
The term silica is used for the compound silicon dioxide,  $\text{SiO}_2$ , which has several crystalline forms as well as amorphous forms, which may be hydrated or hydroxylated. It is the chemical inertness and durability of silica that has made it very popular in many applications.

Natural silicas can be divided into crystalline and amorphous. Crystalline varieties include sands, ground silica (silica flour), and a form of quartz-Tripoli. The amorphous types used as anti-blocks include diatomaceous earth (DE) or diatomite. The natural grades are uncalcinated powders classified according to particle size distribution. During the calcinations process, the moisture (~40% in DE) is also removed due to the high process temperature, which may also cause sintering of DE particles to clusters.

Amorphous synthetic silicas are produced by two different processes: pyrogenic or thermal (generally referred to as fumed silica grades) and the wet process (known as precipitated or particulated silica).

#### 2.8.1.1 Fumed silica

Fumed silica, or fumed silicon dioxide, is produced by the vapor-phase hydrolysis of silicon tetrachloride in an  $\text{H}_2/\text{O}_2$  flame. The reaction are:



Hydrophilic fumed silica bearing hydroxyl groups on its surface is produced by this process. Hydrophobic fumed silica is made by processing fumed hydrophilic silica through in-line hydrophobic treatments, such as with silanes, siloxanes, silazanes. etc. Examples of different types of hydrophobic fumed silica coatings include DMDS (dimethyldichlorosilane), TMOS (trimethoxyoctylsilane), and HMDS (hexamethyldisilazane).

Fumed silica (silicon dioxide) is generally regarded as a unique material because of its unusual particle characteristics, enormous surface area, and high purity. It is a fine, white, and extremely fluffy powder. When added to liquids or polymers with which its refractive index (1.46) is a close match, it appears colorless or clear. Unlike

crystalline silicas, amorphous fumed silica is safe to handle, thus eliminating the serious health problems associated with crystalline silica dust. Its high surface area, ranging from 130-380 m<sup>2</sup>g<sup>-1</sup>, affects dispersibility, rheology control, thixotropic behavior, and reinforcement efficiency. The higher the surface area, the more the rheological control and thixotropic behavior increases, and the greater the potential for reinforcement. However, dispersion becomes more difficult.

Both hydrophilic and hydrophobic silicas are used in solvent-borne coatings to improve rheological properties, and as flow control agents and anti-setting additives for pigments. Fumed silica is a weak acid, bearing hydroxyl groups on its surface. The thickening mechanism of liquid coating systems can be explained in terms of hydrogen-bond formation between neighboring aggregates of silica, leading to the formation of a regular network. Some of these hydrogen bonds may be broken under shear forces, resulting in reduced viscosity. Usually, fumed silica contains 0.5-2.5% moisture, which not only aids the thickening process, but also facilitates curing of some polyurethane pre-polymer systems. Fumed silica is a thixotropic additive, which, when dispersed into epoxy or polyester resins, increases viscosity, imparts thixotropic behavior, and adds anti-settling characteristics during the potlife of the resins. Beside its principal use in coating/paint systems, fumed silica may also be used in thermoplastics. The melt viscosity of poly (ethylene 2, 6-naphthalate) (PEN) was reported to be decreased following the incorporation of small amounts of fumed silica nanoparticles. Additional effects on mechanical properties and crystallization behavior obtained by using untreated and surface-treated silica are reported in literature reviewed. In addition to their function as rheology modifiers, silica particles, colloidal or fumed, and clays are among the most widely studied inorganic fillers for improving the scratch/abrasion resistance of transparent coatings. These fillers are attractive from the standpoint that they do not adversely impact the transparency of coatings due to the fact that the refractive indices of the particles closely match those of most resin-based coatings. The drawback of silica-based fillers is that high concentrations of the particles are generally required to show a significant improvement in the scratch/abrasion resistance of a

coating, and these high loadings can lead to various other formulation problems associated with viscosity, thixotropy, and film formation.

### 2.8.1.2 Reactivity of Silanes toward the Filler

Surface modification of fillers with silanes may generate the following performance benefits:

- improved dimensional stability
- modified surface characteristics (water repellency or hydrophobicity)
- improved wet-out between resin and filler
- decreased water-vapor transmission
- controlled rheological properties (higher loadings with no viscosity increase)
- improved filler dispersion (no filler agglomerates)
- improved mechanical properties and high retention under adverse conditions
- improved electrical properties

Common silanes have the general formulae  $Y-(CH_2)_3Si(X)_3$  (Figure 2.7) and  $Y-(CH_2)_2Si(CH_3)(X)_2$ . The silicon function group X is a hydrolyzable group chosen to react with surface hydroxyl groups of the filler to produce a stable bond, and is usually halogen or alkoxy. The organofunctional group Y is tightly bound to the silicon via a short carbon chain and links with polymer. This group has to ensure maximum compatibility with the resin system. Bonding to the polymer takes place by chemical reactions or physicochemical interactions such as hydrogen bonding, acid-base interaction, interpenetration of the polymer network (entanglement), or electrostatic attraction. The group Y may be non-functional or functional (reactive); examples of the latter are vinyl, amino, methacry, epoxy, mercapto, etc. Most silanes are colorless or slightly yellowish, low viscosity liquids. Both the non-functional and functional organosilanes discussed below are employed in important commercial filler treatments.

Organosilanes rely on the reaction with surface hydroxyl groups to produce a stable covalent bond and stable layer on the filler surface. Thus, they are most effective on fillers with high concentrations of reactive hydroxyls and a sufficient amount of residual surface water. Silica, silicates (including glass), oxides, and hydroxides are





### 2.8.2 Calcium Carbonate

Calcium carbonate is the most common deposit formed in sedimentary rocks. Natural  $\text{CaCO}_3$  used as a filler in plastics is produced from chalk, limestone or marble found in the upper layers of the Earth's crust to a depth of about 15 km. Chalk is a soft textured, microcrystalline sedimentary rock formed from marine microfossils. Limestone is also of biological origin but it is harder and denser than chalk, having been compacted by various geological processes. Marble is even harder, having being subjected to metamorphosis under high pressures and temperatures, which resulted in recrystallization with the separation of impurities in the form of veins.

The sedimentary rocks consisting mainly of calcite crystals are processed by standard mining procedures and then subjected to grinding and classification. In addition to natural ground calcium carbonate (GCC), there also exists a chemically produced from known as precipitated calcium carbonate (PCC), which may be finer and of higher purity, but also more expensive than the natural one.

Calcium carbonate is an abundant, largely inert, low cost, white filler with cubic, block-shaped or irregular particles of very low aspect ratio. Its use yields a cost reduction in a variety of thermoplastics and thermosets, and it can have moderate effects on mechanical properties. In terms of its primary function as a mechanical property improver, its advantages in thermoplastics are slightly increased modulus and often an increase in impact strength. These benefits are accompanied by shrinkage reduction and improved surface finish. In terms of secondary functions, calcium carbonate may act as a surface property modifier, as a processing aid, and as stress concentrator by introducing porosity in stretched films. These functions may be enhanced or modified by the application of suitable surface treatment agents, such as stearates or titanates.

Calcium carbonate occurs in different crystalline forms. The most widespread is calcite, which has either a trigonal-rhombohedral or a trigonal-scalenohedral crystal lattice. The fundamental properties are  $2.7 \text{ g/cm}^3$  of density, 3 Mohs of hardness and 0.0013 g/100mL of water solubility. Another form is the orthorhombic aragonite, which is less stable and can be converted to calcite by heating. Vaterite, a third form, is unstable

and over time will transform into the other two forms. Aragonite has a higher density (2.8-2.9 g/cm<sup>3</sup>), a higher single refractive index (1.7), and a somewhat higher Mohs hardness (3.5-4) than calcite. Its other properties are very similar. Both minerals are white and their refractive indices are not high enough to interface with effective coloration. Commercial GCC grades, wet or dry ground, contain 94-99% CaCO<sub>3</sub>, MgCO<sub>3</sub> as the major impurity, and minor quantities of alumina, iron oxide, silica or manganese oxide. PCC may contain 98-99% CaCO<sub>3</sub>, or even higher concentrations for pharmaceutical grades.

The primary function of calcium carbonate as a filler is to lower costs, while having moderate effects on mechanical properties. However, depending on the particular polymer system, it may also be considered as a multifunctional filler with a variety of specific effects on rheology, processing, and morphology. In any case, the introduction of surface-treated calcium carbonate and of ultrafine grades has undoubtedly led to the development of new applications. The majority of calcium carbonate applications (about 80%) are in polyvinyl chloride, PVA (flexible, plastisols, rigid), and thermosets, primarily fiber glass reinforced unsaturated polyester, UP. The remaining 20% are in polyolefins (primarily injection-molded parts and films), EDPM, polyurethane, polyamide, rubber, ABS, etc. As one of the oldest commodity fillers, a significant amount of technical information has been published on its uses in plastics over the years [13-14].

## 2.9 Nanoparticles in Materials Chemistry and in the Natural Sciences

The major discoveries of the twentieth century can be mainly related to nuclear power engineering, space exploration, development of nanomaterials, semiconducting and microprocessor-based technology. All sciences have made fundamental contributions to the breakthrough in science. Speaking in support of nanomaterials it can be said that the nanoworld is extremely broad and it is practically impossible to find any field in the natural sciences that is not in some way or another connected with nanostructures. Terms such as nanophase, nanohybrid, nanocrystalline and nanoporous materials, nanochemistry, nanophysics, nanostructures, nanocrystals,

nanophase geometry, nanosize hierarchy and architecture, nanostructured organic networks, molecular and nano-level design and finally nanotechnology are most frequently cited currently in the scientific literature as applied to small-scale and small-dimensional phenomena. A peculiar place is occupied in nanochemistry by the particles participating in various biological processes, including supramolecular functional systems to which belong enzymes, liposomes and cells. Fullerenes and nanotubes relate to this group too. These materials are used in chemistry in a number of new reactions, catalytic and sensor systems, fabrication of new compounds and nanocomposites with previously unknown properties. In physics they constitute some of the materials for microelectronics, structures with nanogeometry for information recording systems and are used to transform various natural radiations. In biology and medicine they are being used as novel medicinal preparations and carriers of these preparations to human organs. The relationship between materials science and the natural sciences becomes more and more evident (Fig. 2.9 illustrates size correlation).

The assertions that science and engineering in the twenty-first century will acquire a nano and angstrom character are becoming a reality. In traditional technologies the limits of miniaturization of separate elements (e.g. density of arranging crystals in microelectronics) have already been attained. This motivates the search for some alternative procedures. Fabrication of modern chips is based on so-called planar techniques, being a combination of nanolithography (formation of surface drawings as lines and dots at the nanolevel) and etching. To reduce their size still more new recently developed lithographic procedures are used, particularly electronic, ion-beam and X-ray methods and dry etching, including plasma-chemical, reactive, ionic, etc. These techniques reach below the 100nm size of elements in optoelectronic chips. The part of materials science that studies nanophases differs from the traditional area by not only the creation of new materials but also by the necessity of designing corresponding instruments for manipulating such materials. Among the most promising nanotechnologies of metal materials and their

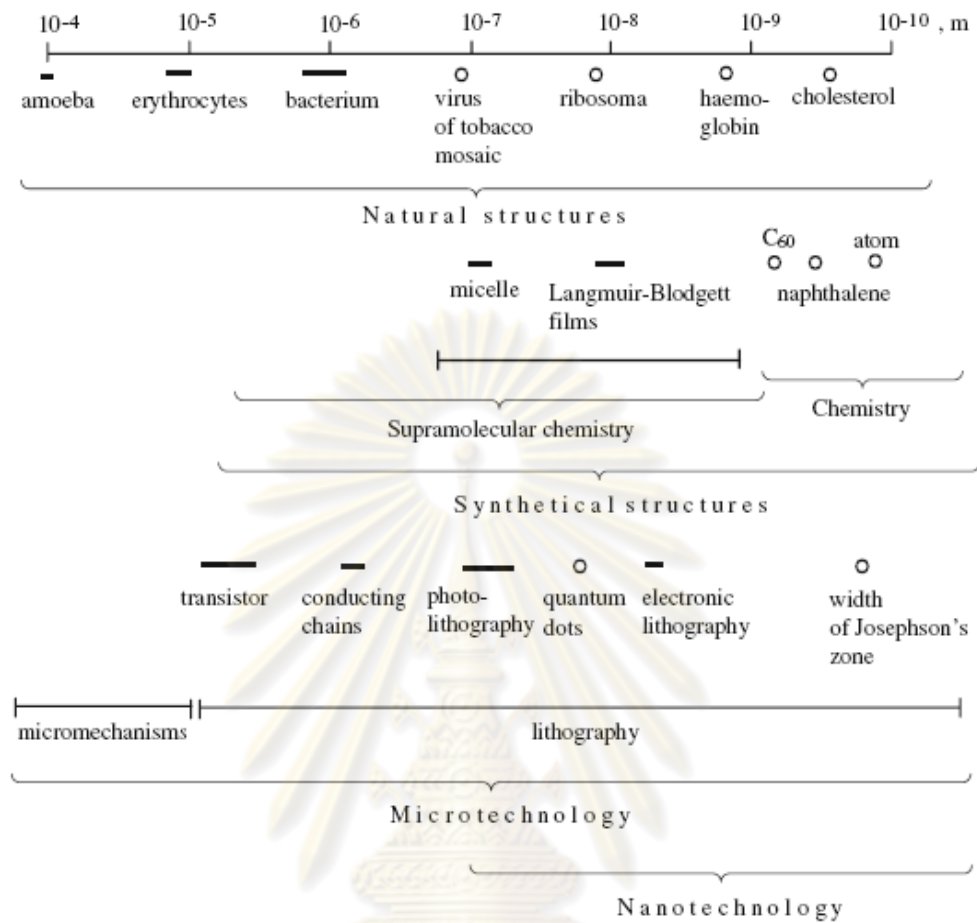


Figure 2.9 Size correlation between synthetic and natural structures [16]

### 2.9.1 Classification of Nanoparticles by Size

Ultradispersed particles can be subdivided by size into three types : nanosize or ultradispersed to about 1–(30–50)nm particles, highly dispersed of size (30–50)–(100–50)nm and micron size particles – flocculi of 100–1000nm. The later rule of individual particles or their agglomerates represent either mono or polycrystals of fractal type. The first two types of particles are colloidal and the latter are coarse dispersed ones. Aerosol particles of metals (~50nm) prepared in normal conditions are spherical or nearly spherical due to the high surface energy of fine particles. The most frequently used terms are *ultrasmall particles* and *nanocrystals* to denote nanoparticles of metals with diameter from 2–5 to 50 nm, as well as colloidal crystallites and subcolloidal particles. The upper threshold of the size of semiconducting nanocrystals in polymer

matrices is the condition which gives the optical homogeneity of compositions (no scattering by the environment at particle size below a quarter of the wavelength of light). The lower boundary is conditioned by the existence of crystalline particles at the interface between the crystalline phase and the quasi-molecular phase. The terms *molecular aggregation* and *crystallite clusters* are used less often.

There are two types of nanoparticles:

1. Clusters of 1–10 nm, the particles of an ordered structure possessing commonly 38–40 atom, and sometimes more, metallic atoms (e.g. Au<sub>55</sub>, Pt<sub>309</sub>, a family of palladium clusters consisting of 500–2000 atoms).
2. Nanoparticles with diameter 10–50 nm and consisting of 10<sup>3</sup>–10<sup>6</sup> atoms. Nanoparticles are also classified by the number,  $N$ , of atoms they consist of. Clusters are subdivided into very small, small and large. Table 2.5 shows the diameter,  $2R$ , for corresponding Na atoms and the relation of  $N_s$  to  $N_v$  atoms. The surface and the bulk appear to be inseparable for very small nanoparticles. For nanoparticles containing 3000 metallic atoms the relation  $N_s/N_v \approx 20\%$  is true, whereas compact metallic particles ( $N_s/N_v \rightarrow 1$ ) are reached only at  $N \rightarrow 10^5$ . Hence, particles can be subdivided by their size into the following four groups (domains):

I – molecular clusters ( $N \leq 10$ );

II – clusters of a solid body ( $10^2 \leq N \leq 10^3$ );

III – microcrystals ( $10^3 \leq N \leq 10^4$ );

IV – particles of dense substances ( $N > 10^5$ ).



Table 2.5 Classification of nanoparticles and clusters by size

Very small	Small	Large
$2 < N \leq 20$	$20 < N \leq 500$	$500 < N \leq 10^7$
$2R_{Na} \leq 1.1 \text{ nm}$	$1.1 \text{ nm} \leq 2R_{Na} \leq 3.3 \text{ nm}$	$3.3 \text{ nm} \leq 2R_{Na} \leq 100 \text{ nm}$
Surface and inner volume are inseparable	$0.9 \geq N_s/N_v \geq 0.5$	$0.5 \geq N_s/N_v$

In Figure 2.10, illustrates the main stages of how an individual atom transforms into a bulk metal through a cluster, nanosize and colloidal particles (active metals).

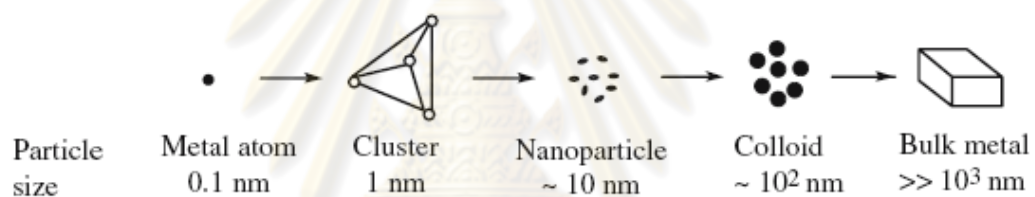


Figure 2.10 The main stages of the transformation metal atoms into a bulk metal[14]

### 2.9.2 Nanoparticle Modifying Action on Polymers

At present a standard way to get the necessary properties or to modify polymer composites is to introduce some substances (pigments, inhibitors, antioxidants, plasticizers, fillers), but the required concentrations are often so great that they considerably change (the whole complex of the material characteristics). The mechanical properties tend to be improved with a general increase of the filler volume. The filler particles are traditionally classified into three broad categories based on their size: macrofillers (~5-50  $\mu\text{m}$ ), microfillers or nanofillers (~0.01-0.1 $\mu\text{m}$ ) and physical hybrids (physical mixture of macro- and microfillers). The decrease of the filler sizes usually reduces the stress concentration, maintains a smooth sample surface, and extends the durability of the composites. However, the smaller the particles are, the more difficult the polymer volume loading process is because of the increase of the

surface area limiting the wetting of small particles by resins and rising to the stress concentrations around the unwetted interfacial defects and filler particles aggregates. The usual result is the failure of composite materials.

Therefore one of the most actual problems of high-molecular compound science is to create systems able to recognize the outer influence or action at the molecular level and to give a corresponding response. Nanocomposites are a class of materials with a filler-induced increase of the characteristics. A change of the phase dimensions on the nanometer level leads to reinforcing of the material properties. Many research studies have been devoted to the influence of nanoscale (single or cluster) particles, mechanical and operational characteristics of the polymer. The influence is based on the particle potential ability to form an ionic or coordination cross-linking, which can limit molecular chains or mobility of the segments and also create cohesion and adhesion cross-linkings. That allows the production of materials with a new architecture, to improve considerably their properties relative to conventional nanocomposites due to maximizing the interfacial adhesion. Such improved properties can be attained in nanocomposites in which the various building blocks (nanoscale metal particles, silica, ceramic sheets like layered silicates) are dispersed in a polymer matrix [15-16].

#### **2.10 Determination of polymer/polymer miscibility**

There are several methods that can determine compatibility of polymer blends, each method has a limitation to determine the compatibility of polymer blends. Some techniques, such as calorimetry, thermomechanical, dynamic mechanical procedures, are based on the determination of the glass transition temperature;  $T_g$ . Other techniques are based on microscopic techniques [17].

#### **2.11 Polymer degradation**

The durability of polymeric material can be studied under several environmental and artificial conditions, which have been summarized in Figure 2.11.

Biodegradation [18] is an environmental degradation which takes place through the action of enzymes and / or chemical decomposition associated with living organisms (bacteria, fungi, etc.) or their secretion products. Microbiological deterioration can

achieved by exo- and endo-enzymes or by products secreted biochemically or chemically from these. Macroorganisms can also eat and, sometimes, digest polymers and give a mechanical, chemical or enzymatic ageing. There are many different degradation modes that in nature combine synergistically to degrade polymers. Biodegradation might be better used as term only when it is essential to distinguish clearly between the action of living organisms and other degradation modes (e.g. photolysis, oxidation, hydrolysis)

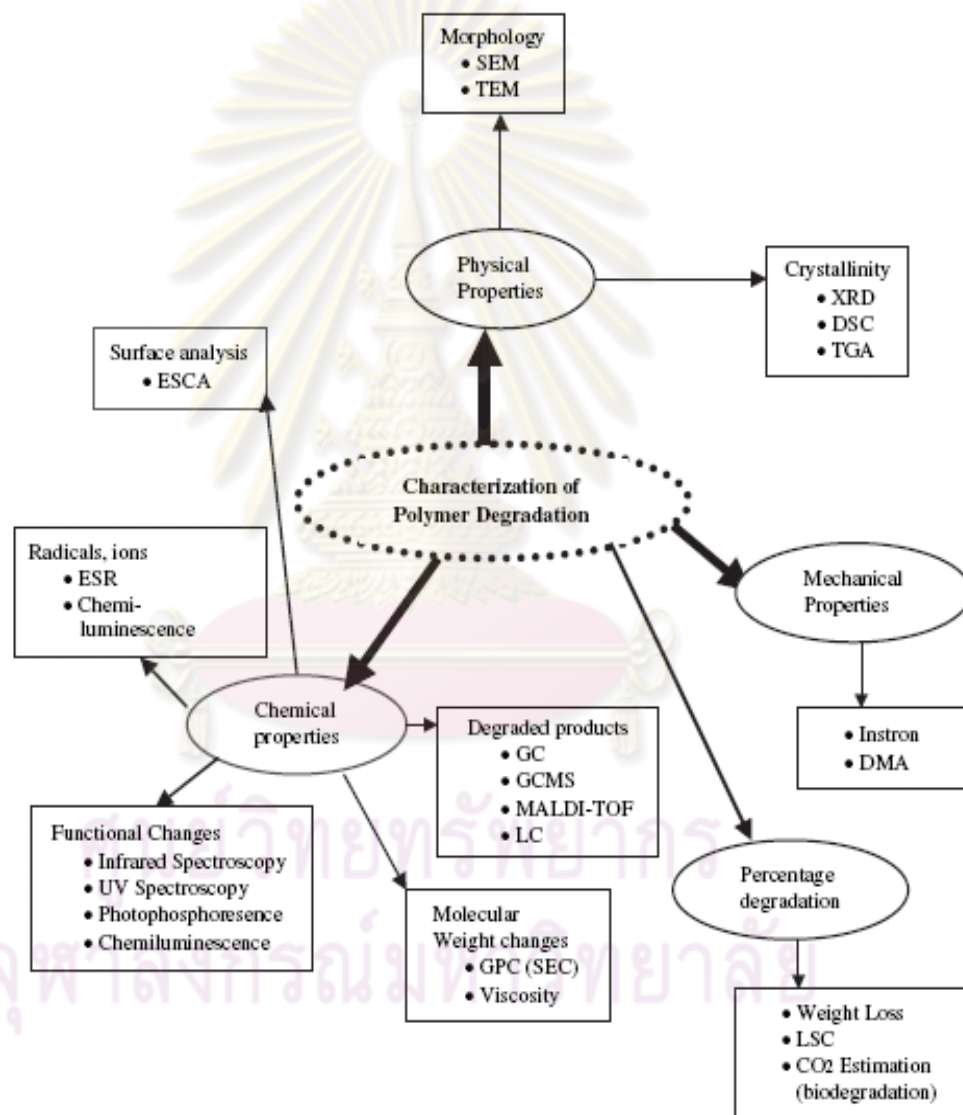


Figure 2.11 Different analytical techniques to analyze the polymer durability [19]

Table 2.6 Reaction catalyzed and reactive bonds of different classes of enzyme [20]

Enzyme class	Reaction catalyzed	Reactive bonds
1. Oxidoreductase	Redox reactions	<ul style="list-style-type: none"> <li>● C=O</li> <li>● C-NH<sub>2</sub></li> </ul>
2. Transferase	Transfer of functional group	<ul style="list-style-type: none"> <li>● One C-groups</li> <li>● Acetyl groups</li> <li>● Peptides</li> </ul>
3. Hydrolase	Hydrolysis	<ul style="list-style-type: none"> <li>● Esters</li> <li>● Peptides</li> </ul>
4. Lyase	Addition to double bonds	<ul style="list-style-type: none"> <li>● HC=CH</li> <li>● C=O</li> </ul>
5. Isomerase	Isomerisation	<ul style="list-style-type: none"> <li>● Racemases</li> </ul>
6. Ligase	Formation of new bonds using ATP	<ul style="list-style-type: none"> <li>● C-O</li> <li>● C-S</li> <li>● C-N</li> </ul>

Chemical structure of the substrate is critically important for any enzymatic attack and the creation of a new kind of enzyme which are summarized in Table 2.6. Enzymes are biological catalysts, with the same action as chemical catalysts, i.e. by lowering the activation energy they can induce or increase in reaction rates in an environment otherwise unfavorable for chemical reaction. A purely enzymatic degradation of a long straight olefin chain dependent on the enzymatic cleavage of the C-C bond should not be expected, since such an endoenzyme does not occur in nature. Oxidation is instead the critical initial step in the degradation of many rather inert organic molecules. Esters bond in PLA could be hydrolyzed by enzyme class of hydrolase and the hydrolysis reaction of PLA shows in Figure 2.12 [21].

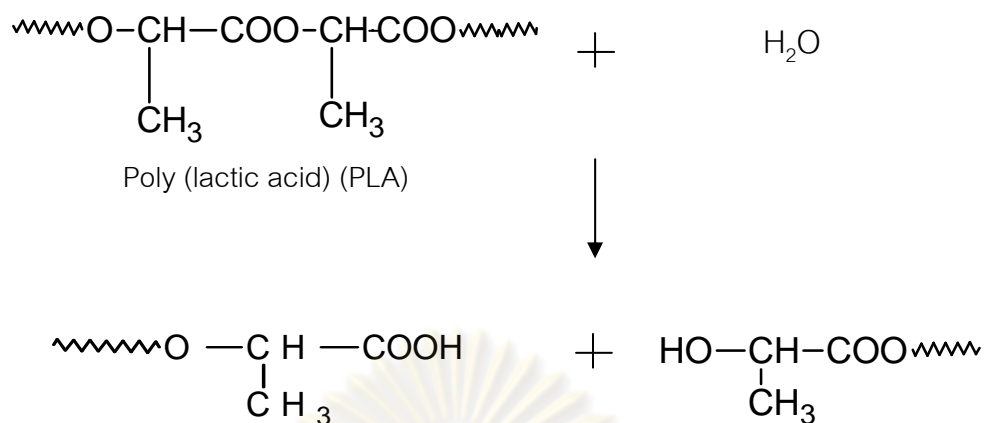


Figure 2.12 Hydrolysis reaction of PLA [21]

### 2.12 Literature review

Jiang *et al* [22] studied blends of PLA and PBAT with increased toughness while maintaining biodegradability. PLA and PBAT blends were prepared by mixing different percentages with the increase in PBAT content (5 – 20 wt %). The blend showed decreased tensile strength and modulus; however, elongation and toughness were dramatically increased. The impact strength of the blend was also significantly improved at 10 % or higher of PBAT addition. With the addition of PBAT, the failure mode changed from brittle fracture of the neat PLA to ductile fracture of the blend as demonstrated by tensile test and scanning electron microscopy (SEM) micrographs. Melt elasticity and viscosity of the blends increased with the concentration of PBAT. The blend comprised an immiscible, two-phase system with the PBAT evenly dispersed in the form of ~ 300 nm domains within the PLA matrix. The PBAT component accelerated the crystallization rate of PLA but had little effect on its final degree of crystallinity.

Xiong *et al* [23] studied the effect of nano-SiO<sub>2</sub> on physical and biodegradable properties of starch/PVA blended films. Starch/PVA film with nano-SiO<sub>2</sub> was compared with film without nano-SiO<sub>2</sub>. The result has shown that the mechanical properties, transmittance, and water resistance of a starch/PVA film were all improved significantly with the addition of nano-SiO<sub>2</sub>. The film's tensile strength, breaking elongation, and transmittance increased by 79.4%, 18%, and 15%, respectively, and the water absorption decreased by 70% while maintaining biodegradability. The permeation took



place for the small-size effect and quantum tunneling effect of nano-SiO<sub>2</sub>. It was easy to insert in polymer chains and destroy the ordered structure. The intermolecular hydrogen bond was formed in nano-SiO<sub>2</sub> and starch/PVA, and the strong chemical bond C-O-Si was also formed in nano-SiO<sub>2</sub>/starch/PVA hybrid materials. Therefore, the miscibility and compatibility were increased and an interpenetrating network structure was formed to prevent the water molecules from dissolving, which greatly increased the water resistance and mechanical properties of the film.

Hiljanen-Vainio *et al* [24] studied two lactic-acid-based poly (ester-urethanes) (PEUs: PEUa and PEUb), a linear and a branch, were reinforced through blending with several organic and inorganic fillers of different particle sizes and shapes such as talc, kaolin, silicate fillers and calcium carbonate with the purpose of studying the effects of the fillers on mechanical properties and morphology. In general, addition of particulate or fibrous filler increased the stiffness almost linearly with filler content, particularly at lower filler loadings. The most significant reinforcement was achieved with glass fibres, even though processing of the samples by compression moulding did not contribute to orientation. In addition, some blend compositions containing particulate silicate-type fillers showed improvement in tensile strength. This finding is probably explained by interactions like hydrogen bonding between the silicates and the hydroxyl end groups of PEU. DMTA did not show any significant changes in the glass transition temperature of the PEU, but further evidence of stiffening was obtained. In general, all fillers exhibited surprisingly good mixing and contact with the PEU matrix, even at relatively high concentrations. Despite the reinforcing effect of the fillers, the composites were still brittle, and further toughening or compatibilization is required.

Liu *et al* [25] studied the effect of nanokaolin and precipitated silica as the main reinforcing agents in filled styrene butadiene rubber (SBR), natural rubber (NR), butadiene rubber (BR) and ethylene-propylene diene methylene (EPDM) on the vulcanizing, mechanical, heat-resisting properties and microstructure of the corresponding rubber composites. The result has shown that nanokaolin/rubber composites have excellent elasticity. The tensile capability is close to that of rubber filled with precipitated silica, but the tear strength and modulus are inferior to that of

precipitated silica. In natural rubber, tensile strength of the composites filled with nanokaolin is considerably higher than that filled with precipitated silica. The low cost endows nanokaolin with wide applied potential. The suitable modification of nanokaolin can make kaolinite platelets dispersed in rubber matrix in directional parallel arrangements, with 20-50 nm in thickness. The tightly linked interface at the nanoscale range between the kaolin sheets and rubber molecules is the main reason for the improvements of mechanical properties and thermal stability.

Zhang et al [26] studied the effect of organically modified montmorillonite (MMT) clay and nano-sized precipitated calcium carbonate (NPCC) in filled polylactide (PLA) nanocomposites on physical and mechanical properties. The result has shown that the strain-at-break of PLA increased with NPCC concentration ranging from 0 to 7.5 wt%, whereas it only increased with MMT concentration up to 2.5 wt% and decreased at higher concentrations. The tensile strength of PLA nanocomposites decreased with NPCC, whereas it increased with MMT up to 5 wt%. All PLA/NPCC nanocomposites showed clear stress yielding on the stress-strain curves but without noted necking. For PLA/MMT nanocomposites, stress yielding was only noted for the PLA/2.5 wt% MMT composite with significant necking. The different reinforcing effects of these two nanoparticles could be mainly attributed to the differences in microstructures and interactions between the nanoparticles and PLA in the respective nanocomposites.

Elias et al [27] studied the effect of silica nanoparticles on the morphology and the rheological properties of an immiscible polymer blend (polypropylene/polystyrene). The result has shown that the rheological data obtained with the hydrophobic silica were more difficult to model since the existence of a thick interphase. The hypothesis that hydrophilic silica is homogeneously dispersed in PS droplets and that hydrophobic silica is dispersed in PP matrix was much closer to the actual situation. It can be then conclusion that stabilization mechanism of PP/PS blend by hydrophilic silica is the reduction in the interfacial tension whereas hydrophobic silica acts as a rigid layer preventing the coalescence of PS droplets.

## CHAPTER III

### EXPERIMENTAL

#### 3.1 Materials

##### 3.1.1 Poly (lactic acid) (PLA)

The commercial PLA (Natureworks PLA 2002D) in pellet form exhibits a density of  $1.26 \text{ g/cm}^3$ , having melt flow index (MFI) of 4-8 g/10min, exhibits a number average molecular weight of 120,000 g/mol and a glass transition temperature and melting point of 51 and  $150 \text{ }^\circ\text{C}$ , respectively.

##### 3.1.2 Poly (butylenes adipate-co-terephthalate) (PBAT)

The PBAT (Ecoflex F BX 7011, BASF Corp.) in pellet form exhibits a density of  $1.23 \text{ g/cm}^3$ , having melt flow index (MFI) of 2 g/10min, exhibits a number average molecular weight of 24,400 g/mol, and a glass transition temperature and melting point of  $-28$  and  $117 \text{ }^\circ\text{C}$ , respectively.

##### 3.1.3 Hydrophilic fumed silica ( $\text{SiO}_2$ ) nanoparticles

The hydrophilic fumed silica ( $\text{SiO}_2$ ) (AEROSIL 200) was supplied by Degussa. The silica particle is an average primary particle size of 12 nm. Its specific surface area is  $200 \pm 25 \text{ m}^2/\text{g}$ .

##### 3.1.4 Hydrophobic fumed silica ( $\text{mSiO}_2$ ) nanoparticles

The hydrophobic fumed silica ( $\text{SiO}_2$ ) (AEROSIL R972) was supplied by Degussa. The silica particle is an average primary particle size of 16 nm and treated with dimethyldichlorosilane (DDS). Its specific surface area is  $110 \pm 20 \text{ m}^2/\text{g}$ .

##### 3.1.5 Nano-sized precipitated calcium carbonate (NPCC)

The nano-sized precipitated calcium carbonate (NPCC) (FCC-600) was supplied by Chemmin Corporation (Thailand). It was coated with stearic acid for better

dispersion. The calcium carbonate particles are in cubic shape with an average primary particle size of 60 nm. Its specific surface area is 22 m<sup>2</sup>/g.

### 3.1.6 Proteinase K

Proteinase K from *Tritirachium album* in a lyophilized powder, from Invitrogen, has an enzymatic activity of not less than 20 units/mg protein. It is stable over a wide pH range (4-12.5), with optimal activity at pH 6.5-9.5.

### 3.1.7 Sodium azide (NaN<sub>3</sub>)

Sodium azide S2002, ReagentPlus<sup>®</sup> grade, was supplied by Sigma-Aldrich with 99.5% purity in a powder form. Molecular weight is 65.01 g/mole.

### 3.1.8 TRIS hydrochloride buffer

Tris(hydroxymethyl)aminomethane hydrochloride, (NH<sub>2</sub>C(CH<sub>2</sub>OH)<sub>3</sub>.HCl), that show chemical structure in Figure 3.1. It was supplied by Sigma-Aldrich in a powder form with purity >99%. Molecular weight is 157.6 g/mole.

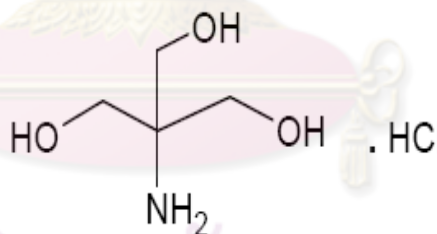


Figure 3.1 TRIS hydrochloride

## 3.2 Instruments and Apparatus

Instruments and apparatus used in this research are as follows:

1. Twin screw extruder (Model LTE-26-40, Lab Tech Engineering, Thailand)
2. Blown film extrusion (Model MGPB-30, Mach Group (1992), Thailand)
3. Compression molding (Model LP-S-50 E/W, Lab Tech Engineering, Thailand)
4. Differential Scanning Calorimeter  
(Model DSC1 Star<sup>®</sup> system, Mettler Toledo, Switzerland)

5. Dynamic Mechanical Analysis  
(Model Star<sup>®</sup> SW 9.20, Mettler Toledo, Switzerland)
6. Universal Testing Machine (Model H10K-T, Tinius Olsen, England)
7. Scanning Electron Microscope (Model JSM6480LV, JEOL, Japan)
8. Water Vapour Permeability Tester (Model WDDG, Brugger, Germany)
9. Dual-beam Spectrophotometer (Model Datacolor 650, Datacolor, USA)
10. Fourier Transform Infrared (FT-IR) spectroscopy  
(Model Tensor 37, Bruker, USA)
11. Analytical balance (Model XP 205, Mettler Toledo, Switzerland)
12. Vacuum oven (Model J-DV01, JISIO, Japan)
13. Incubator shaker (Model LSI-3016 A, Lab Tech, UK)

### 3.3 Polymer blend nanocomposites preparation

A twin-screw extruder was employed to compound PLA/PBAT/SiO<sub>2</sub>, PLA/PBAT/mSiO<sub>2</sub> and PLA/PBAT/NPCC polymer blend nanocomposites. The extruder had a screw diameter of 26 mm. and an  $L/D$  ratio of 40. The extruder had five controlled temperature zones which were set to range from 150 (next to the feeding segment) to 180 °C (die adaptor). The screw speed was maintained at 50 rpm for all runs. Before extrusion, PLA and PBAT resin were dried at 60 °C for 8 h, SiO<sub>2</sub>, mSiO<sub>2</sub> and NPCC were dried at 90 °C for 8 h in a vacuum oven in order to remove any trace of moisture to prevent potential hydrolytic degradation during the melt processing in the extruder. In general, the hydrolytic degradation reduces molecular weight of the biodegradable polymers which actually induces the decrease of mechanical properties. The mixture of PLA/PBAT and nanofillers was manually premixed by tumbling in a plastic zip-lock bag, and subsequently fed into the extruder for melt compounding. The extrudate was cooled in a water bath and subsequently granulated by a pelletizer. Polymer films (thickness 300 μm) and sheet (thickness 2 mm) were prepared by compression molding using a LP-S-50 P/W, ASTM melt press. Crushed blend samples were heated at 200 °C between Teflon sheets for 1 min, then pressure (5 MPa) was applied at 200 °C for 1 min and 1



min cooling. Biodegradable polymer blend/  $\text{SiO}_2$ ,  $\text{mSiO}_2$  and NPCC nanocomposite were prepared with various compositions as shown in Table 3.1.

Table 3.1: Compositions and sample code name of PLA/PBAT/ fumed silica and NPCC polymer blend nanocomposites

Sample code	PLA ( wt% )	PBAT ( wt% )	Nano-sized fumed silica (PHR)		NPCC (PHR)
			Hydrophilic	Hydrophobic	
PL100PB0	100	0	0	0	0
PL50PB50	50	50	0	0	0
PL40PB60	40	60	0	0	0
PL30PB70	30	70	0	0	0
PL0PB100	0	100	0	0	0
PL50PB50S1	50	50	1	0	0
PL50PB50S3	50	50	3	0	0
PL50PB50S6	50	50	6	0	0
PL50PB50MS1	50	50	0	1	0
PL50PB50MS3	50	50	0	3	0
PL50PB50MS6	50	50	0	6	0
PL50PB50C1	50	50	0	0	1
PL50PB50C3	50	50	0	0	3
PL50PB50C6	50	50	0	0	6

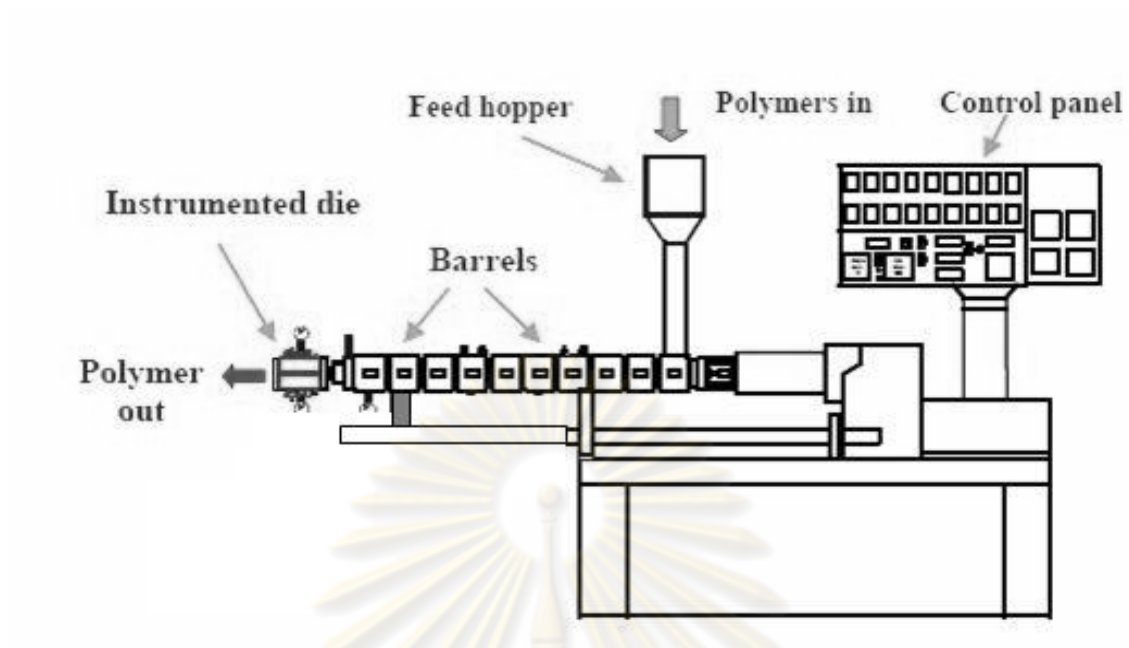


Figure 3.2 Twin screw extruder for blending

### 3.4 Thermal analysis

#### 3.4.1 DSC analysis

The thermal properties of PLA, PBAT and PLA/PBAT/SiO<sub>2</sub>, PLA/PBAT/mSiO<sub>2</sub> and PLA/PBAT/NPCC polymer blend nanocomposites were studied using DSC1 Star<sup>®</sup>. DSC measurements were performed on 5-15 mg samples. Samples of pellet form were heated from 30 to 220 °C at 10 °C/min (1<sup>st</sup> heating), cooled to -80 °C at the same scan rate (1<sup>st</sup> cooling), then heated again to 220 °C at 10 °C/min (2<sup>nd</sup> heating). DSC studies revealed the significant thermal properties and crystallization behavior of the samples, such as glass transition temperature ( $T_g$ ), cold crystallization temperature ( $T_c$ ), the heat of crystallization ( $\Delta H_c$ ), melting temperature ( $T_m$ ), and the heat of melting ( $\Delta H_m$ ).  $T_g$  were measured from inflection point in the second heating thermogram. Crystallization and melting enthalpies were evaluated from the integrated areas of melting peaks. Aluminium was used as calibration standards. DSC feature is shown in Figure 3.3.

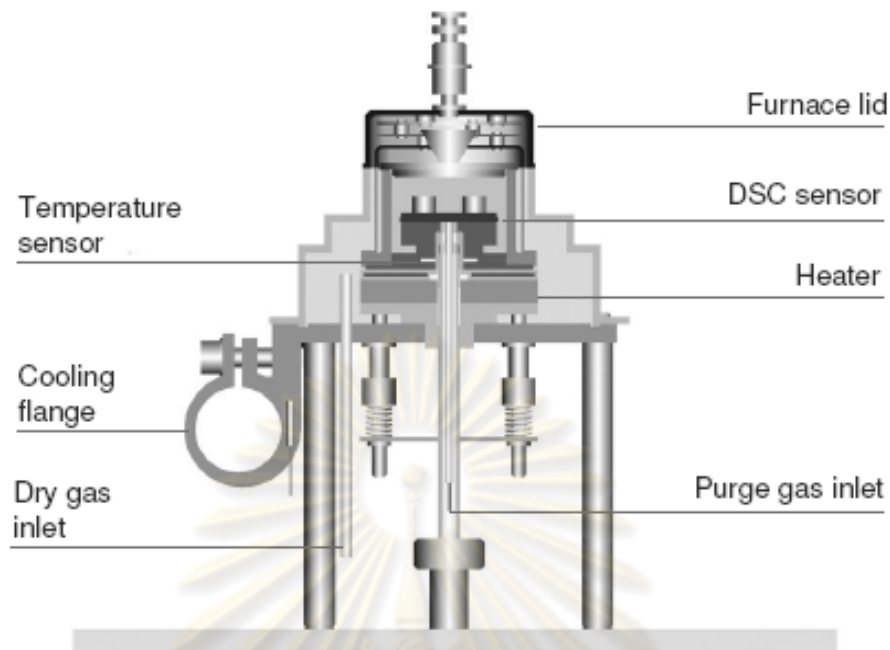


Figure 3.3 Typical DSC: Differential Scanning Calorimeter

#### 3.4.2 DMA analysis

The thermal properties of PLA, PBAT and PLA/PBAT/SiO<sub>2</sub>, PLA/PBAT/mSiO<sub>2</sub> and PLA/PBAT/NPCC polymer blend nanocomposites were studied using DMA Star<sup>®</sup> SW 9.20. The samples used for DMA analysis were prepared by compression molding at 200 °C into thick sheet. Specimens (4 x 2 x 45 mm<sup>3</sup>) were cut from the sheet, vibrated in extension mode at a frequency of 1 Hz and temperature ramp from -60 to 100 °C.

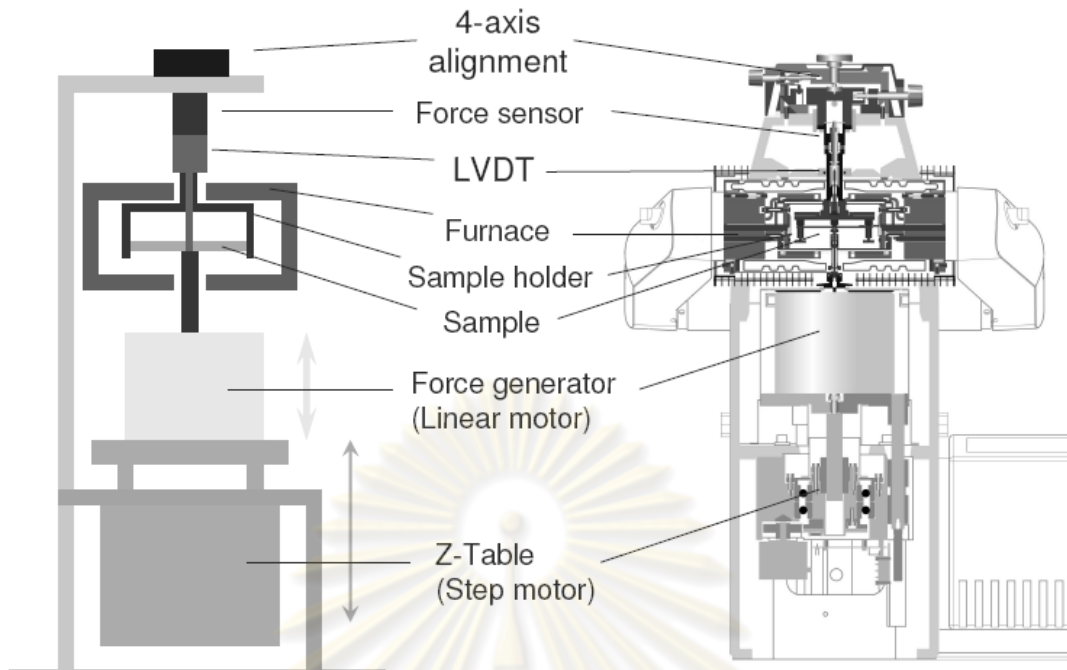


Figure 3.4 Typical DMA: Dynamic Mechanical Analysis cells

### 3.5 Morphological observation

The SEM samples for morphology studies were directly taken from the broken pieces in liquid nitrogen for characterizing morphology. Morphology of the fracture surface of the blends were examined using scanning electron microscopy (SEM) at 15 kV accelerating voltage. The samples were coated with gold before analysis. Then the degraded samples were examined on its sheet surface after the enzyme degradation.



Figure 3.5 SEM: Scanning Electron Microscope

### 3.6 FT-IR analysis

Interactions between PLA/PBAT polymer blend and nanoparticles was studied by Fourier Transform Infrared Spectroscopy (FTIR) on film samples. The wavenumber range, from 400 to 4000  $\text{cm}^{-1}$ , was scanned 32 times for spectrum integration. The scanning resolution was 4  $\text{cm}^{-1}$ .



Figure 3.6 Fourier Transform Infrared (FT-IR) spectroscopy

### 3.7 Mechanical properties

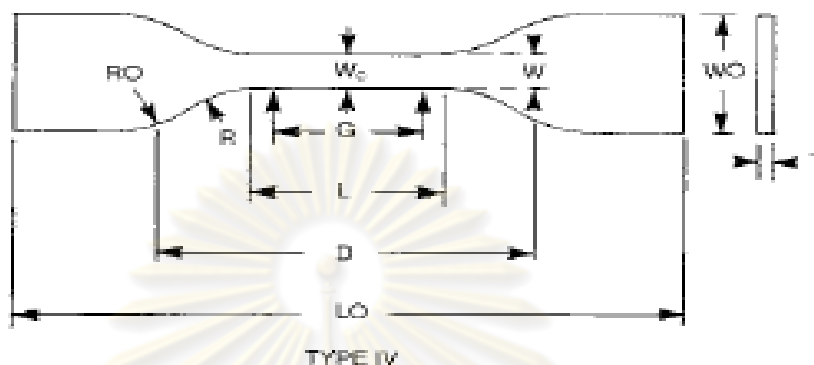
#### Tensile properties measurement

To investigate mechanical properties of the polymer blend nanocomposites, tensile tests were carried out according to ASTM D638 type IV using a Tinius Olsen H10 KT tensile tester. The dumbbell specimens (2.0 mm thickness) for tensile tests were die cutting method from the final plate. The test was carried out at a cross head speed of 5.0 mm/min, from both ends with a load cell of 500 N, and a gauge length of 25 mm. Tensile strength, modulus and % elongation were calculated from the load elongation curves obtained for three replicates for each sample.

The mechanical properties of specimens (300  $\mu\text{m}$  thickness) after enzyme degradation observation were performed according to ASTM D882-02 using a Tinius Olsen H10 KT tensile tester. The test was carried out at a cross head speed of 5.0



mm/min with a load cell of 500 N. Tensile strength, modulus and % elongation were calculated from the load elongation curves obtained for two replicates for each sample.



W	: Width of narrow section	6
L	: Length of narrow section	33
WO	: Width overall	19
LO	: Length overall	115
G	: Gauge length	25
D	: Distance between grips	65
R	: Radius of fillet	14
T	: Thickness	2.0

All dimension in millimeters (mm)

Figure 3.7 Tensile testing apparatus and dumbbell test specimen

### 3.8 Water vapor transmission rate (WVTR) and water vapor permeability (WVP) of the films

The water vapor transmission of the films was measured using the ASTM E96 method. A glass cup with 10 g of  $\text{CaCl}_2$  was closed with a sample of film firmly fixed on top. The films were cut circularly with a diameter of 10 cm. and then were sealed using melted paraffin. The cups were weighed with their contents and were placed in a

desiccator containing saturated KCl solution in a beaker at the bottom, providing 90% relative humidity(RH) at 25 °C. The cups were weighed every 24 hours until a steady increase in weight was achieved. The water vapor transferred through the films and absorbed by the desiccant was determined from the gain weight of the cup. The water vapor transmission rate (WVTR) and water vapor permeability (WVP) were calculated as follows:

$$\text{WVTR} = \frac{\Delta W}{\Delta t \times A}$$

$$\text{WVP} = \frac{\text{WVTR}}{\Delta P} L$$

where  $\Delta W/\Delta t$  is the amount of gain water per unit time of transfer, A is the area exposed to water transfer ( $\text{m}^2$ ), L is the film thickness (m), and  $\Delta P$  is the water vapor pressure difference between both sides of the film (Pa) [28].

### 3.9 Optical transporence analysis

The percentage of the light transmittance (T) of the film was measured by using Datacolor 650 Dual-beam Spectrophotometer at different wavelengths (400 nm, 500 nm, 600 nm, 650 nm, and 700 nm).



Figure 3.8 Dual-beam Spectrophotometer

### 3.10 Enzyme degradation observation

For enzymatic degradation studies, each specimen (10 mm x 10 mm x 0.30 mm) was placed in a vial filled with 5 ml of Tris HCl buffer solution (pH = 8.6) containing 1.0 mg proteinase K and 2.0 mg sodium azide. The vials were allowed to shake in a shaker thermostated at 37 °C. The buffered enzyme system was changed every 24 h to

restore the original level of enzymatic activity. For a given experiment, two replicate samples were withdrawn from the degradation medium, and washed with distilled water. After the specimens were vacuum dried at room temperature for 1 week. Then sample were investigated for their appearance by SEM and weight loss by weighing.

For tensile properties measurement after enzyme degradation observation, each specimen (10 mm x 100 mm x 0.30 mm) was placed in a petri dish filled with 20 ml of Tris HCl buffer solution (pH = 8.6) containing 4.0 mg proteinase K and 4.0 mg sodium azide. The vials were allowed to shake at a shaker thermostated at 37 °C. The buffered enzyme system was changed every 24 h to restore the original level of enzymatic activity. For a given experiment, two replicate samples were withdrawn from the degradation medium, and washed with distilled water. Then the specimens were vacuum dried at room temperature for 1 week.



ศูนย์วิทยทรัพยากร  
จุฬาลงกรณ์มหาวิทยาลัย

## CHAPTER IV

### 4.1 Thermal analysis of PBAT/PLA blends

#### 4.1.1 DSC measurement of PBAT/PLA polymer blend

Thermal analysis of the PBAT/PLA blend is shown in Table 4.1 and Figures 4.1. From the DSC thermograms, it could be seen that the melting temperature ( $T_m$ ) and their enthalpy of the blends showed endothermic melting peaks in the 2<sup>nd</sup> heating program. The crystallization temperature ( $T_c$ ) and their enthalpy also were investigated in a cooling program after the 1<sup>st</sup> heating program.

A small effect of the PBAT content on  $T_m$  of PBAT/PLA was observed. In Table 4.1, Figure 4.1 and appendix Fig.A-1, the  $T_m$  of the blends was close to that of the neat PLA. This indicated that the PLA was a matrix phase in the blends and the two polymers were still immiscible blend. Because all the blends revealed a typical two-phase system, immiscible blends, showing two glass transition temperatures (Table 4.1). The  $T_m$  of PL30PB70 in second heating scan which was the highest of polymer blends, suggesting maximum degree of crystallinity ( $\Delta H_c$ ) from cooling scan.

Table 4.1  $T_m$  and  $T_c$  of PBAT/PLA blends with various PBAT contents

(1<sup>st</sup> heating scan, cooling and 2<sup>nd</sup> heating scan, 10°C/min).

Sample code	First Heating		Cooling		Second Heating			
	$T_m$ (°C)	$\Delta H_m$ (J/g)	$T_c$ (°C)	$\Delta H_c$ (J/g)	$T_{g1}$ (°C)	$T_{g2}$ (°C)	$T_m$ (°C)	$\Delta H_m$ (J/g)
PL100PB0	150.27	31.17	-	-	-	52.71	152.30	-
PL50PB50	150.01	12.43	62.64	15.76	-35.39	53.26	147.66	13.47
PL40PB60	151.19	9.44	65.82	14.61	-36.61	50.18	145.66	10.47
PL30PB70	149.05	4.36	68.32	16.57	-33.03	56.69	148.70	5.84
PL0PB100	116.95	11.19	41.08	22.92	-31.85	-	116.76	16.92

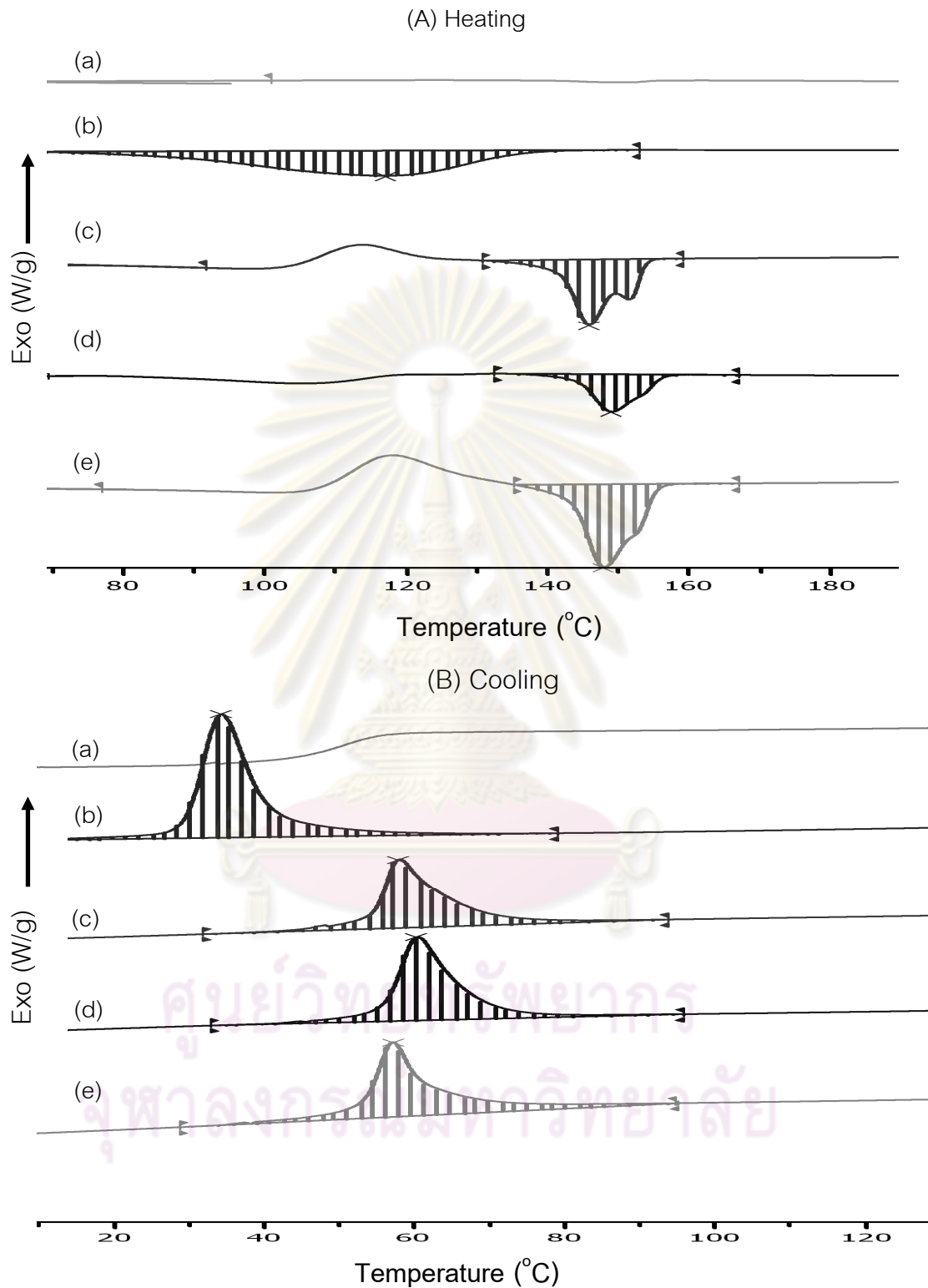


Figure 4.1 DSC thermograms of PLA, PBAT and their blends:

(a) neat PLA      (b) neat PBAT      (c) PL40PB60

(d) PL30PB70      (e) PL50PB50



The  $T_c$  of neat PLA did not displayed a cold crystallization exotherm. This result suggested that neat PLA was not able to crystallize within the cooling time frame because the PLA was primarily amorphous. Comparing curves c-e with a, the incorporation of PBAT was occurred at cold crystallization temperature, indicating an enhanced crystalline ability of PLA. Therefore, it could be concluded that the addition of PBAT greatly increased the crystallization rate of PLA. In the DSC thermogram (Figure 4.1A), the addition of PBAT clearly separated the melting peak into two individual peaks as shown in curves c-e. The peaks at higher temperatures corresponded to the shoulder was PLA phase. The peaks at lower temperatures was suggested the presence of a new crystalline structure induced by PBAT.

#### 4.1.2 DSC measurement of PBAT/PLA polymer blend nanocomposites

Thermal analysis of the PBAT/PLA blend in the absence and presence of fillers are shown in Table 4.2 and Figures 4.2 to 4.6. From the DSC thermograms, it could be seen that the melting temperature ( $T_m$ ) of the blends showed endothermic melting peaks in the 1<sup>st</sup> and 2<sup>nd</sup> heating program. The crystallization temperature ( $T_c$ ) and their enthalpy also were investigated in a cooling program after the first heating program.

The presence of fillers in PBAT/PLA blend showed apparent shift in  $T_m$  values which were summarized in Table 4.2 and supporting by DSC thermograms in Figures 4.3 A, 4.4A and 4.5A. In this study, Figures 4.3A, 4.4A and 4.5A after filled with  $\text{SiO}_2$  (all content),  $\text{mSiO}_2$  (6 phr) and NPCC (1 and 3 phr) showed clearly two endothermic melting peaks indicated that the miscibility of PBAT and PLA obviously decreased while after filling with  $\text{mSiO}_2$  (1 and 3 phr) and NPCC (6 phr) they showed slightly one endothermic melting peaks which indicated enhancement of the miscibility of the PBAT/PLA blend. Thus, the modified surface fillers ( $\text{mSiO}_2$  and NPCC) were able to bring the two polymer phases to a level of miscibility depend on particle loading which indicated by the  $T_m$  from DSC thermograms.

The  $T_c$  of PBAT/PLA filled with fillers were increased at all content and type as shown in Table 4.2 and Figures 4.3 B, 4.4B and 4.5B. Higher  $T_c$  values indicated an increased crystalline ability of PLA. The higher crystallization temperature also indicated

an enhancement of crystalline ability of PLA. On the other hand, the lower of crystallization temperature also indicated lower degree of crystallization. These results implied that the interfacial adhesion between PBAT and PLA was enhanced by reactions between fillers and polymers.

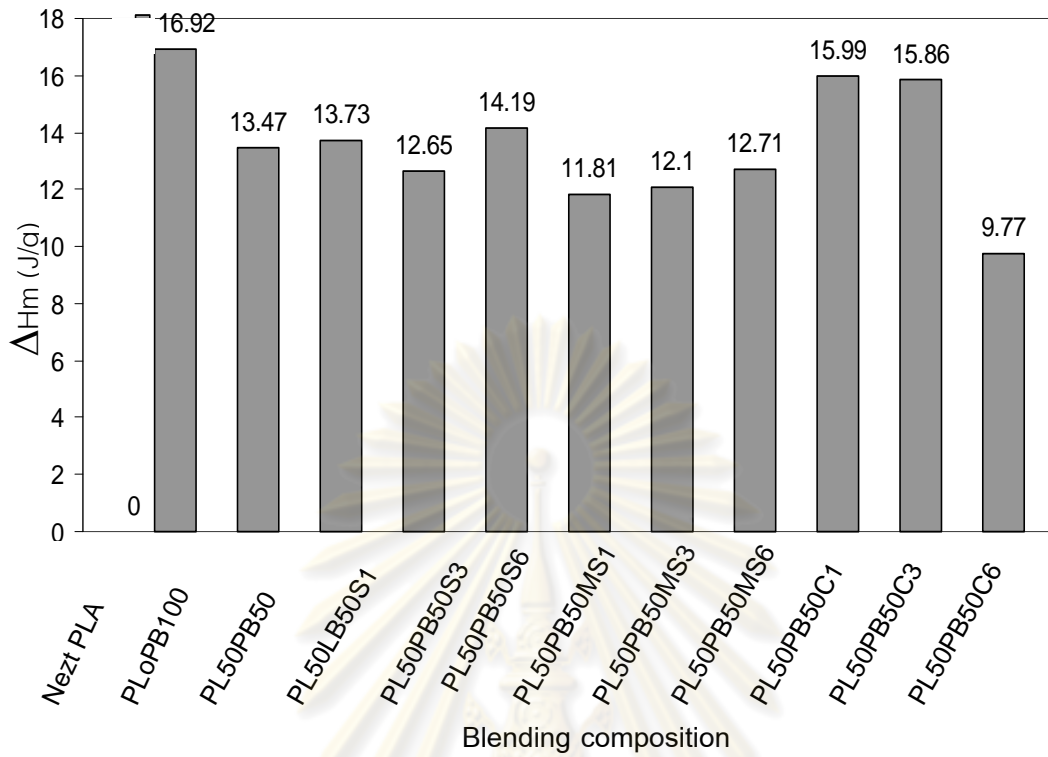
From figure 4.2B, the incorporation of SiO<sub>2</sub> (3 phr), mSiO<sub>2</sub> (1 phr) and NPCC (1 phr) increased trend of enthalpy of crystallization in blends. Therefore, the enthalpy component from the DSC thermograms indicated the effect of fillers in the blend.

Table 4.2 Thermal properties of PBAT/PLA blends with various filler types and contents

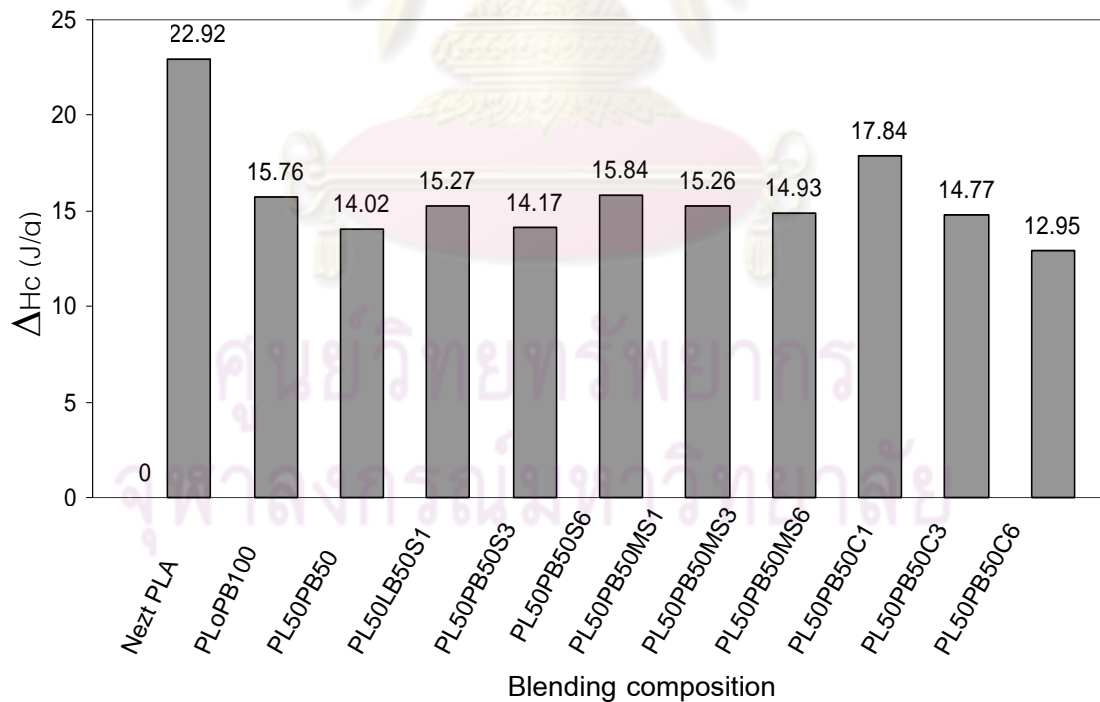
Sample code	1 <sup>st</sup> heating		Cooling	2 <sup>nd</sup> heating
	T <sub>m</sub> (°C)	ΔH <sub>m</sub> (J/g)	T <sub>c</sub> (°C)	T <sub>m</sub> (°C)
PL50PB50	150.01	12.43	62.64	147.66
PL50PB50S1	147.15	12.75	87.02	151.46
PL50PB50S3	146.86	10.97	80.5	144.85
PL50PB50S6	146.50	11.42	79.93	144.64
PL50PB50MS1	149.12	8.99	72.45	148.09
PL50PB50MS3	152.40	9.66	67.31	148.38
PL50PB50MS6	152.64	10.34	70.22	146.45
PL50PB50C1	149.34	11.20	63.55	147.46
PL50PB50C3	150.09	12.94	64.59	149.57
PL50PB50C6	150.99	12.67	63.89	148.36

จุฬาลงกรณ์มหาวิทยาลัย

(A) Enthalpy of Tm of PLA, PBAT and their blends



(B) Enthalpy of Tc of PLA, PBAT and their blends

Figure 4.2 Enthalpy of Tm and Tc of PLA, PBAT and their blends (2<sup>nd</sup> heating&cooling)

(A) Enthalpy of melting temperature (B) Enthalpy of crystallization temperature

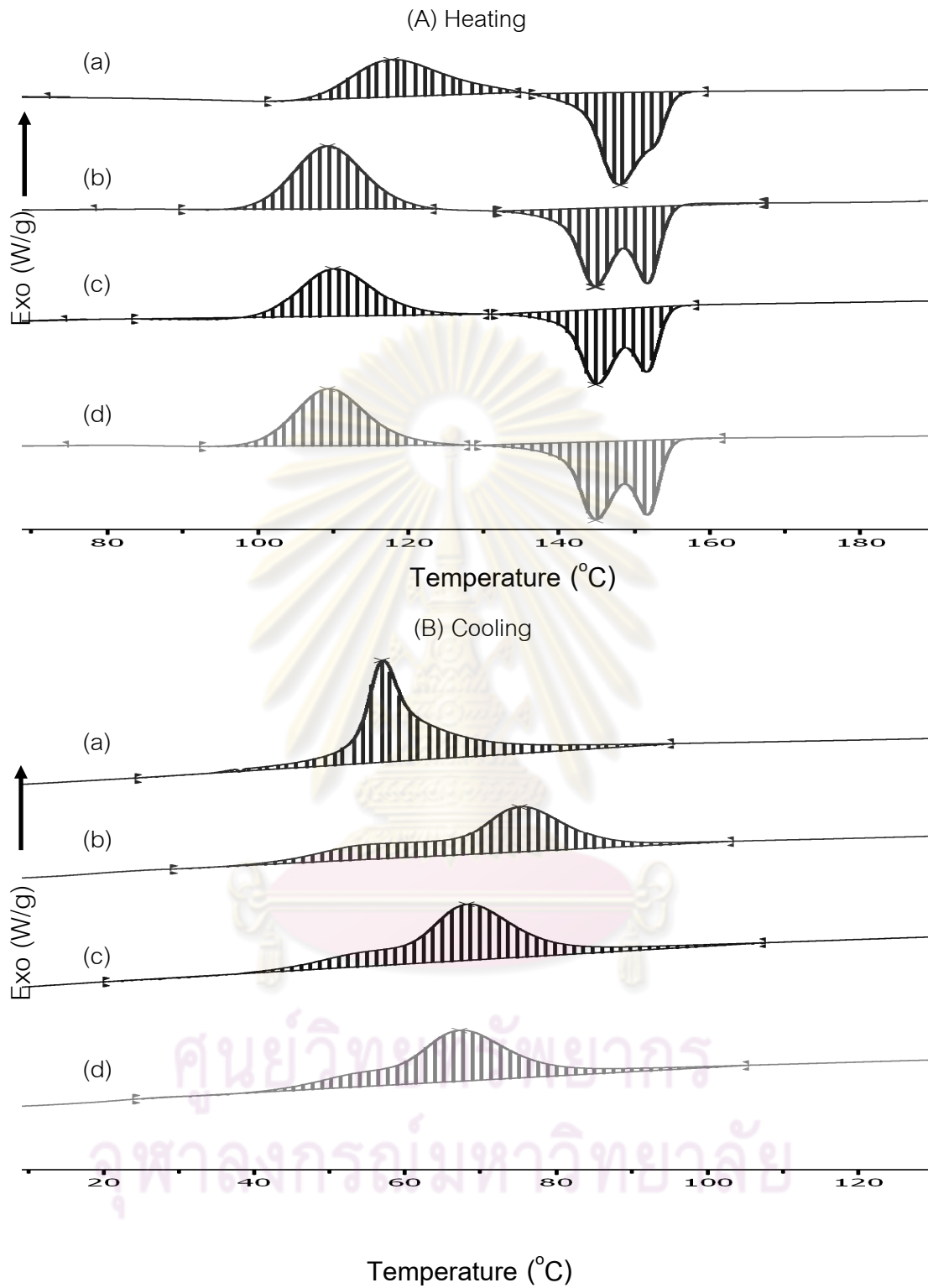


Figure 4.3 DSC thermograms of PLA, PBAT and their blends with  $\text{SiO}_2$ :  
 (a) PL50PB50 (b) PL50PB50S1 (c) PL50PB50S3 (d) PL50PB50S6

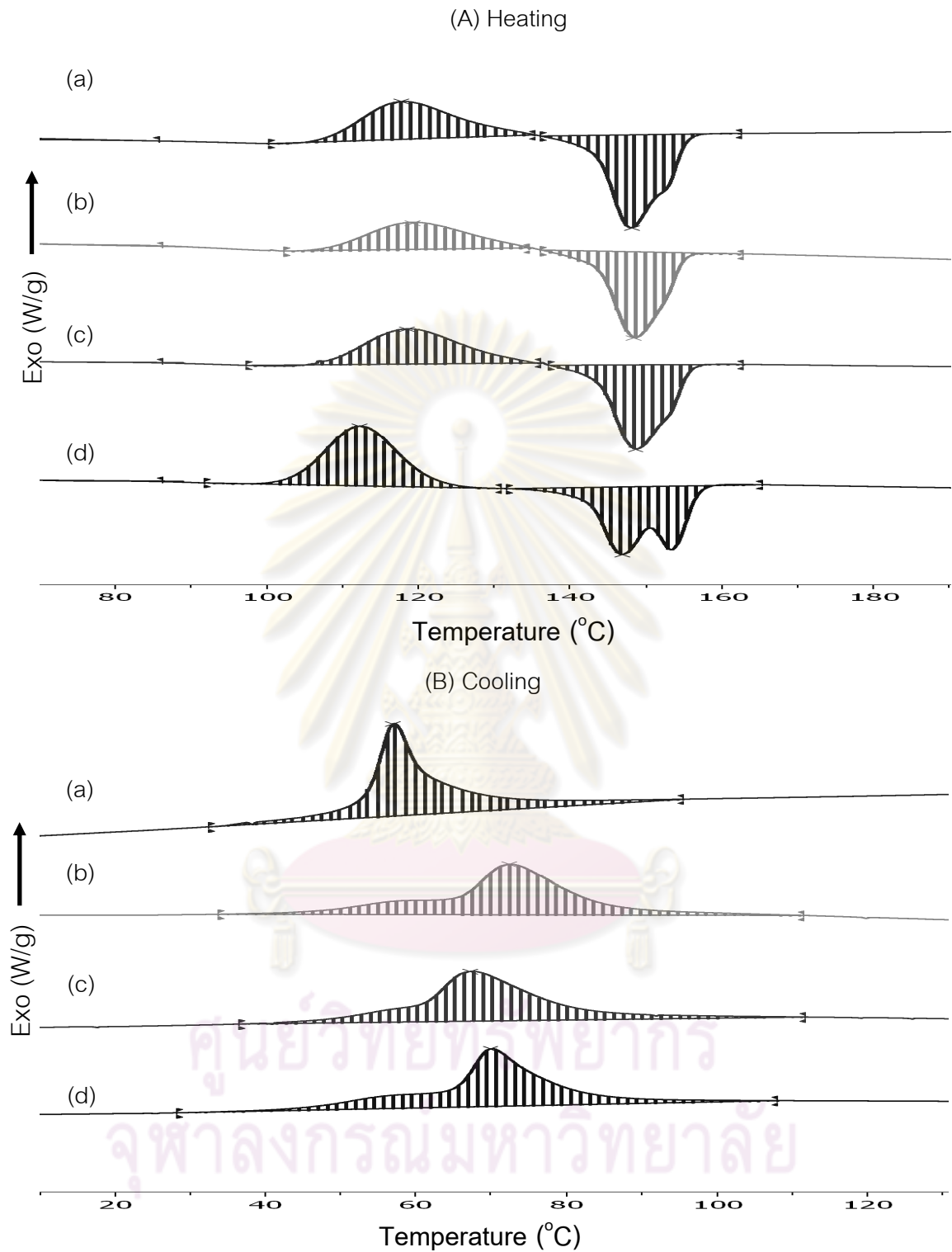


Figure 4.4 DSC thermograms of PLA, PBAT and their blends with mSiO<sub>2</sub>:  
 (a) PL50PB50 (d) PL50PB50MS1 (e) PL50PB50MS3 (f) PL50PB50MS6

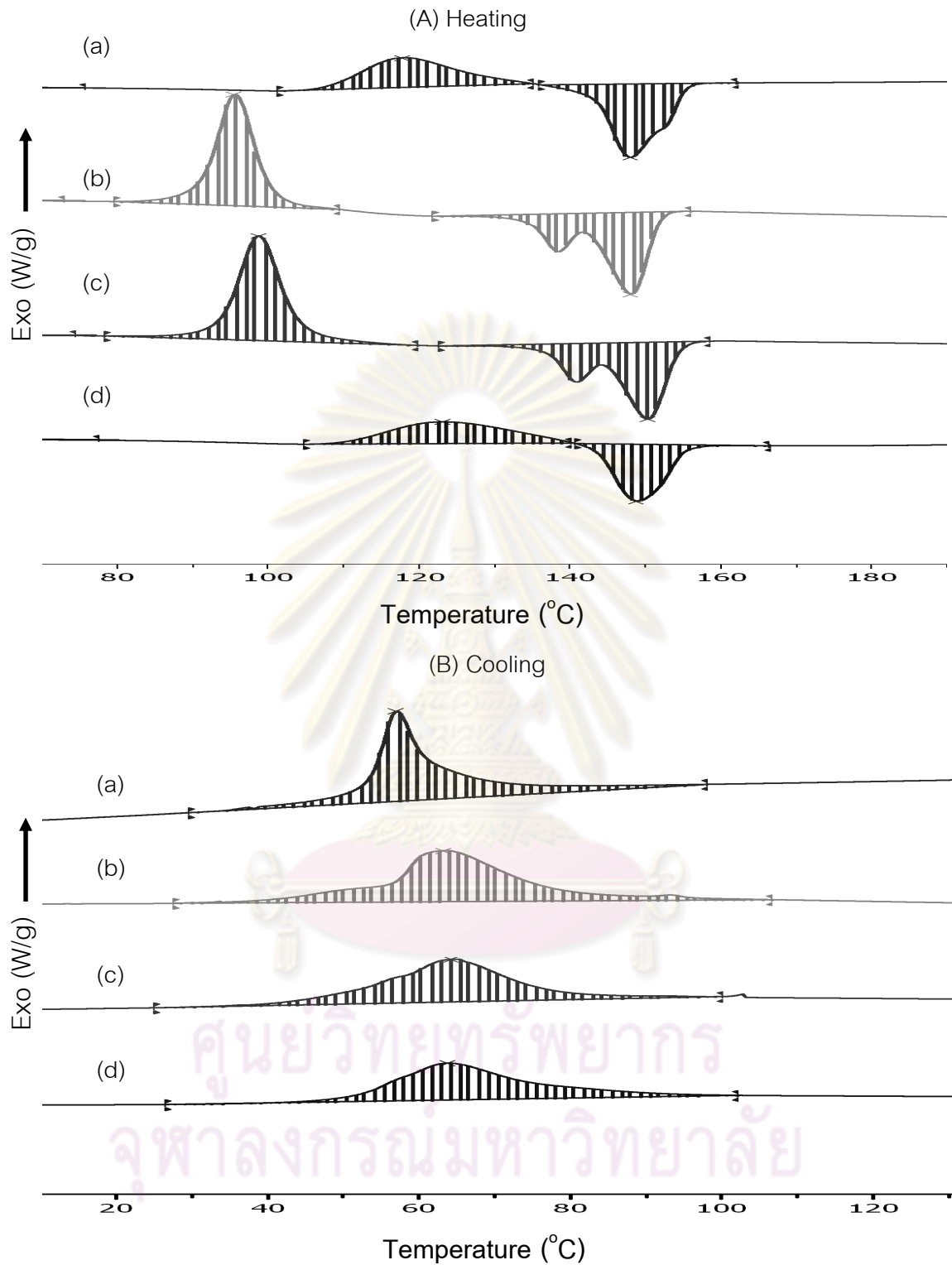


Figure 4.5 DSC thermograms of PLA, PBAT and their blends with NPCC:

(a) PL50PB50 (b) PL50PB50C1 (c) PL50PB50C3 (d) PL50PB50C6

(A) Heating



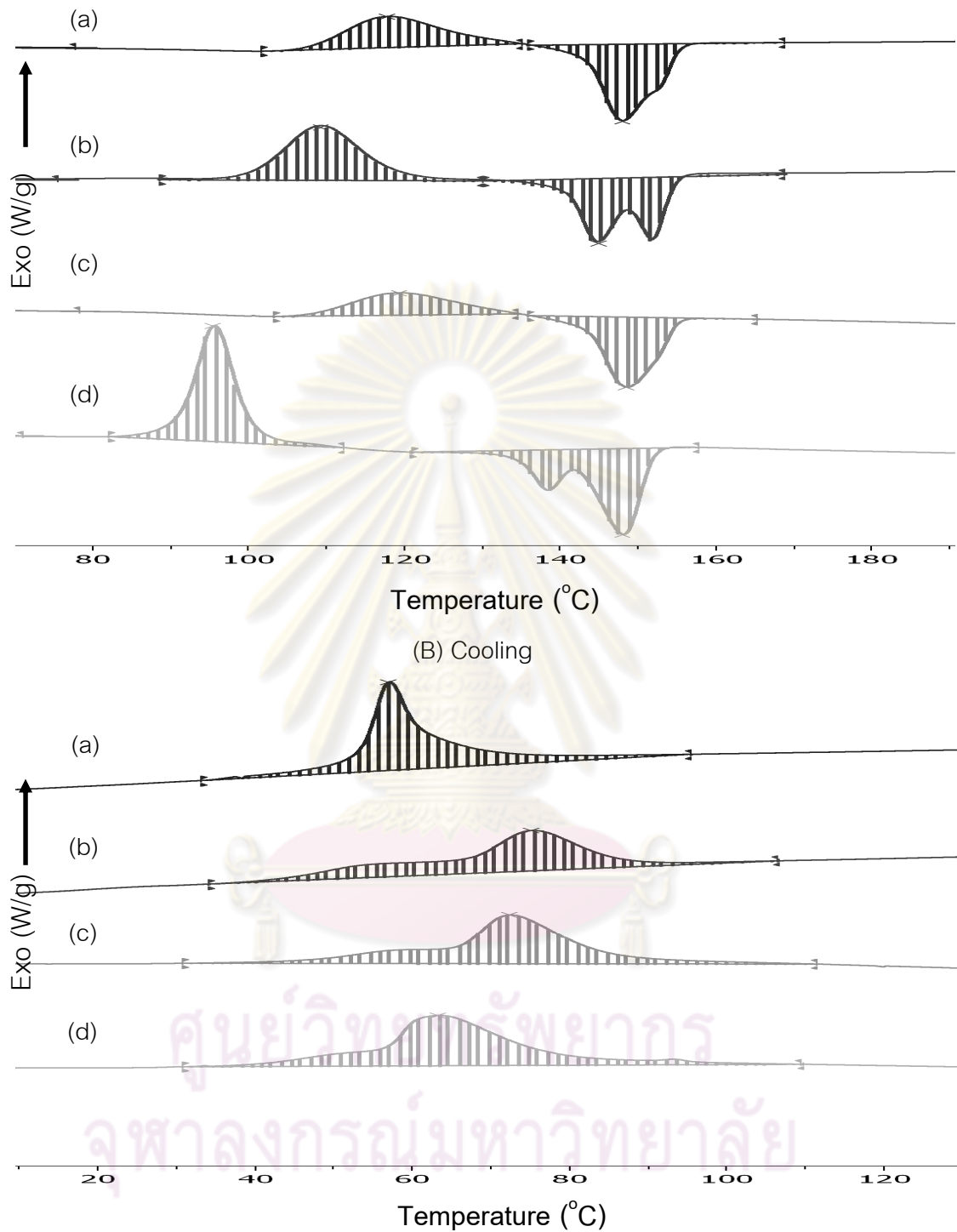


Figure 4.6 DSC thermograms, comparison of PBAT/PLA blends filled with  $\text{SiO}_2$ ,  $\text{mSiO}_2$  and NPCC at 1 phr :

(a) PL50PB50 (b) PL50PB50S1 (c) PL50PB50MS1 (d) PL50PB50C1

## 4.2 Morphology of PBAT/PLA blend in the absence and presence of SiO<sub>2</sub>, mSiO<sub>2</sub> and NPCC by SEM

The morphologies of the blends of PBAT/PLA with SiO<sub>2</sub>, mSiO<sub>2</sub> and NPCC as reinforcement filler are shown in Figure 4.7. In Figure 4.7a, the blend showed a kind of immiscible, two-phase structure with PBAT dispersing evenly in PLA matrix and cavitation caused by debonding can be clearly identified. As shown in Figure 4.7a, the matrix phase was PLA and the dispersed phase was PBAT. After the addition of 3 phr of SiO<sub>2</sub> and mSiO<sub>2</sub>, the blends of PLA showed finer and smaller particles of PBAT scattering in the matrix as seen in Figures b and d. Addition of NPCC, the blends illustrated that the shape dispersed phases of PBAT were changed from spherical to elongated shape and PBAT inclusion smaller (Figure 4.7f). As a result, the fracture surfaces appeared coarser due to this size reduction. PBAT inclusion size reduction also indicated the presence of NPCC in the composites significantly changed inclusion flow, dispersion, and agglomeration. As shown in Figure 4.7g (high magnification), the PBAT inclusions were recognizable as well-defined individual fiber in PBAT/PLA/NPCC composite. This caused by the shear amplification effect which occurred in extrusion compounding when the polymer melt flowed through small gaps formed by nanoparticles. In Figure 4.7e, the addition of mSiO<sub>2</sub> revealed lighter boundary at interface indicating that the interfacial adhesion increased between the dispersed and matrix phases. Figures 4.7 b, and e, addition of SiO<sub>2</sub> nanoparticles indicated that the PLA/PBAT blends were immiscible and SiO<sub>2</sub> were dominantly dispersed in the PBAT phase. Therefore it could be concluded that the SiO<sub>2</sub> possessed a preferential affinity into one phase and this phenomenon made unique morphological properties of the nanocomposite system. This result was already observed in the previous work [29] on PP/EVA silica blends with hydrophilic and hydrophobic silica. In this study, it could be observed by SEM micrographs shown in Figure 4.7. Therefore, this corresponds well with the prediction based on the surface tensions. It was assumed that the presence of silica particles induced a decrease in the effective interfacial tension which tended to reduce the dispersed phased size, which hydrophilic silica was efficient at producing a

relatively uniform distribution of drop sizes and the distribution shifts to smaller diameter whereas hydrophobic silica particles act as a rigid layer preventing the coalescence of PBAT droplets. The hydrophilic silica was preferentially located in the dispersed phase (Figure 4.7c), by contrast, for hydrophobic silica which located closer to the interface (Figure 4.7e). As results, silica was distributed non-homogeneously in the blend. Depending on their wetting ability (wetting parameter) in which the interactions were more favorable according to the wetting parameter, the silica particles are confined in one of the two phases or could be confined at the interface between the two polymers. The mode of addition of the silica seemed to have weak effect on its localization. However, the decrease of the effective interfacial tension due to the presence of silica particles in the volume of the dispersed droplets was difficult to understand. One explanation could arise from the thermodynamic origin of the interfacial tension. From a thermodynamic point of view, interfacial tension is defined as formula  $\alpha = \partial G / \partial A$  where  $G$  is the free enthalpy of the system and  $A$  is the interfacial area between the two phases. An increase in the interfacial area causes an increase in the free energy. The free energy can be viewed as the elastic energy stored by the droplet during its deformation. Generally, nanofillers prefer to be well dispersed in the polymer which has a lower interfacial tension. Therefore, it could be concluded that the PLA/SiO<sub>2</sub> interfacial tension was stronger than PBAT/SiO<sub>2</sub> interfacial tension.

ศูนย์วิทยทรัพยากร  
จุฬาลงกรณ์มหาวิทยาลัย

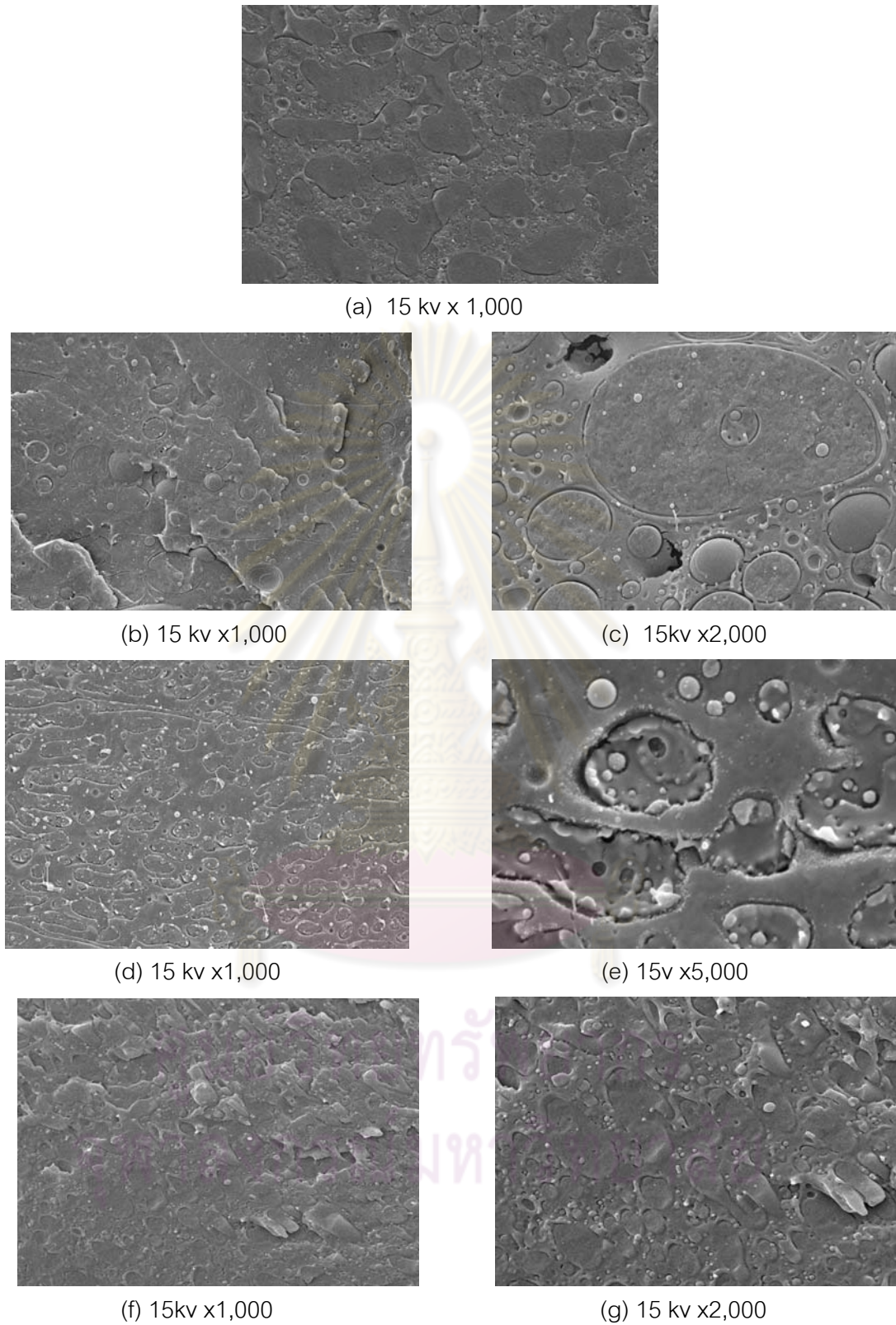


Figure 4.7 SEM images of the blends: (a) PL50PB50 (b) PL50PB50S3 (c) zoom of image b (d) PL50PB5MS3 (e) zoom of image d (f) PL50PB50C3 and (g) zoom of image f



### 4.3 Mechanical properties of PBAT/PLA blend in the absence and presence of fillers content

The mechanical properties of neat PBAT, neat PLA and their blends are shown in Figures 4.8- 4.13. In this study, tensile test was used to determine the mechanical properties of the blended nanocomposites in term of tensile modulus, tensile strength and elongation at break. Tensile modulus was used to indicate the stiffness of materials which was determined by the first linear slope of stress-strain curve. The strength of a material is defined as the maximum stress that the material can sustain under uniaxial tensile loading. In addition, elongation at break is defined as strain at rupture of the specimen. It is worthwhile to mention that the single polymer (PLA) had higher tensile strength and modulus than PBAT in which PLA had very stiffness and PBAT had high elongation and more ductile than PLA. It was well known that polymer composites filled with inorganic materials have attracted great interest due to the improvement of stiffness. The improvement was explained that the inorganic filler served as a reinforcement agent. Therefore, the addition of inorganic materials into polymer matrix could help improving the stiffness of materials. However, interfacial interaction between polymer and inorganic filler should also be considered because it strongly affected the improvement of mechanical properties. Besides inorganic filler, the crystalline part of polymer also enhanced the stiffness of polymer. In general, the stiffness of materials increased with increasing degree of crystallinity.

#### 4.3.1 Mechanical properties of PBAT/PLA blends

Mechanical behavior of the specimen in tensile test changed from brittle of neat PLA to ductile of the blends. This was demonstrated as shown in Figures 4.8 - 4.10. Neat PLA showed a distinct tensile strength and modulus and the elongation was only about 5.97 %. Surprisingly, it was noticed that the elongation of the blend was tremendously increased (>300%), and the elongation continuously increased with increase in PBAT content (Figure 4.10). Tensile strength and modulus of PBAT/PLA blends decreased with increasing PBAT content (Figures 4.8-4.9) and the blends showed clearly a decreasing trend when the amount of PBAT was increased. Tensile strength decreased by 48.65% from 45.90 (neat PLA) to 23.57 MPa (50%PBAT), while

modulus decreased by 82.35% from 1469.32 (neat PLA) to 259.44 MPa (50%PBAT). This was expected since PBAT had a lower tensile strength and modulus than PLA. Therefore, the debonding progress with the stress was higher than the bonding strength at the interface between the PLA matrix and PBAT domain. Because there was not sufficient interfacial adhesion between PBAT and PLA, interfacial debonding took place. With the debonding progress, PLA matrix stranded between PBAT particles deformed more easily to achieve the shear yielding. The interfacial adhesion had a great influence in the various toughened micromechanical deformation process. When there was an interfacial adhesion, the plastic deformation occurs via a single cavitation process inside the modifier particle, whereas when there was not adequate adhesion, the micromechanical deformation process was initiated with debonding. Mechanical properties of PBAT/PLA blend were investigated by tensile testing. In keeping with that reported by Ludvik et al. [30], and recently by Signori et al. [31] the addition of PBAT to PLA, to give PBAT-PLA blends, resulted in a strongly improvement of PLA ductility.

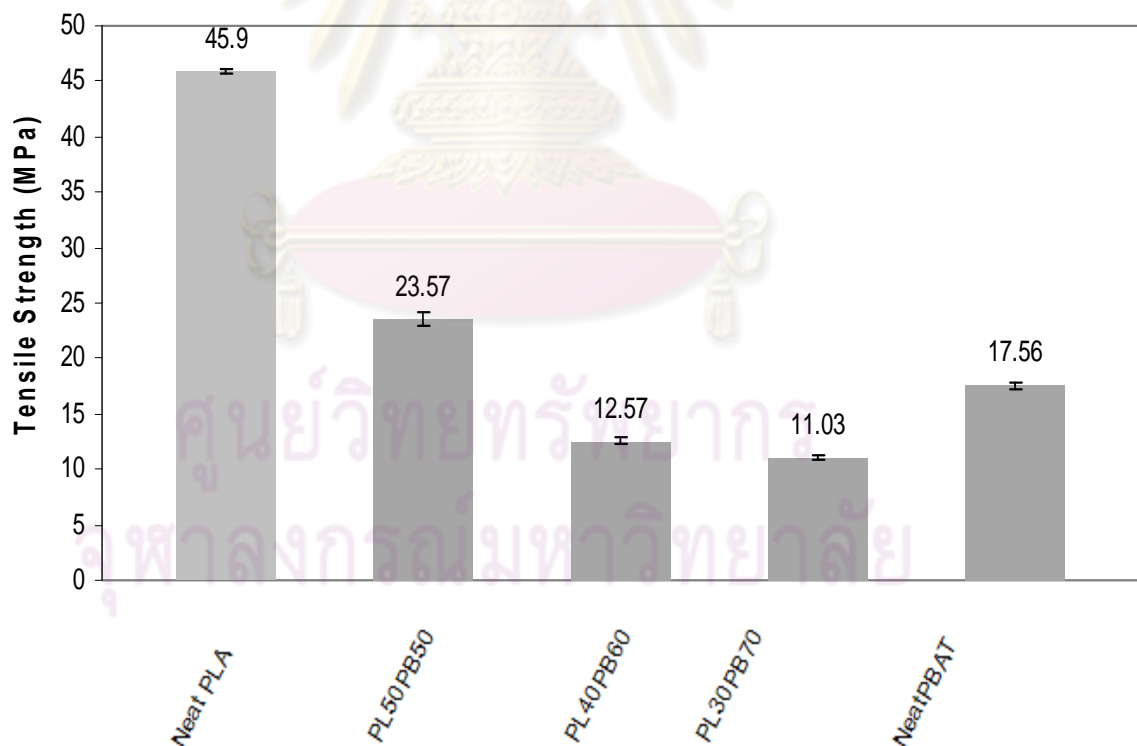


Figure 4.8 Tensile strength of neat PLA, PBAT and their blends



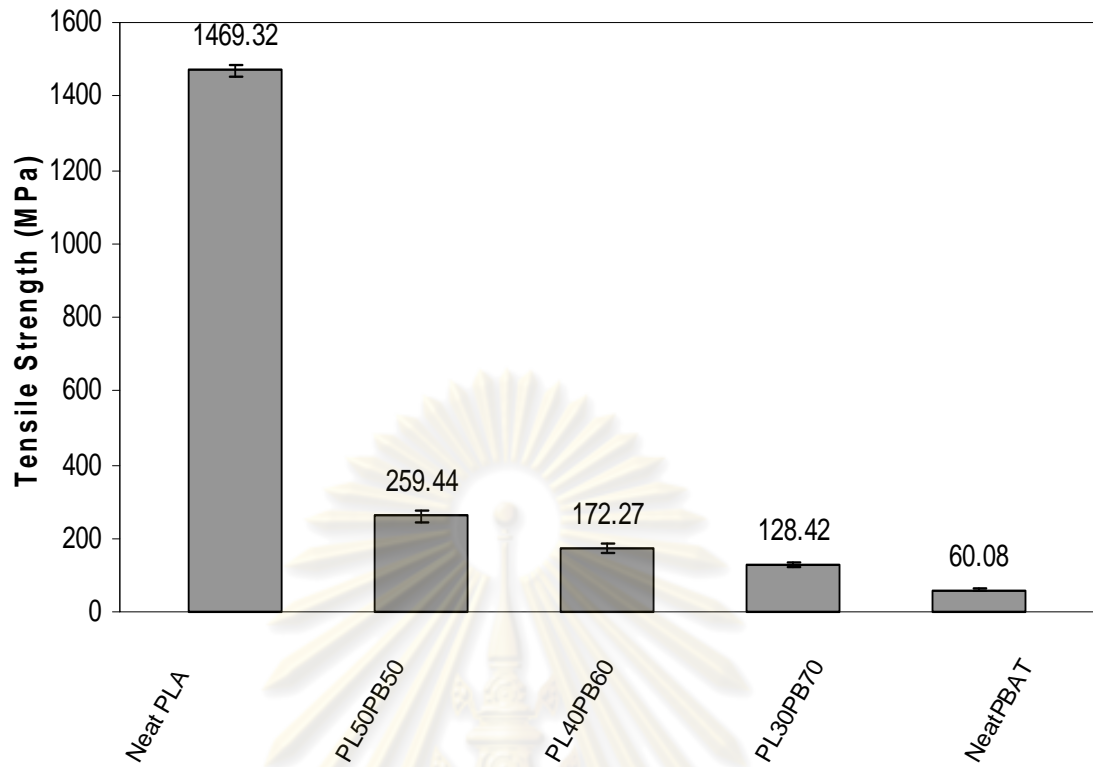


Figure 4.9 Tensile modulus of neat PLA, PBAT and their blends

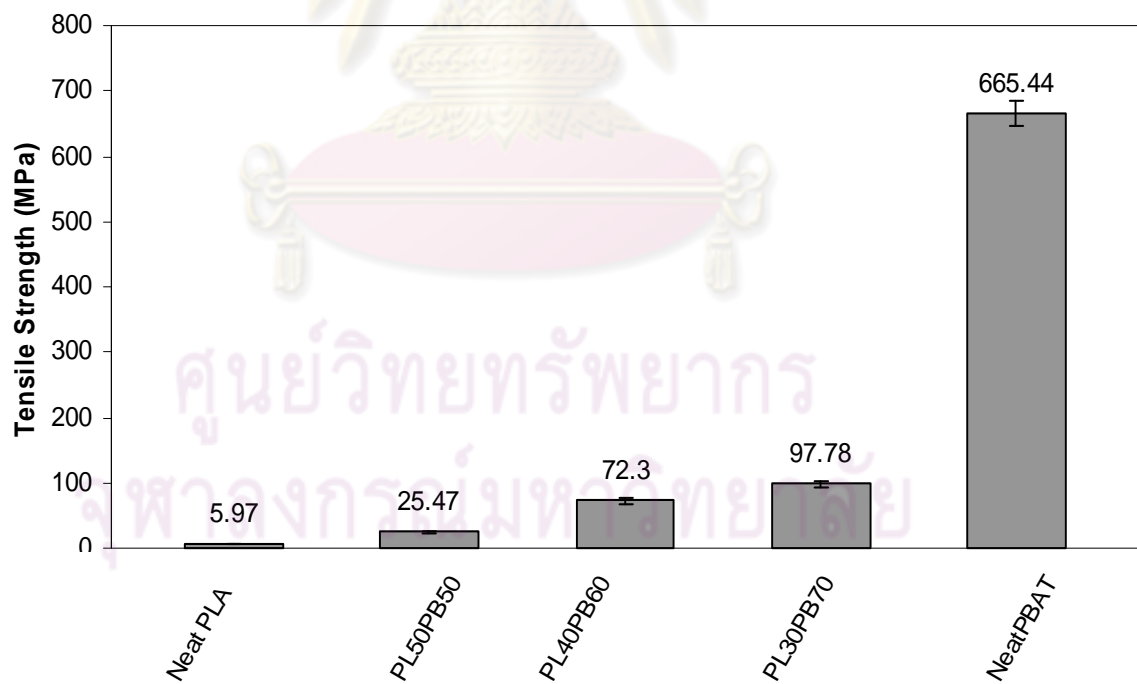


Figure 4.10 The elongation of neat PLA, PBAT and their blends

#### 4.3.2 Mechanical properties of PBAT/PLA polymer blend nanocomposites

Figures 4.11 -4.13 show mechanical properties of PBAT/PLA (50/50 wt %) blend in the absence and presence of fillers at various contents. The strength of material for micro- and nano-particulate composites was relies on the effectiveness of stress transfer between matrix and fillers. Factors like particle size, particle/matrix interfacial strength and particle loading significantly affected the composite strength. As shown in Figure 4.11, tensile strength of PBAT/PLA/SiO<sub>2</sub> with 1 and 3 phr of SiO<sub>2</sub> and PBAT/PLA/NPCC with 3 and 6 phr of NPCC were higher than that of the PBAT/PLA blend. These results indicated that the interfacial adhesion between PBAT and PLA was enhanced by interaction between fillers and polymer which a strong interfacial bonding between particles and matrix which was critical for effective stress transfer leading to high composite strength. As shown in Figure 4.7 of SEM, after the addition of fillers, the blends of PLA showed finer and smaller particles of PBAT scattering in the matrix due to the decrease of the effective interfacial tension that implied the enhancement of interfacial adhesion. Addition of mSiO<sub>2</sub> in the PBAT/PLA blends, the elongation gradually increased. These results also indicated that the silane modification of the SiO<sub>2</sub> had influence on the elongation. The effects of this silane flexible interlayer were also observed as (a) a decrease in the strengthening effect of the rigid unmodified particles and (b) an increase in the ductility compared with untreated silica. In addition, the different result of SiO<sub>2</sub>, mSiO<sub>2</sub> and NPCC involved on particle dispersion as seen in SEM analysis. Comparison of PBAT/PLA/SiO<sub>2</sub>, PBAT/PLA/mSiO<sub>2</sub> and PBAT/PLA/NPCC at 1 phr in the tensile strength showed that PBAT/PLA/SiO<sub>2</sub> and PBAT/PLA/NPCC had higher strength than that of PBAT/PLA/mSiO<sub>2</sub>. In addition, PBAT/PLA/SiO<sub>2</sub> had higher tensile strength than PBAT/PLA/NPCC. This result implied the effect of higher aspect ratio and lower particle size of SiO<sub>2</sub>. From the above results, the strength of particulate composites was determined not only by prominent effect of the particle/matrix interfacial adhesion but also by particle loading, particle dispersion and particle size. Various trends of the effect of particle loading, particle dispersion and particle size on composite

strength had been observed due to the interplay between these four factors, which could not always be separated.

As shown in Figure 4.12, the tensile modulus of the PBAT/PLA blends with all fillers was increased at about 11.97 – 47.61 % when  $\text{SiO}_2$ ,  $\text{mSiO}_2$  and NPCC were incorporated in all contents. Hence, addition of rigid particles to polymer matrix could easily improve the modulus since the rigidity of inorganic fillers was generally much higher than that of organic polymers. The direct factor was mainly responsible for the improvement of composite modulus because the crystallinity of semi-crystalline polymers, and hence the composite modulus, was affected by the filler while interfacial adhesion had little effect on the tensile modulus of particulate-filled composites. Higher of tensile modulus implied an increased mobility of polymer chain as enhanced crystalline ability of PLA matrix. Comparison of PBAT/PLA/ $\text{SiO}_2$ , PBAT/PLA/ $\text{mSiO}_2$  and PBAT/PLA/NPCC at 1phr in the tensile modulus, it was observed that PBAT/PLA/ $\text{SiO}_2$  and PBAT/PLA/NPCC had higher tensile modulus than that of PBAT/PLA/ $\text{mSiO}_2$  due to higher crystalline ability of PLA matrix as shown in  $\Delta H_m$  (1<sup>st</sup> heating) from DSC (Table 4.2) results which were 12.75 J/g ( $\text{SiO}_2$ ), 11.20 J/g (NPCC) and 8.99 J/g ( $\text{mSiO}_2$ ). In addition, PBAT/PLA/ $\text{SiO}_2$  had higher tensile modulus than PBAT/PLA/NPCC due to higher crystalline ability of PLA matrix.

Surprisingly, Figure 4.13, the incorporation of  $\text{SiO}_2$ ,  $\text{mSiO}_2$  and NPCC at all contents, indicated that the elongation of the blends were increased (65.02 – 130.58%) from PBAT/PLA blends. These results indicated that interfacial bonding between PBAT and PLA was enhanced by the addition of fillers which had high surface area. This could be explained by interfacial interaction and particle dispersion between inorganic material and polymer matrix which demonstrated by SEM micrographs as shown in Figure 4.7. Furthermore, the highest elongation of PBAT/PLA/ $\text{mSiO}_2$  was explained by silane flexible layer of  $\text{mSiO}_2$  with increase in the ductility. It may be concluded that the modified and unmodified fillers were acted as reinforcement agents from interfacial properties in this study [32].

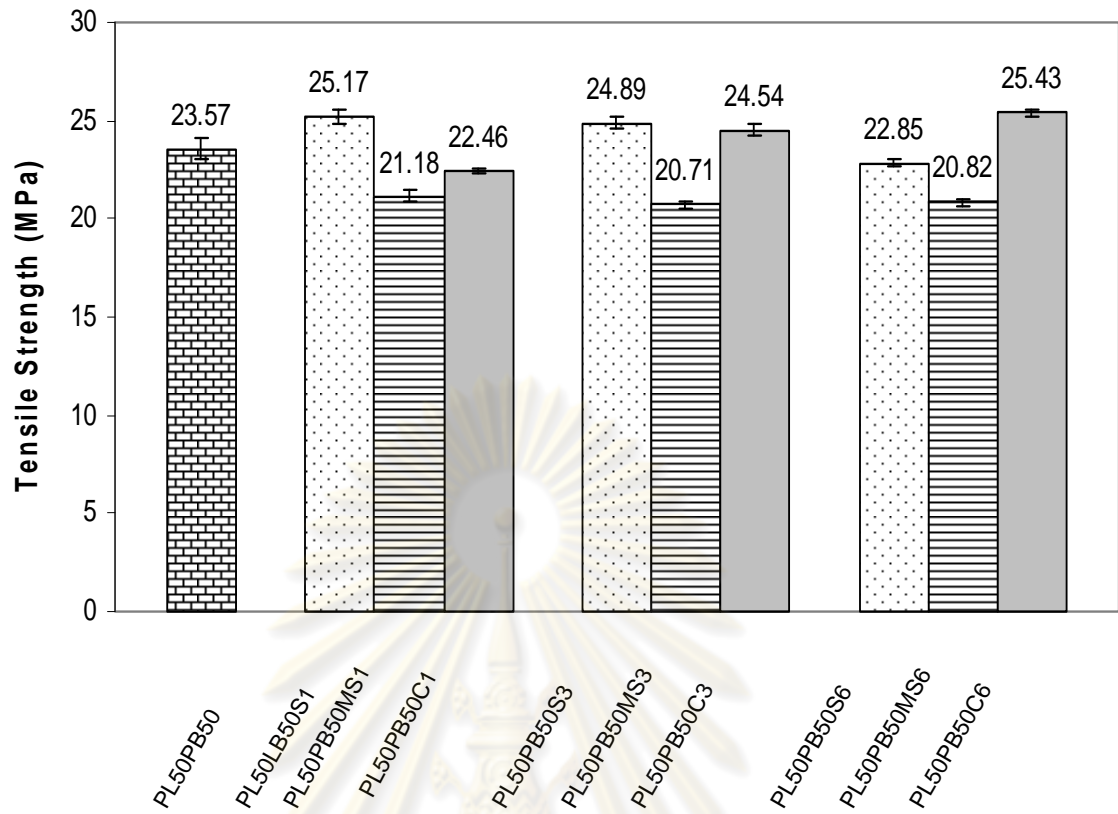


Figure 4.11 Tensile strength of PBAT/PLA (50/50 wt %) and their composites

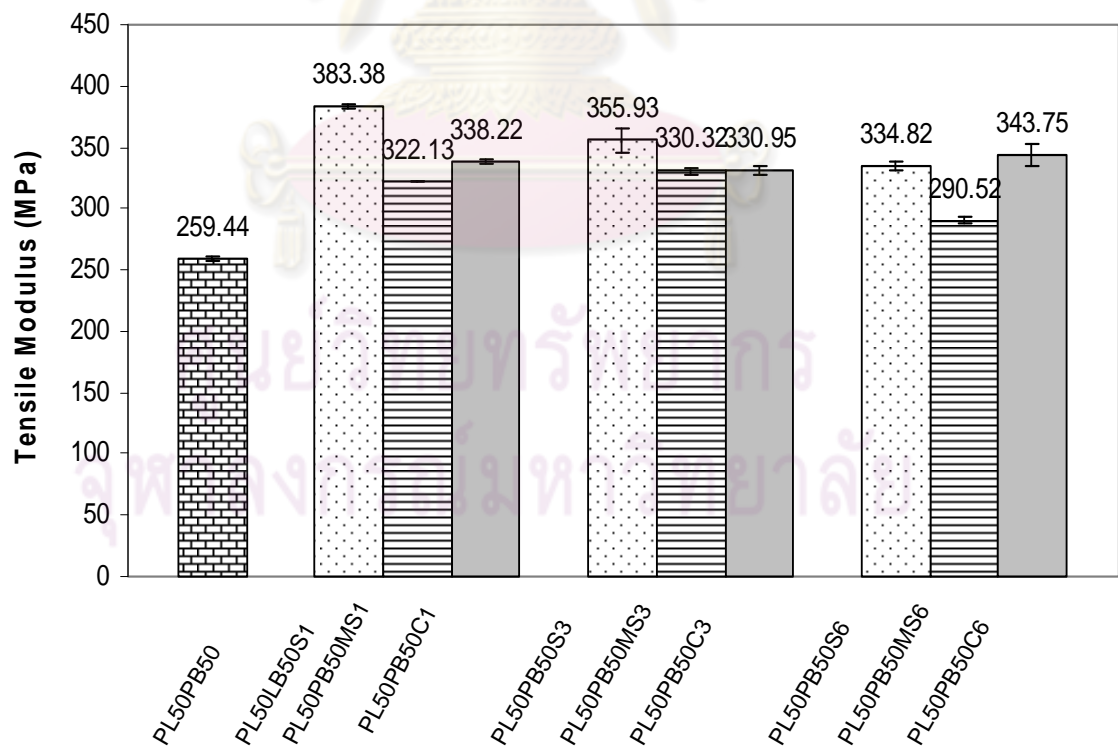


Figure 4.12 Tensile modulus of PBAT/PLA (50/50 wt %) and their composites

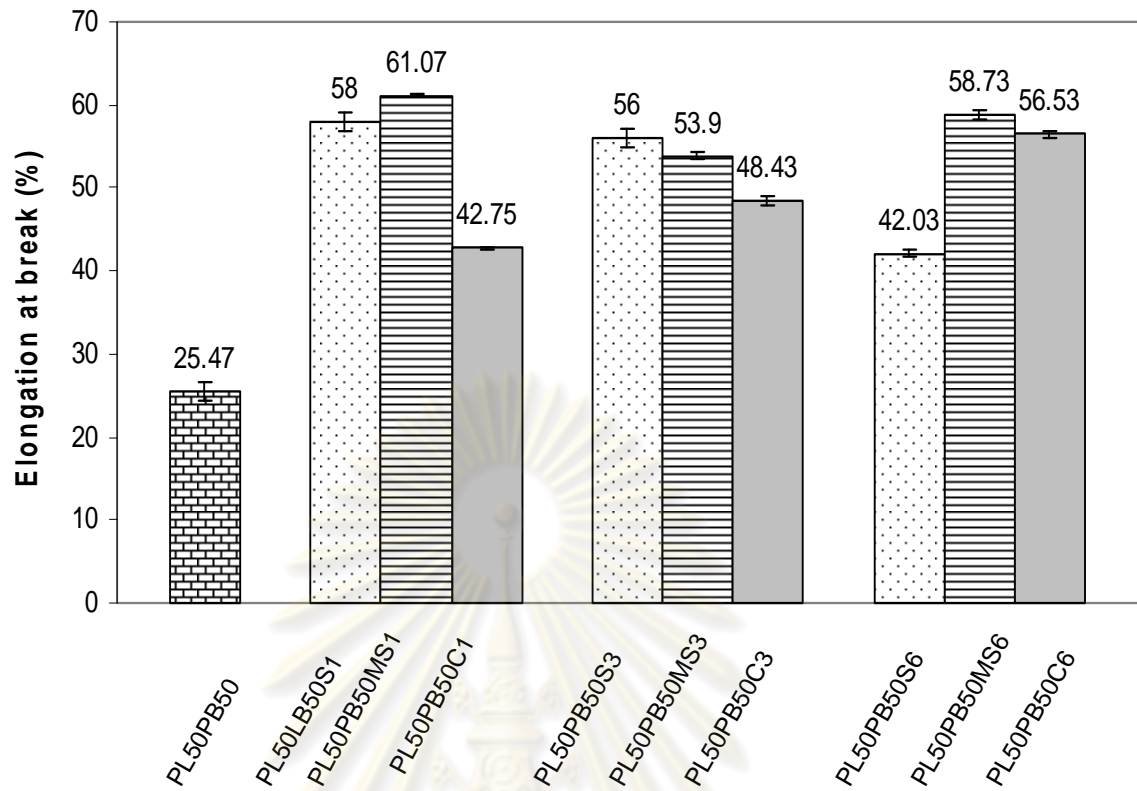


Figure 4.13 The elongation of PBAT/PLA (50/50 wt %) and their composites

ศูนย์วิทยทรัพยากร  
จุฬาลงกรณ์มหาวิทยาลัย

#### 4.4 Optical transparence of the blend films

Generally, the transparency of blend films was due to the degree of particle dispersion in the matrix polymer. The light transparence (%T) at different wavelengths for the films is shown in Table 4.3. As indicated in the table, all of the films' transmittance increased with the increase in wavelengths. PL50PB50 had the best light transparence among all of the blend films but it was still lower than that of the neat PLA. As shown in Table 4.3 it indicated that addition of fillers decreased the transmittance of the blend film, suggesting high reflective index of fillers. In addition, two types of fumed silica had higher reflective index than calcium carbonate. This reason indicated that fumed silica blend films had higher transmittance than calcium carbonate blend films.

Table 4.3 The light transparence ( $T$  %) at different wavelengths for the film

Sample code	Wavelengths						
	400 nm	450nm	500nm	550nm	600nm	650nm	700nm
PL100PB0	84.56	84.07	83.99	83.62	83.54	83.6	83.64
PL0PB100	43.43	49.58	52.75	54.66	83.54	58.18	59.13
PL50PB50	45.97	49.8	52.76	54.53	83.54	57.66	58.43
PL50PB50S1	42.73	46.72	49.6	51.37	83.54	54.69	55.55
PL50PB50S3	41.51	45.75	48.67	50.41	83.54	53.65	54.41
PL50PB50S6	43.32	47.25	50.19	51.98	83.54	55.34	56.14
PL50PB50MS1	13.33	18.53	22.13	24.64	20.95	28.87	30.48
PL50PB50MS3	20.38	26.52	30.49	33.08	20.95	36.92	38.06
PL50PB50MS6	12.29	17.84	22.23	25.17	20.95	29.42	30.79
PL50PB50C1	6.91	12.18	16.00	18.76	20.95	23.29	24.99
PL50PB50C3	16.78	24.12	28.45	31.64	20.95	37.12	39.07
PL50PB50C6	18.02	25.15	29.56	32.97	20.95	39.12	41.34



#### 4.5 Interactions between PBAT/PLA blends in the absence and presence of fillers

The hypothesis of polymer-polymer and polymer-particle intermolecular interaction was that interfacial bonding occurred between the hydroxyl group of polymer or fillers and carbonyl groups of polymer matrix.

In Figures 4.14-4.16, the IR spectra of PLA virgin (a), PBAT virgin (b), PL50PB50 (c), and PL50PB50S6 (d) films show polymer-particle interaction. The absorption band at  $1754\text{ cm}^{-1}$  of PLA (a) samples indicated carbonyl groups. The absorption band at  $1714\text{ cm}^{-1}$  of PBAT (b) samples indicated carbonyl groups. In the blends from the spectra of PL50PB50 (d) in Figures 4.14-4.16, the absorption peak at  $1714$  and  $1754\text{ cm}^{-1}$  were not changed from virgin PBAT and PLA, suggesting the lack of intermolecular bonding between PBAT and PLA.

Figures 4.14-4.16 (e) presents the IR spectra of PBAT/PLA blends nanocomposites. Figure 4.14 (e) shows that the PBAT/PLA/SiO<sub>2</sub>, PBAT/PLA/mSiO<sub>2</sub> and PBAT/PLA/NPCC exhibited the absorption peaks at  $1715$  and  $1754\text{ cm}^{-1}$ , which was not shifted from virgin PLA and PBAT, suggesting the lack of intermolecular bonding between fillers and PBAT/PLA molecules. From FT-IR results, the polymer-particles interaction between PBAT/PLA and fillers exhibited no significantly change of absorption peaks. These results suggested that intermolecular interactions between polymer molecules and filler particles were interfacial adhesion resulted from surface tension property.

ศูนย์วิทยทรัพยากร  
จุฬาลงกรณ์มหาวิทยาลัย

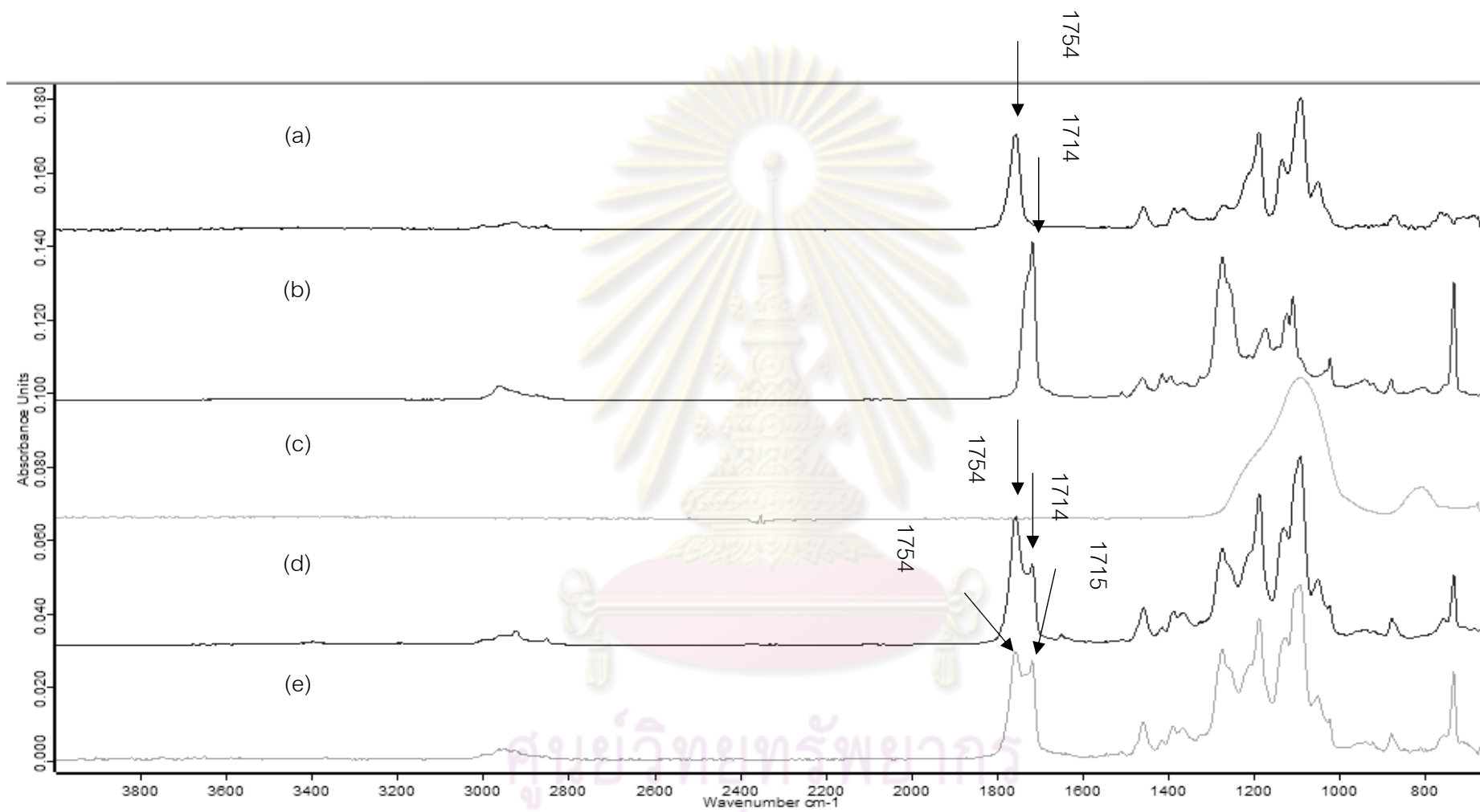


Figure 4.14 IR spectra of PLA (a), PBAT (b),  $\text{SiO}_2$  (c), PL50PB50 (d), and PL50PB50S6 (e)

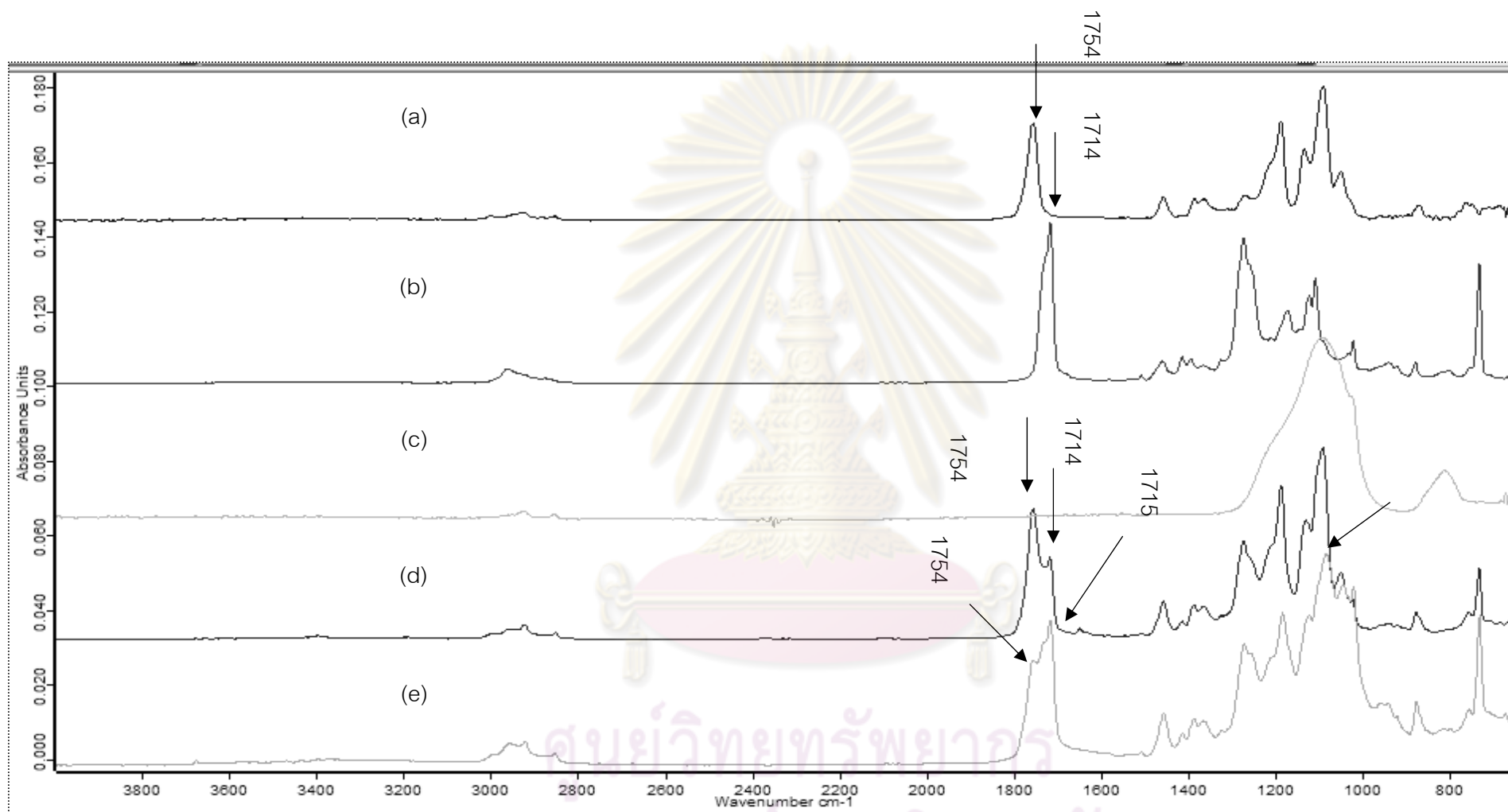


Figure 4.15 IR spectra of PLA (a), PBAT (b),  $\text{mSiO}_2$ (c), PL50PB50 (d), and PL50PB50MS6 (e)

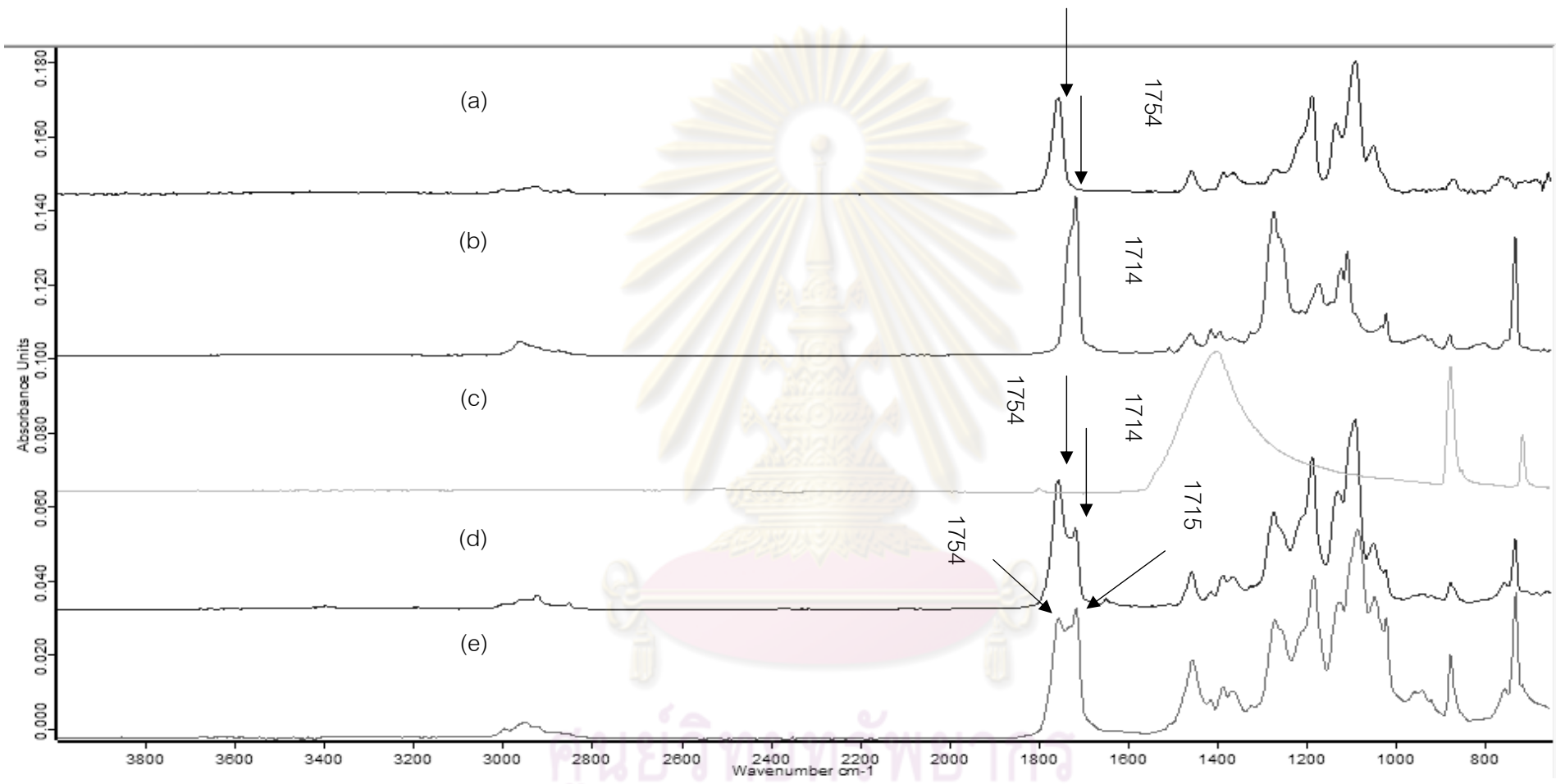


Figure 4.16 IR spectra of PLA (a), PBAT (b), CaCO<sub>3</sub>(c), PL50PB50 (d), and PL50PB50C6 (e)

#### 4.6 Dynamic mechanical properties

Figure 4.17 shows the storage modulus, loss modulus, and tan delta of the PBAT/PLA blend in the absence and presence of fillers, as function of temperatures. Here, the DMA was performed to show that exposing the composites at elevated temperatures would affect the stiffness of the composite material. As seen in Figure 4.17(a) and Table 4.4, the storage modulus at 60 °C of fillers addition in polymer blend was higher than the absence fillers in polymer blend. This was due to the reinforcement imparted by the fillers, which allowed stress transfer from the matrix to the fillers. In Table 4.4, fillers reinforced PBAT/PLA polymer blend nanocomposite showed a high storage modulus of about 5.01 (SiO<sub>2</sub>), 5.92 (mSiO<sub>2</sub>), 4.20 (NPCC) GPa at 60 °C. Figure 4.16 (b) shows the variation of the tan delta of the PBAT/PLA in the absence and presence of fillers with temperature. From the Tan delta curves in Figure 2(b), the glass transition temperature (T<sub>g</sub>) was observed. The T<sub>g</sub> was usually interpreted as the peak of either the tan delta or the loss modulus curves obtained during the dynamic mechanical test. As seen in Figure 2(b) and Table 4.4, due to the fillers present in the PBAT/PLA blend, the T<sub>g</sub> of PBAT phase shifted to higher temperature. The shifting of T<sub>g</sub> to higher temperatures was associated with the decreased mobility of the polymer chains, due to the addition of fillers. Furthermore, the stress field surrounding the particles induced the shift in T<sub>g</sub>. In DMA tan delta, two T<sub>g</sub> peaks indicated that the blend was still a two-phase system, immiscible blend.

As seen in Table 4.4, the addition of 1 phr of fillers increased the storage modulus of the PBAT/PLA blends, i.e., the storage modulus of PL50PB50S1, PL50PB50MS1 and PL50PB50C1 were higher than that of PBAT/PLA blend due to the reinforcement imparted by the fillers that allowed stress transfer from the matrix to the fillers. The storage modulus of the PBAT/PLA blend in the absence and presence of fillers decreased with the increase of temperature. The reduction of modulus was associated with softening of the matrix at higher temperature.

**Table 4.4** The storage modulus of the PBAT/PLA blend filled with fillers nanoparticle.

Sample code	Tg (°C)	Storage modulus (MPa)			Improvement by the fillers at 60°C (modulus %)
		at 25 °C	40 °C	60 °C	
	PBAT matrix				
PBAT virgin	-31.80	23.46	17.64	11.88	-
PL50PB50	-38.50	182.76	130.14	3.56	-
PL50PB50S1	-32.00	97.67	85.95	5.01	40.73
PL50PB50MS1	-34.50	110.29	81.62	5.92	66.29
PL50PB50C1	-33.50	189.17	152.75	4.20	17.97

ศูนย์วิทยทรัพยากร  
จุฬาลงกรณ์มหาวิทยาลัย



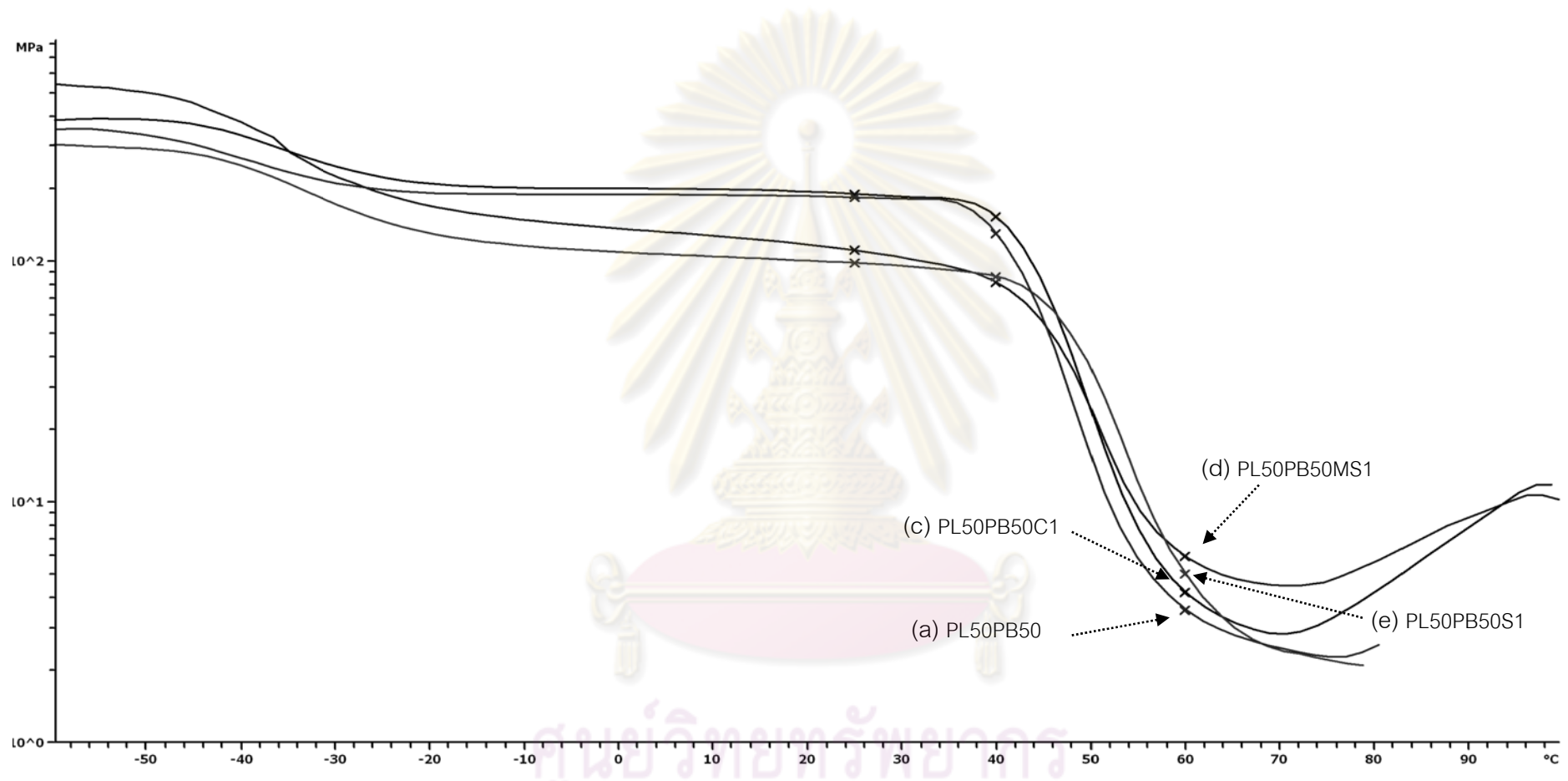


Figure 4.17 (a) Temperature dependence of storage modulus at 60 °C

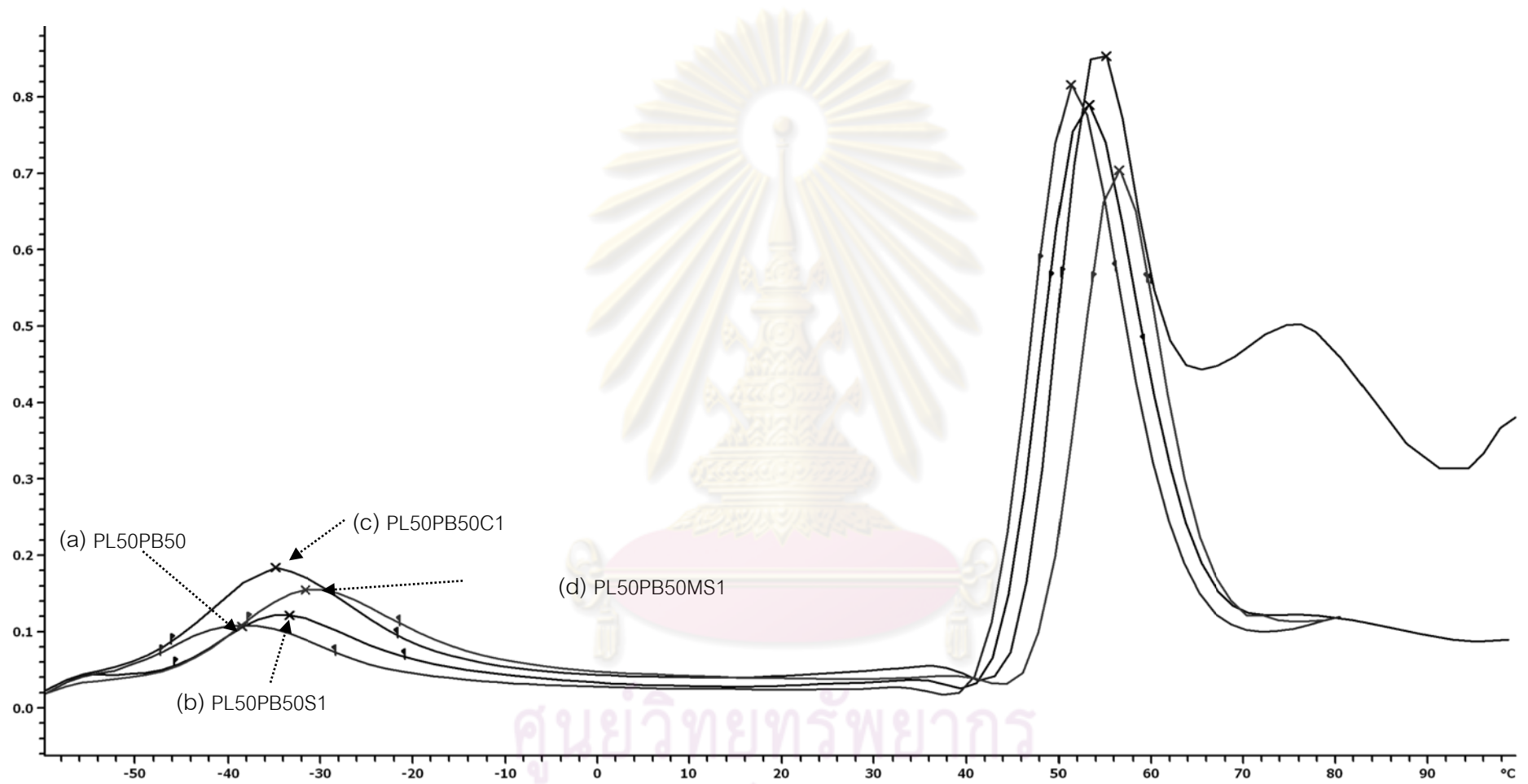


Figure 4.17 (b) Temperature dependence of tan delta ( $T_g$  of PBAT)

#### 4.7 Water vapor transmission rate (WVTR) and water vapor permeability (WVP)

WVTR is a measurement of the ease of moisture to penetrate and pass through a material. The film WVTR was calculated, and the results are shown in Figure 4.18. It could be seen that the presence of  $\text{SiO}_2$ ,  $\text{mSiO}_2$  and NPCC decreased WVTR in the whole. The WVTR of the films decreased with the presence of fillers. This might indicate the existence of intermolecular interactions and a decrease in the mobility of both the PBAT and PLA when fillers were added to the PBAT/PLA blend.

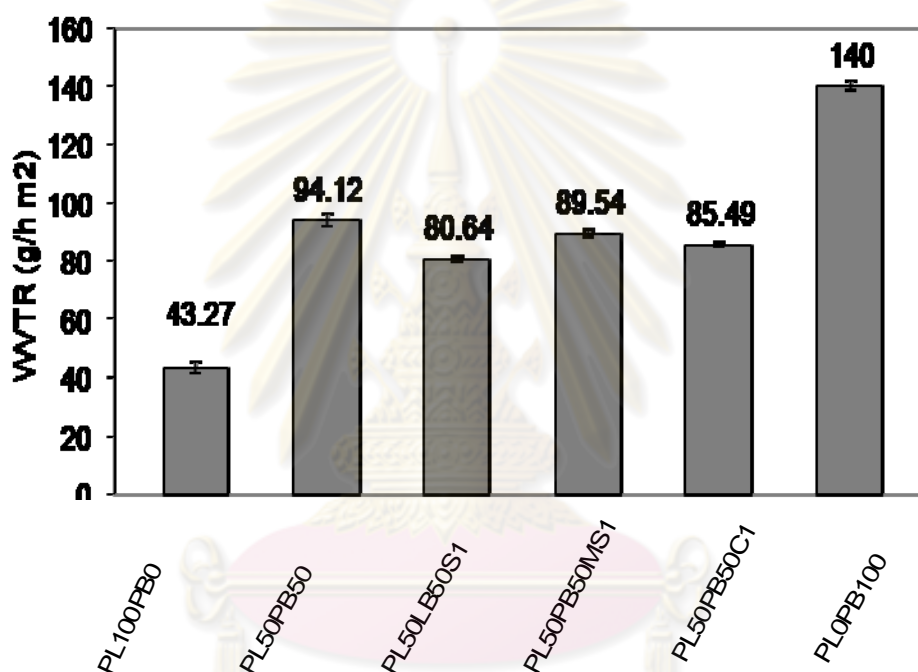


Figure 4.18 Water vapor transmission rate (WVTR) of films

#### 4.8 Enzymatic degradation study of PBAT/PLA blend in the absence and presence of SiO<sub>2</sub> at 1 phr

##### 4.8.1 Observation by SEM

The scanning electron micrographs (Figures 4.19-4.20 a - d) of PBAT/PLA (50/50 wt %) blend in the absence (PL50PB50) and presence (PL50PB50S1) of SiO<sub>2</sub> at 1 phr films indicated the damaged areas of PLA that was a starting point of the degradation. In SEM micrographs, comparing of Figures 4.19 b - 4.20 b with Figures 4.19e - 4.20e, incorporation of SiO<sub>2</sub> decreased amounts of black spots and damaged holes of the PLA degradation phase on PBAT/PLA. The degraded polymer exhibited higher amount of abnormal holes on PL50PB50 surface than that of PB50PL50S1 surface. Figures b and d, (at 120 hours) showed that the damaged hole areas of PLA degradation were higher than those of films at 8 hours. These indicated that the biodegradation rates in long term were higher than those in short term.



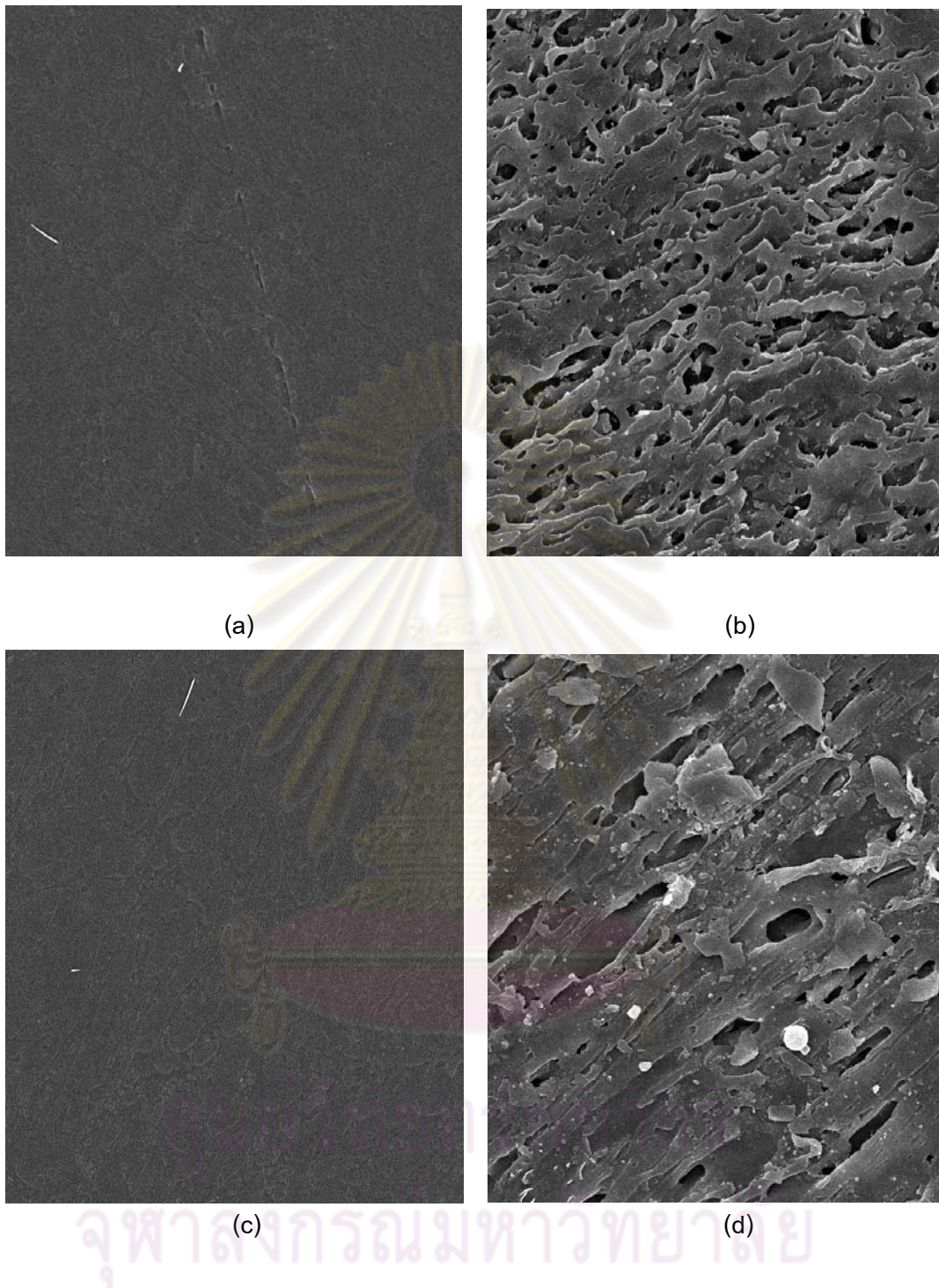


Figure 4.19 Scanning electron micrographs after 8 hours of enzymatic exposure  
at 15 kV 1,000 x

- (a) PL50PB50 (control)    (b) PL50PB50 (8 hrs)  
(c) PL50 PB50S1 (control) (d) PL50PB50S1 (8hrs)



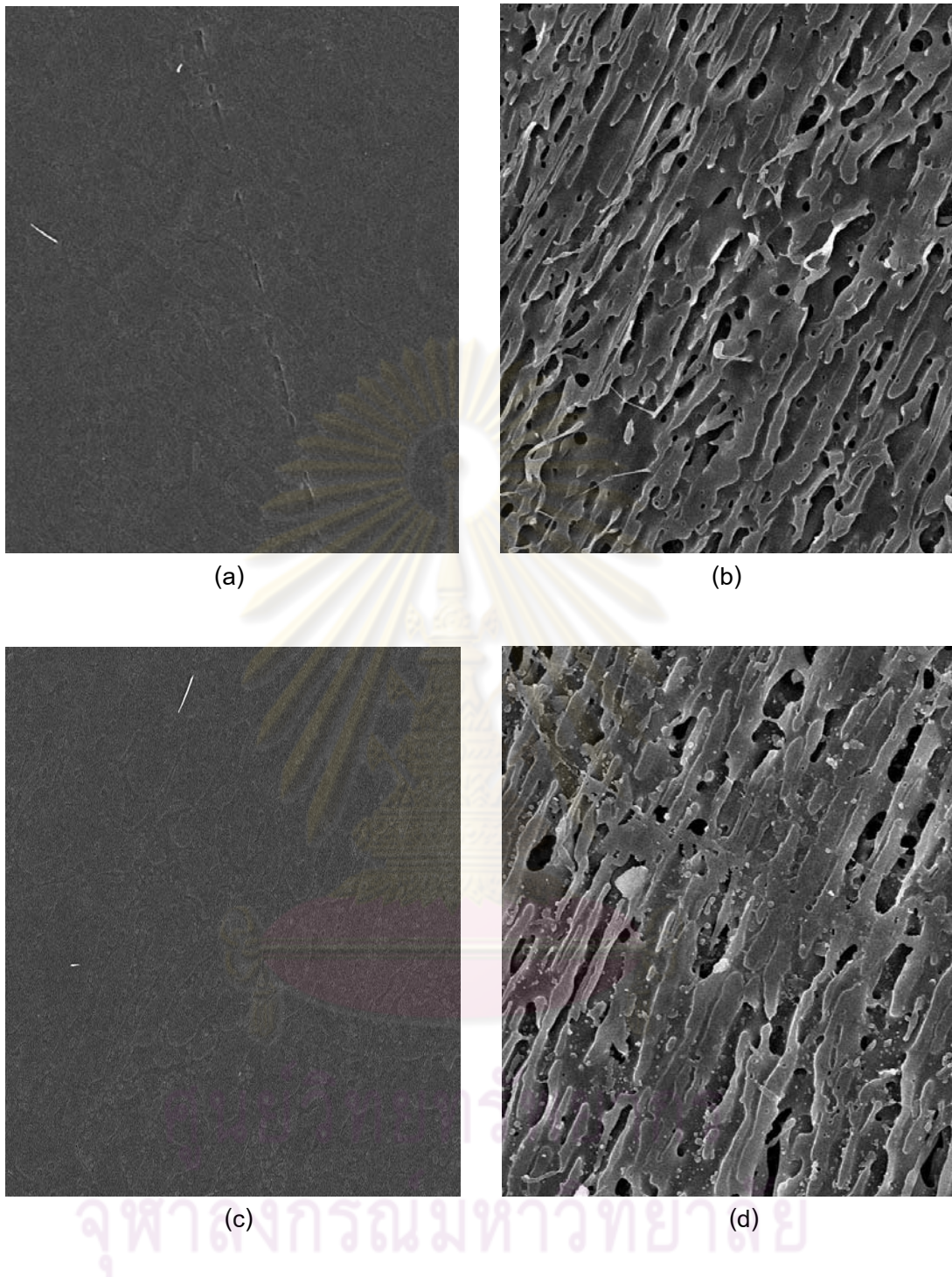


Figure 4.20 Scanning electron micrographs after 120 hours of enzymatic exposure  
at 15 kV 1,000 x

- (a) PL50PB50 (control)    (b) PL50PB50 (120 hrs)  
(c) PL50 PB50S1 (control)    (d) PL50PB50S1 (120hrs)



#### 4.8.2 Weight loss investigation

The percentages of weight loss from enzymatic degradation are shown in Figure 4.21. This illustrated more than 15 % weight loss after 120 hrs degradation of PBAT/PLA blend in the absence of  $\text{SiO}_2$  and more than 12 % weight loss after 120 hrs degradation of PBAT/PLA blend in the presence of  $\text{SiO}_2$ . The degradation rate of PBAT/PLA blend in the absence of  $\text{SiO}_2$  was higher than that of PBAT/PLA blend in the presence of  $\text{SiO}_2$ . This phenomena could be explained as follows: the PLA area of degradation phase in PL50PB50S1 was lower than that of the PL50PB50 as shown in Figure 4.21. The presence of  $\text{SiO}_2$  content increased interfacial adhesion between PBAT and PLA and crystalline ability of PLA, thus implied a hampered activity of Proteinase K enzyme. Hydrolysis reaction of PLA was hampered from the PBAT disperse phase and crystalline ability increasing of PLA matrix.

Basically, silica nanoparticles increased interfacial adhesion between the PBAT and PLA which caused difficulties to degrade by enzymatic degradation.

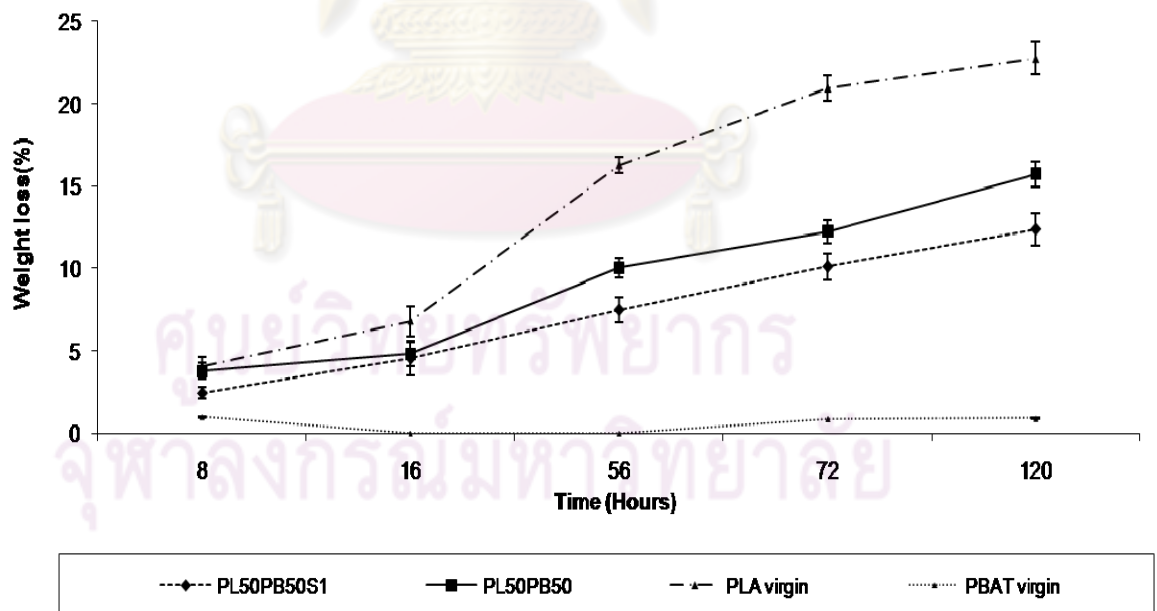


Figure 4.21 Weight loss of the PL50PB50 and PL50PB50S1 on digestion times

4.8.3 Mechanical properties after enzymatic degradation

Tensile modulus and yield stress results are shown in Figure 4.22-4.23. Both PL50PB50 and PL50PB50S1, the tensile modulus and yield stress were slightly decreased when digestion times increased. With the addition of SiO<sub>2</sub> at 1 phr, the tensile modulus and yield stress were higher than those without SiO<sub>2</sub>. This result was confirmed with weight loss from enzymatic degradation which increasing trend in weight loss resulted in reducing trend in tensile modulus and yield stress.

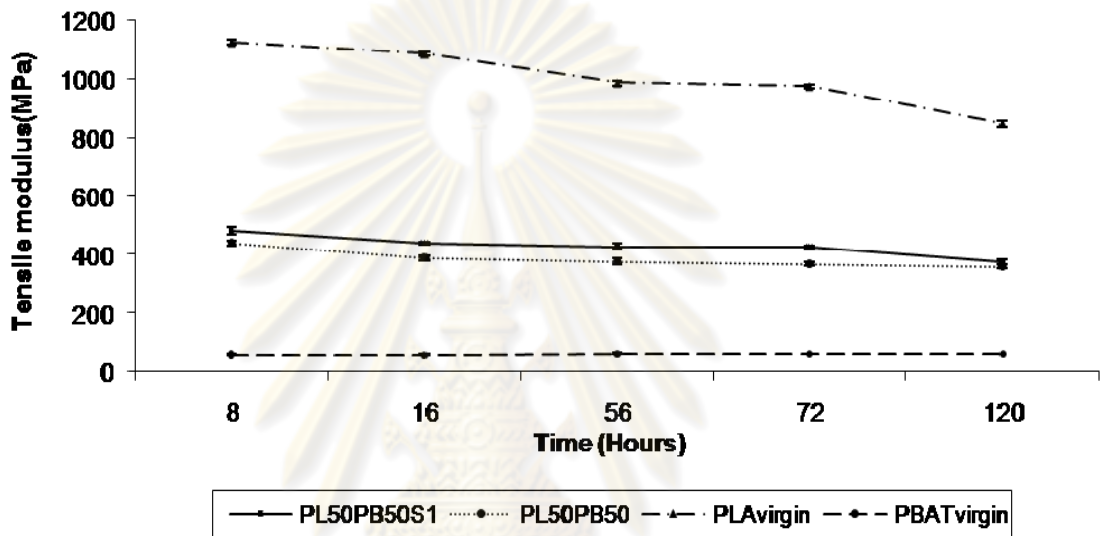


Figure 4.22 Comparison of tensile modulus between PL50PB50 and PL50PB50S1

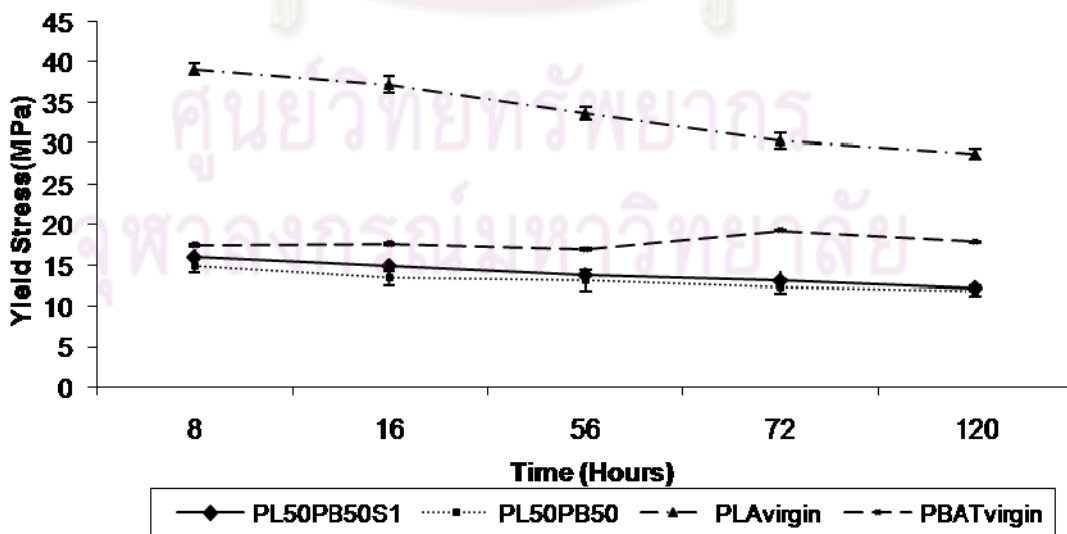


Figure 4.23 Comparison of yield stress between PL50PB50 and PL50PB50S1

## CHAPTER V

### CONCLUSION AND FUTURE DIRECTION

#### 5.1 Conclusion

The blends of PBAT/PLA with  $\text{SiO}_2$ ,  $\text{mSiO}_2$  and NPCC as reinforced fillers were prepared by twin screw extrusion.  $\text{SiO}_2$ ,  $\text{mSiO}_2$  and NPCC as reinforced fillers obviously effected the physical properties and biodegradability of PBAT/PLA blends. The addition of PBAT was found to accelerate the crystallization rate of PLA but had little effect on its final degree of crystallinity. Similar to other blend systems, the semi-crystalline PLA experienced extensive cold crystallization, and the PLA was almost totally amorphous in the molded products at the normal processing condition. With the PBAT addition, the tensile toughness of the PLA blend was greatly increased with severe loss in tensile strength and modulus. The material changed from brittle (PLA) to ductile failure with the addition of PBAT. Blend of PBAT/PLA (50/50 wt %) with  $\text{SiO}_2$ ,  $\text{mSiO}_2$  and NPCC as reinforced fillers were prepared by twin screw extrusion. Incorporated with fillers, the tensile strength, modulus and elongation of the PBAT/PLA blend were increased. SEM micrographs revealed that they had better miscibility than the PBAT/PLA blend. DSC results indicated that the blend was still a two-phase system. The presence of fillers was found to enhance the crystallization rate and degree of crystallinity of PBAT /PLA blends. DMA results revealed that the addition of fillers increased the storage modulus. The optical transmittance of the blends with fillers was decrease. FT-IR results showed that the polymer-particle interactions between PBAT/PLA polymer molecules and  $\text{SiO}_2$ / $\text{mSiO}_2$ /NPCC particles were attributed to interfacial adhesion. With the presence of fillers content, the permeability of the films was also improved. Finally, the enzymatic degradation test showed that the addition of nano- $\text{SiO}_2$  had significant influence the biodegradability of the films.

## 5.2 Future direction

In this research, the addition of  $\text{SiO}_2$ ,  $\text{mSiO}_2$  and NPCC nanoparticles as reinforced fillers could lead to some improvements of the mechanical properties of PBAT/PLA blends. However from the SEM results, less compatibility was found. Therefore future work should be in the direction of finding new compatibilizers, for example, triethyl citrate and tributylacetyl citrate to enhance greater mechanical properties of PBAT/PLA blends to be as close as PP.



ศูนย์วิทยทรัพยากร  
จุฬาลงกรณ์มหาวิทยาลัย

## REFERENCES

- [1] Zhang, Q.-X., Yu, Z.-Z., Xie, X.L., Naito, K., and Kagawa, Y. Preparation and crystalline morphology of biodegradable starch/clay nanocomposites. Polymer 48(2007): 7193-7200.
- [2] Tang, S., Zou, P., Xiong, H., and Tang, H. Effect of nano-SiO<sub>2</sub> on the performance of starch/polyvinyl alcohol blend films. Carbohydrate Polymers 72(2008): 521-526.
- [3] Gu, S-Y., Zhang, K., Ren, J., and Zhan, H. Melt rheology of polylactide/poly(butylenes adipate-co-terephthalate) blends. Carbohydrate Polymer 74(2008): 79-85.
- [4] Aso, O., Eguiazabal, J.I., and Nazabal, J. The influence of surface modification on the structure and properties of a nanosilica filled thermoplastic elastomer. Composites Science and Technology 67(2007): 2854-2863.
- [5] Zuiderduin, W. C. J., Huétink, J., and Gaymans, R. J. Rigid particle toughening of aliphatic polyketone. Polymer 47(2006): 5880-5887.
- [6] Pandey, J.K., Raghunatha Reddy, K., Pratheep Kumar, A., and Singh, R.P. An overview on the degradability of polymer nanocomposites. Polymer Degradation and Stability 88(2005): 234-250.
- [7] Chandra, R., and Rustigi, R. Biodegradable polymer. Progress in Polymer Science 23(1998): 1273-1335.
- [8] Bordes, P., Pollet, E., and Averous, L. Nano-biocomposites: biodegradable polyester/nanoclay systems. Progress in Polymer Science (2008).
- [9] Simon, G.P. Polymer Characterization Techniques and Their Application to Blend. New York: American Chemical Society, 2003: 22-460.
- [10] Sodergard, A., and Stolt, M. Properties of lactic acid based polymers and their correlation with composition. Progress in Polymer Science 27(2002): 1123-1163.

- [11] Nolan-ITU Pty Ltd. Biodegradable Plastics-Developmental Impacts. Available from: [http:// www.environment.gov.au/ settlements/publications/waste-degradables/biodegradable/chapter3.html#3-2](http://www.environment.gov.au/settlements/publications/waste-degradables/biodegradable/chapter3.html#3-2). October, 2002.
- [12] Rudnik, E. Compostable Polymer Materials. Netherlands: Elsevier, 2008: 14-64.
- [13] Xanthos, M. Functional Fillers for Plastics. New Jersey:Wiley-VCH, 2005: 3-284.
- [14] Furstner, A., Active Metal. New York: Weinheim-VCH, 1996: 17-338.
- [15] Fischer, H. Polymer nanocomposites: from fundamental research to specific applications. Materials Science and Engineering 23(2003): 763-772.
- [16] Pomogailo, A.D., and Kestelman, V.N. Metallopolymer Nanocomposites. New York: Springer series in materials science, 2005: 3-23.
- [17] Sperling, L.H. Introduction to Physical Polymer Science. New York:Wiley, 2006: 687-741.
- [18] Li, S., Tenon, M., Garreau, H., Braud, C., and Vert, M. Enzymatic degradation of stereocopolymers derived from l-, dl- and meso-lactides. Polymer Degradation and Stability 67(2000): 85-90.
- [19] Yu, L., Dean, K., and Li, L. Polymer blends and composites from renewable resources. Progress in Polymer Science 31(2006): 576-602.
- [20] Griffin, G.J.L. Chemistry and Technology of Biodegradable Polymers. London: Backie Academic and Professional, 2001: 3-154.
- [21] Dan, G., and Gerald, S. Degradable Polymers. London: Chapman and Hall, 1997: 1-271.
- [22] Jiang, L., Wolcott, M.P., and Zhang, J. Study of biodegradable/(poly)butylenes adipate-co-terephthalate blends. Biomacromolecules 7(2006): 199-207.
- [23] Xiong, H. G., Tang, S. W., Tang, H. L., and Zou, P. The structure and properties of a starch- based biodegradable film. Carbohydrate Polymers 71(2007): 263-268
- [24] Hiljanen-Vainio, M., Heino, M., and Seppala, J.V. Reinforcement of biodegradable poly (ester-urethane) with fillers. Polymer 39(1998): 865-872.



- [25] Lii, Q., Zhang, Y., and Xu, H. Properties of vulcanized rubber nanocomposites filled with nanokaolin and precipitated silica. Applied Clay Science 42(2008): 232-237.
- [26] Jiang, L. Zhang, J., and Wolcott. Michael, P. Comparison of polylactide/nano-sized calcium carbonate and polylactide/montmorillonite composites: reinforcing effects and toughening mechanisms. Polymer 48(2007): 7632-7644.
- [27] Elias, L., Fenouillot, F., Majeste, J.C., and Cassagnau, Ph. Morphology and rheology of immiscible polymer blends filled with silica nanoparticles. Polymer 48(2007): 6029-6040.
- [28] Li, B., Kennedy, J.F., Peng, J.L., Yie, X., and Xie, B.J. Preparation and performance evaluation of glucomannan-chitosan-nisin ternary antimicrobial blend film. Carbohydrate Polymers 65(2006): 488-494.
- [29] Elias, L., Fenouillot, F., Majeste, J.C., Alcouffe, P., and Cassagnau, P. Immiscible polymer blends stabilized with nano-silica particles: Rheology and effective interfacial tension. Polymer 49(2008):4378-4385.
- [30] Ludvik, C.N., Glenn, G.M., Klamczynski, A.P., and Wood, D.P. Cellulose Fiber/Bentonite Clay/Biodegradable Thermoplastic Composites. Journal of Polymer and Environment 15(2007): 251-257.
- [31] Signori, F., Coltelli, M.B., and Bronco, S. Thermal degradation of poly(lactic acid) (PLA) and poly(butylene adipate-co-terephthalate) (PBAT) and their blends upon melt processing. Polymer degradation and Stability 94(2009): 74-82.
- [32] Fu, S-Y., Feng, X-Q., Lauke, B., and Mai, Y-W. Effects of particle size, particle/matrix interface adhesion and particle loading on mechanical properties of particulate-polymer composites. Composites Part B: Engineering 39(2008): 933-961.



APPENDICES

ศูนย์วิทยทรัพยากร  
จุฬาลงกรณ์มหาวิทยาลัย

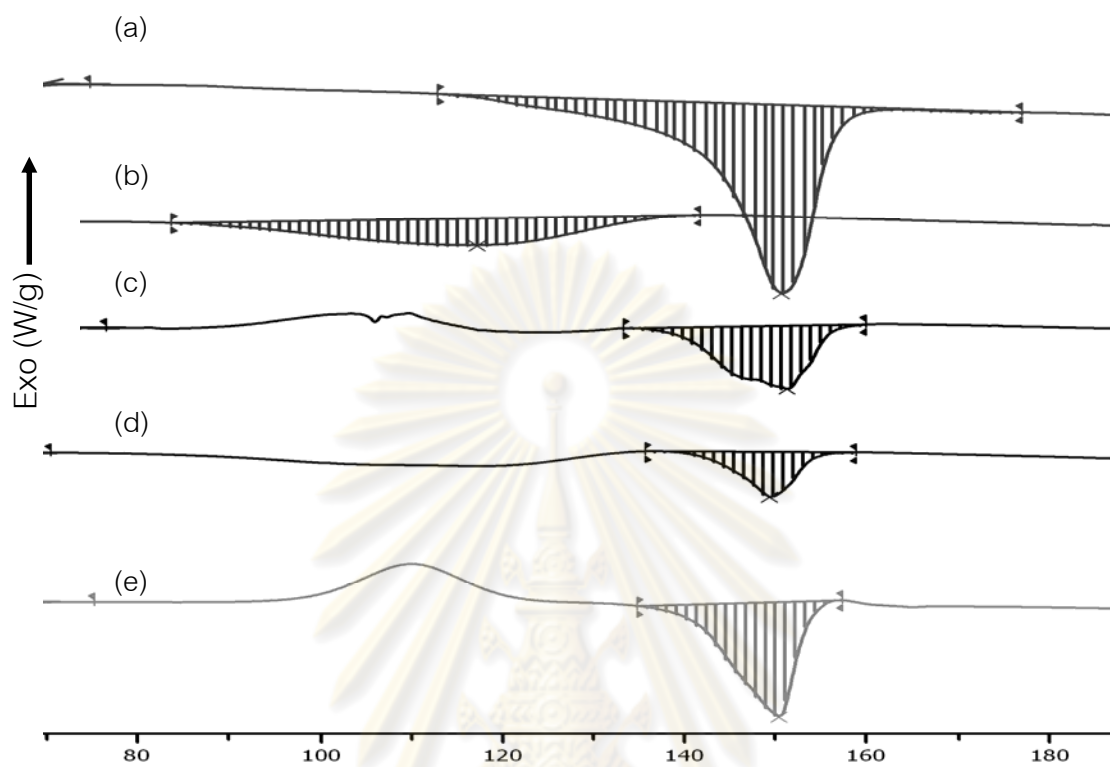


Figure A-1  $T_m$  and  $\Delta H_m$  of PLA in neat form and blends at various PBAT contents

(1<sup>st</sup> heating scan, 10°C/min) : (a) neat PLA (b) neat PBAT (c) PL40PB60

(d) PL30PB70 (e) PL50PB50

ศูนย์วิทยทรัพยากร  
จุฬาลงกรณ์มหาวิทยาลัย

Table A-1 Mechanical properties of PBAT/PLA blend with various PBAT contents.

Sample code	Tensile strength	Tensile modulus	Elongation at break
	Mpa	Mpa	%
PLA (Virgin)	45.90±0.23	1469.32±3.73	2.97±0.75
PBAT (Virgin)	17.56±0.34	60.08±0.59	665.44±5.15
PL50PB50	23.57±0.58	259.44±1.69	25.47±1.07
PL40PB60	12.57±0.17	172.27±3.03	72.30±2.32
PL30PB70	11.03±0.17	128.42±2.48	97.78±1.86

ศูนย์วิทยทรัพยากร  
จุฬาลงกรณ์มหาวิทยาลัย

Table A-2 Mechanical properties of PBAT/PLA blend with absence and presence of fillers content.

Sample code	Tensile strength	Tensile modulus	Elongation at break
	Mpa	Mpa	%
PL50PB50	23.57±0.58	259.44±1.69	25.47±1.07
PL50PB50S1	25.17±0.35	383.38±1.97	58.00±4.05
PL50PB50S3	24.89±0.26	355.93±9.76	56.00±4.87
PL50PB50S6	22.85±0.09	334.82±12.69	42.03±2.41
PL50PB50MS1	21.18±0.27	322.13±0.22	61.07±0.12
PL50PB50MS3	20.71±0.04	330.32±0.21	53.90±0.95
PL50PB50MS6	20.82±0.04	290.52±0.65	58.73±0.85
PL50PB50C1	22.46±0.09	338.22±1.48	42.75±0.22
PL50PB50C3	24.54±0.02	330.95±0.27	48.43±0.18
PL50PB50C6	25.43±0.17	343.75±0.52	56.53±0.4

ศูนย์วิทยทรัพยากร  
จุฬาลงกรณ์มหาวิทยาลัย

Table A-3 Thermal properties ( $T_{g1}$  and  $T_{g2}$ ) of PBAT/PLA blends with various filler types and content (2<sup>nd</sup> heating scan, 10°C/min)

Sample Code	$T_{g1}$ (°C)	$T_{g2}$ (°C)
PI100PB0	-	52.71
PL0PB100	-31.85	-
PL50PB50	-35.39	53.26
PL50PB50S1	-36.69	53.56
PL50PB50S3	-36.29	52.31
PL50PB50S6	-35.99	52.19
PL50PB50MS1	-33.96	55.22
PL50PB50MS3	-33.33	56.00
PL50PB50MS6	-33.41	54.35
PL50PB50C1	-34.93	48.15
PL50PB50C3	-33.54	51.00
PL50PB50C6	-32.70	57.06

ศูนย์วิทยทรัพยากร  
จุฬาลงกรณ์มหาวิทยาลัย



Table A-4 The glass temperature ( $T_g$ ) from DMA analysis of the PBAT/PLA blend filled with nanoparticle fillers.

Sample code	$T_g$ ( $^{\circ}\text{C}$ )	
	PBAT	PLA
PBAT virgin	-31.80	-
PL50PB50	-38.50	51.50
PL50PB50S1	-32.00	56.80
PL50PB50MS1	-34.50	53.00
PL50PB50C1	-33.50	53.90



คุนยวทยทรพยากร  
จุพาลงกรณมหาวิทยาฬย

## BIOGRAPHY

Miss Kanrawee Bosuwan was born on May 5, 1983 in Pranakhonsriyutthaya, Thailand. Her permanent address is 27/2 Moo.3, Tambon Clongsrabua, Amphoe Pranakhonsriyutthaya, Pranakhonsriyutthaya 13000. She graduated with a Bachelor's degree of Education, major in chemistry, Faculty of Education, Chulalongkorn University in 2005. She has worked in the department of R&D at Advance Packaging Co., Ltd. for 2 years. She began her master study in Petrochemistry and Polymer Science Program, Faculty of Science, Chulalongkorn University, Bangkok, Thailand since 2006 and finished her study in 2009.

### Presentation Experience

Poster presentation at the 2<sup>nd</sup> The National Conference on Science and Technology (NCST2009) organized by Faculty of Science and Technology, Sakon Nakhon Rajabhat University in the topic of "Physical Properties of Biodegradable Polymer Blends filled with Silica Nanoparticles".

ศูนย์วิทยทรัพยากร  
จุฬาลงกรณ์มหาวิทยาลัย